Polyolefin Hybrids with Designed Topologies and Compositions: Synthesis, Characterization and Properties

Hideyuki Kaneko

2009

TABLE OF CONTENTS

GENERAL INTRODUCTION

1. Polyolefin

Along with metals, ceramics, wood, glass and paper, plastics are indispensable materials for a modern society and are literally daily used in such applications as films and sheets, synthetic leathers, pipes, containers, automotive parts, electric and electronic parts, medical and sanitary products, toys, construction materials, agricultural materials and so on. Since the discovery of phenol resin in 1907 by Bakeland, a variety of plastics, such as methacrylic resin, polystyrene, poly(vinyl chloride), polyamide, polyethylene, polyester, polyurethane, poly(ethylene telephthalate), polycarbonate, polypropylene and polyimide, have been developed rapidly and their worldwide production has reached about 162 million tons in 2005 (Figure 1). The reasons for their dramatic development include a wide range of physical properties and excellent processability compared with conventional materials such as metals and ceramics, not to mention competence in cost and availability.

Among these plastics, polyolefin, represented by polyethylene (PE) and polypropylene (PP), is the most widely used commercial polymers with over 100 million tons per year, or more than 60 % of the total plastic production. Their well-balanced combination of chemical and physical properties, such as mechanical strength, flexibility, toughness and chemical stability along with low cost production, superior processability and recyclability, has positioned itself as the most preferred commercial polymers of choice. In addition, polyolefin is green materials because they are composed of only carbon and hydrogen and, therefore, they are also useful and preferable in terms of a reduction of environmental burdens.

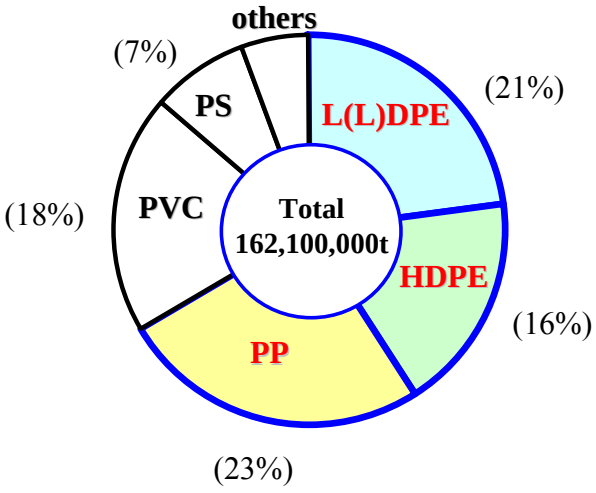

Figure 1. World thermoplastic market in 2005.

2. Development of Polyolefin

Since the commercialization of low density polyethylene (LDPE), polyolefin chemistry and industry have continuously evolved to create a large number of new polyolefin products. Today's prosperity of polyolefin owes much to the development of olefin polymerization catalyst and the consequent highly precise control of polymer structure. Figure 2 shows the constituent factors for controlling the polyolefin structure and property, including the diversity in monomers, stereoregularity, molecular weight, molecular weight and composition distributions, monomer sequence, topology and functionality. Since the discovery of Ziegler-Natta catalyst, these factors have been controlled more precisely and widely along with the progress of polymerization catalyst, resulting in a wide variety of polyolefin families with some excellent properties.

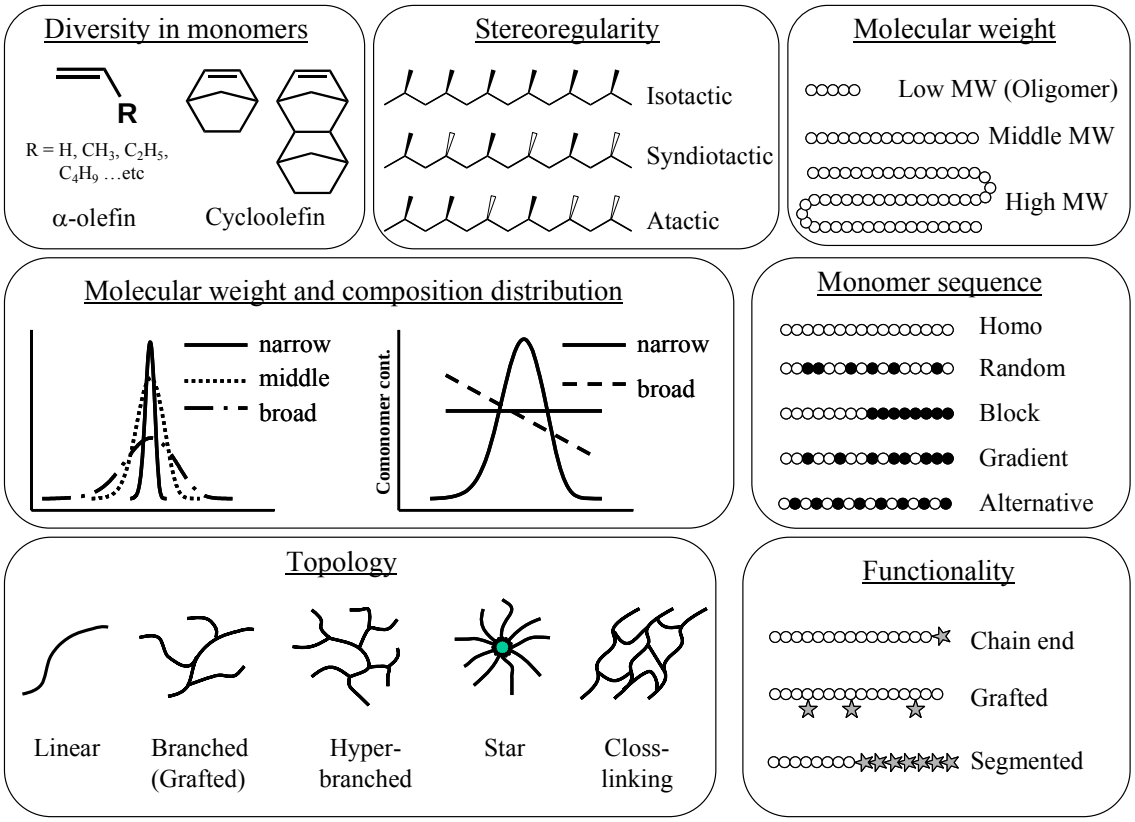

Figure 2. Constituent factors for controlling the structure and property of polyolefin.

2.1. Genesis of Polyolefin

In 1933, low density polyethylene (LDPE) was discovered by Imperial Chemical Industries (ICI, England) and it was then commercialized in 1939. LDPE is produced by radical polymerization process in the presence of air or organic peroxide as a radical initiator at high temperature (100 – 350 ^{o}C) and high pressure (1000 – 4000 atm) [1]. Therefore, though ethylene homopolymer in nature, LDPE contains a considerable number of long- and short-chain alkyl and hydrocarbon branches along the polyethylene backbone and consequently represents variable features of low density (lightweight), softness and high impact strength. In addition, the microstructure, such as number of branches, branch length, molecular weight and molecular weight distribution, is reflected in its properties and processability. Because of these characteristics, LDPE has been mainly used as films.

2.2. Conventional Polyolefin by Ziegler-Natta Catalyst

After 20 years from the discovery of LDPE, Ziegler and Natta found a novel coordination polymerization system using transition-metal catalyst to create new polyolefin families such as high density polyethylene (HDPE), linear low density polyethylene (LLDPE) and isotactic polypropylene (i-PP) [2-5]. HDPE has higher crystallinity, stiffness and heat resistance than LDPE because of few or no short-chain branches in its backbone and then it is used in the field of structural materials such as containers, bottles and groceries. LLDPE is a copolymer of ethylene with a small amount of α-olefins carrying a pendant alkyl group. Owing to some short-chain branching from the α-olefin comonomer units, LLDPE shows low density, softness, good toughness and transparency compared with HDPE and it is mainly used for films. i-PP is used for several injection molding and extrusion processes due to its excellent rigidity, toughness and heat resistance. Thus, Ziegler-Natta catalyst enabled not only the incorporation of α-olefins, such as propylene and 1-butene, into polyolefin but also their stereoregular polymerization, and all of these common polyolefins thereby led to birth of polyolefin industries around the world.

2.3. Advancement of Polyolefin by Improved Catalysts

Even after the historic breakthrough achieved by Ziegler and Natta, it had been continued to improve the existing polyolefin and create new generations of polyolefin by the progress of polymerization catalyst and process. For example, $MgCl_2$-supported $TiCl_4$ catalyst, discovered by Kashiwa in 1968, showed not only high activity but also narrowed molecular weight and composition distributions to realize the high

performance HDPE and LLDPE with well-controlled structure [7-10]. In addition, this catalyst enabled to increase the α-olefin content in LLDPE, leading to the creation of new classes of PE called VLDPE (having lower densities than LLDPE). In the case of propylene polymerization, $MgCl_2$-supported $TiCl_4$ catalyst enabled a good balance among high activity, high isospecificity, narrow molecular weight and composition distributions and good comonomer response in combination with the so-called electron donor including ester, ether and alkoxysilane compound to improve the properties of i-PP families, such as homopolymer (HP), random copolymer (RCP) and impact copolymer (ICP), and to create new class of polyolefins, such as isotactic poly(1-butene) and isotactic poly(4-methyl-1-pentene).

Alternatively, the vanadium-based catalyst system, which is discovered by Natta, is also active for olefin polymerization [11]. One of the advantages of this catalyst system is that it can produce the polymers with the narrowest molecular weight and composition distribution among all Ziegler-Natta catalyst systems. For example, narrow composition distribution is especially important for elastomer production, since a broad distribution could lead to the formation of high crystalline polymer fractions, which is evidently undesirable for elastomer applications. Therefore, it is commercially used mainly for the production of some ethylene-based copolymers, such as ethylene/propylene random copolymer (EPR), ethylene/1-butene random copolymer (EBR) and ethylene/propylene/diene copolymer (EPDM). These elastomeric materials are useful for impact modifier and precursor of rubber. In addition, this catalyst system excels at introduction of cyclic olefins and therefore, cyclic olefin copolymer (COC) is also produced industrially.

2.4. New Polyolefin Families by Single-Site Catalysts

In 1980, Kaminsky and Sinn found that the combination of dicyclopentadienyl zirconiumdimethyl and methylamuminoxane catalyzed the polymerization of ethylene with high activity [12,13]. One of the most important features for metallocenes is that they are molecularly well-defined homogeneous catalysts which can produce polymers with narrower and well-controlled molecular weight and composition distributions at very high catalytic activity than heterogeneous and thus ill-defined Ziegler-Natta catalyst. Another important feature of metallocenes is the facile introduction of bulky monomers such as higher α-olefins and cyclic olefins. Owing to these features, metallocene-catalyzed LLDPE has been rapidly commercialized and mainly used as film resin. Its narrow molecular weight and composition distributions bring about uniform and thin lamellae and, therefore, uniform fine crystals and many tie molecules

are formed, leading to high film clarity and high impact strength, respectively. Thus, a part of Ziegler-Natta catalysts was replaced by metallocenes in the production of LLDPE. Needless to say, it is an irreversible trend in polyolefin industries that metallocenes supersede vanadium-based catalysts in the production of elastomer and COC. Furthermore, it is noteworthy that metallocenes established the production of a new class of polymers such as PE with much lower density (so-called "Plastomer"), syndiotactic polypropylene (s-PP), ethylene/styrene copolymer, syndiotactic polystyrene and long-chain-branching polymers.

2.5. Challenges in Polyolefin and Catalysis

The great successes of metallocenes have also reminded the fact that the precise control of polymer structure, as realized by single-site nature and customized design of catalysts, should be key success factors in development of polyolefins. However, the precisely control of sequence, topology and functionality were not achieved well even by the latest metallocene catalyst.

In 1995, non-metallocene catalyst based on late transition metals, so-called post-metallocenes, was reported [14] and attracted considerable attention to their specific polymerization behaviors such as living polymerizations of α-olefins, the formation of short-chain-branching polyethylene and copolymerization of ethylene with polar monomers. Moreover, early transition metal post-metallocenes were the topics because of their extremely high activities in ethylene homopolymerization and living polymerizations of olefins at high temperatures [15]. Therefore, the post-metallocene catalyst would be considered to have a great potential for further precise control of polymer structures to produce new classes of polyolefins.

Block copolymer and gradient copolymer obtained by controlling monomer sequence have been expected to have distinctive properties due to the combination of different compositions. By olefin living polymerization with vanadium-based catalysts or post-metallocene catalysts, several kinds of block copolymers, such as PE-*b*-EPR [16-20], PE-*b*-poly(ethylene-*co*-1-hexene) [21], s-PP-*b*-EPR [22,23] and PP-*b*-EPR-*b*-s-PP [19], as well as gradient EPR copolymers [24,25], were successfully synthesized and demonstrated good rubber-elastic properties. Recently, it has been reported that so-called "olefin block copolymers (OBCs)", or multi-block copolymers of PE and ethylene/1-octene random copolymer (EOR), were synthesized by chain shuttling polymerization with post-metallocene catalyst [26-30]. These multi-block copolymers consist of hard and soft segments and thereby are expected as modifier for polyolefins.

On the other hand, topology control has long been a great challenge for polyolefin

chemistry and however there are only a few reports about it. The long-chain branched copolymer based on ethylene [31-33], which can be produced by metallocene catalyst system, showed the excellent properties balance between processability and toughness. The long-chain branched PP [34-36] can be prepared by metallocene catalyst system and have good balance of melt elasticity and mechanical properties. In addition, the new methodology for controlling chain topology has recently reported [37-39]. In the chain-walking polymerization of ethylene using post-metallocene catalyst, the polymer chain topology ranging from linear to hyperbranched structures can be simply controlled by varying ethylene pressure and polymerization temperature. The obtained hyperbranched polyethylene had very low viscosities and showed a Newtonian flow behavior due to the absence of chain entanglements. The change of chain topology from hyperbranched to linear leads to much higher viscosity and non-Newtonian flow behavior due to chain entanglements. Progress in catalysts and production processes is expected to allow further precise control of these factors.

3. Polyolefin Hybrids: New Challenges for Functionalization

Despite the development of polyolefin with catalyst innovation, as reviewed above, there are still large areas of properties occupied by non-polyolefin, including styrenic/(meth)acrylic polymers prepared by radical polymerization, engineering plastics, super engineering plastics, thermosetting plastics and thermoplastic elastomers, all of which are much more expensive and less environmentally friendly materials. As shown in Figure 3, polyolefin is far inferior to the non-polyolefin consisting of some polar and aromatic groups, particularly in terms of physical properties, such as stiffness and heat-resistance. In order to improve the properties of polyolefin and broaden their application into highly profitable fields, the introduction of functional groups or segments into polyolefin backbone is widely-recognized as very important and effective approach, and consequently extensive studies have been actively carried out for such approaches.

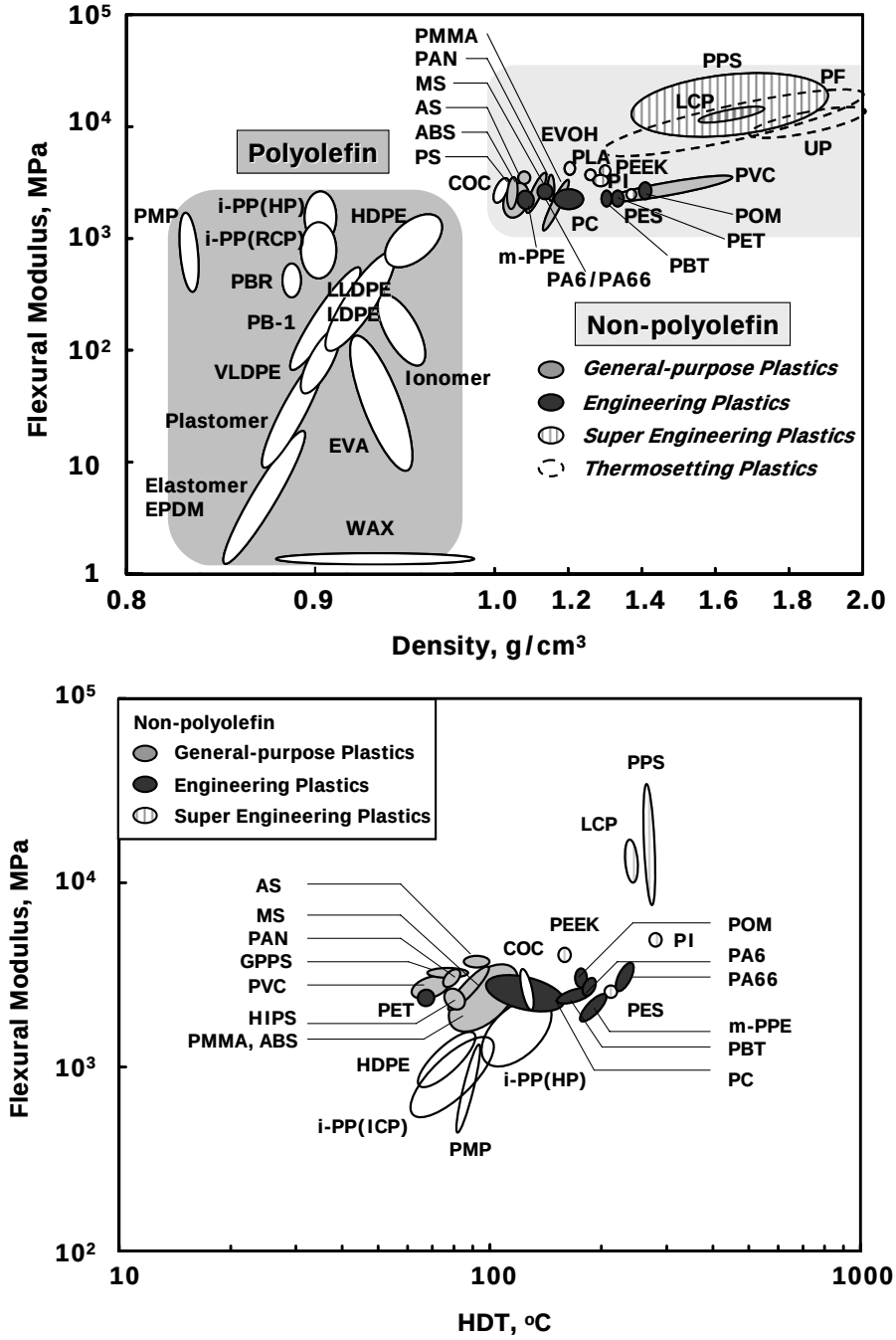

HDPE: high density PE, LDPE: low density PE, LLDPE: linear low density PE, VLDPE: very low density PE, i-PP(HP): isotactic PP, i-PP(RCP): propylene random copolymer, i-PP(ICP): propylene impact copolymer, PB-1: poly(1-butene), PMP: poly(4-methyl-1-pentene), EPDM: ethylene-propylene-diene terpolymer, PBR: propylene-butene copolymer, EVA: ethylene-vinyl acetate copolymer, COC: cyclic olefin copolymer, PMMA: poly(methyl methacrylate), PAN: polyacrylonitrile, MS: styrene-methyl methacrylate copolymer, AS: styrene-acrylonitrile copolymer, ABS: acrylonitrile-butadiene-styrene copolymer, PS: polystyrene, PVC: poly(vinyl chloride), HIPS: high impact PS, GPPS: general purpose PS, m-PPE: modified polyphenylene ether, PA6: 6-nylon, PA66: 6,6-nylon, PC: polycarbonate, PBT: polybutylene telephtalate, PET: polyethylene telephthalate, POM: polyoxymethylene, PI: polyimide, PEEK: polyether ether ketone, PES: poly(ether sulfone), PPS: polyphenylene sulfide, LCP: liquid crystalline polymer, PF: phenol resin, UP: unsaturated polyester, EVOH: ethylene-vinyl alcohol copolymer, PLA: polylactide.

Figure 3. Product ranges of leading commercial polymers in terms of flexural modulus and product density (upper figure) and in terms of flexural modulus and heat distortion temperature (lower figure).

3.1. Introduction of Functional Pendant Groups

The presence of functional groups in non-polar polyolefin chains imparts functionalized polyolefins with some novel functions and properties, such as adhesiveness, paintability, hydrophilicity, reactivity, etc. Several methods for preparation of functionalized polyolefins have been reported [40] and, in general they are divided broadly into two classes of approaches to the synthesis of functionalized polyolefins, namely, chain end functionalization and side chain functionalization as shown in Figure 4.

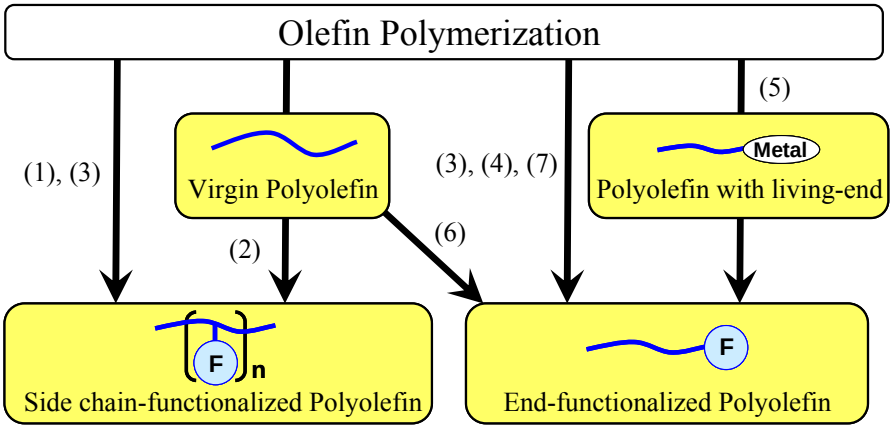

Functionalization Methods of Polyolefin
(1) Direct radical copolymerization of ethylene with polar monomers
(2) Radical grafting of polar monomers
(3) Transition-metal catalyzed copolymerization of olefin with polar monomers
(4) Chain transfer reaction by functional agents in olefin polymerization
(5) Olefin living polymerization and successive quenching with polar monomers
(6) Pyrolysis of polyolefin
(7) Chain transfer reaction with β-hydride elimination

Figure 4. Synthetic methods of functionalized polyolefins.

Direct radical copolymerization and radical grafting of polar monomers are the most common and industrially applicable methods to produce some functionalized polyolefins. For example, ethylene copolymers with polar monomers, such as vinyl acetate, ethyl acrylate and glycidyl methacrylate, are produced by direct radical copolymerization under high pressure. Radical grafting on polyolefins is also important, where polar monomers include methacrylates, acrylates and styrenes, among others [41-52]. In particular, maleic anhydride(MAH)-modified polyolefin [53] is well known as a commercially available functionalized polyolefin with a wide range of olefin compositions, MAH contents and molecular weight. The grafting-on method is

advantageous over the direct radical copolymerization, in that it is applicable to not only ethylenic but also propylenic and higher α-olefinic polymers. Because of its accessibility and high reactivity, MAH-modified polyolefins are widely used for various purposes such as additives, adhesives, coatings and reactive compatibilizers for polymer blends.

On the other hand, transition-metal-catalyzed olefin copolymerization with polar monomers has also been attracting much attention and has been attempted to produce new functionalized polyolefins with precisely controlled structure. Metallocene [54-85] or post-metallocene [86-100] catalyst systems have been employed with polar monomers such as (meth)acrylates and functional α-olefins with a methylene spacer, usually to give olefin/polar monomer random copolymers. It has been reported that kinds and contents of functional groups significantly affect their physical properties. Under some specific conditions, however, end-functionalized polyolefin can also form even in these copolymerizations. For example, Imuta *et al.* suggested that in ethylene/allyl alcohol copolymerization, the latter comonomer protected with a certain alkylaluminum compound acted as chain-transfer agent, resulting in terminally-hydroxylated polyethylene with high functionality [79]. In addition, it is well known that alkylaluminums [101,102], primary silanes ($RSiH_3$) [103-106], secondary boranes (R_2BH) [107,108], thiophene [109,110] and *p*-methylstyrene [111] act as efficient chain transfer agents in olefin polymerization to yield the polyolefins capped by the moiety of those chain transfer agents. End-functionalized polyolefin can be also obtained by olefin living polymerization and subsequent transformation of chain end. It has been reported the introduction of various functional groups into the chain end of the polypropylene prepared by living polymerization with a vanadium catalyst system. However, because of catalyst deactivation by functional groups, olefin polymerization in the presence of polar monomers or chain transfer agents using transition-metal catalysts still stop short of the commercial production of functionalized polyolefins.

Terminally-unsaturated polyolefin, which is prepared by pylolysis of polyolefin or chain transfer reaction with β-hydride elimination in metallocene or post-metallocene catalyzed polymerization, is also useful as one of the end-functionalized polyolefins with reactive C-C double bond and the precursor of the end-functionalized polyolefins with other functional groups. Such polyolefins possessing vinyl or vinylidene terminal are used as a macromonomer for olefin polymerization to give the branched polyolefins. In addition, these unsaturated structures can be converted to other functional groups, such as hydroxyl group, epoxy group, amino group, halide group, maleic anhydride group and so on [112-117].

3.2. Introduction of Functional Segments

Recent advances in polyolefin chemistry have led to the creation of polyolefin-based polymer hybrids, named "Polyolefin Hybrids", consisting of polyolefin segments and other polyolefin or polar polymer segments (Figure 5). In particular, the introduction of the functional segments prepared by polymerization of polar monomers into polyolefin backbone has been one of the most important research fields for polymer chemists [118-122] and these polyolefin hybrids with functional (polar) segments are expected as new value-added materials possessing unique and improved properties.

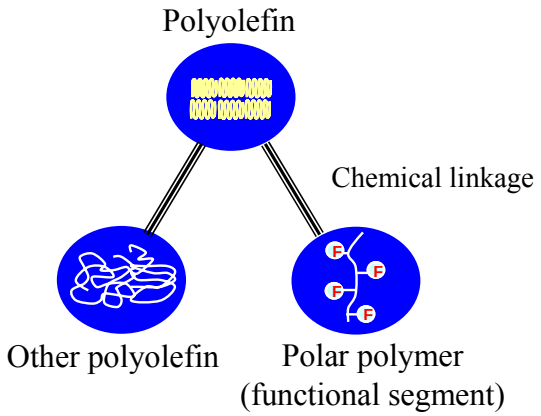

Figure 5. Polyolefin-based polymer hybrids, "*Polyolefin Hybrids*".

From an industrial point of view, the grafting method of polar segments by ionizing radiation (X-ray, γ-ray and *e*-beams) in the presence of air, ozone or UV as accelerators or radical initiators is well known as a useful method for polyolefin hybrids [51,52,123]. However, it had been difficult to obtain the well-defined polymer structures because of side reactions by radical species such as recombination, disproportionation, cross-linking and chain scission, resulting in loss of their properties. Alternatively, sequential living anionic polymerization of conjugated dienes and styrene has been also used to prepare the liner triblock copolymers such as polystyrene-*b*-polybutadiene-*b*-polystyrene (SBS), polystyrene-*b*-polyisoprene-*b*-polystyrene (SIS) and their hydrogenated copolymers, polystyrene-*b*-poly(ethylene-*co*-butylene)-*b*-polystyrene (SEBS) and polystyrene-*b*-poly(ethylene-*co*-propylene)-*b*- polystyrene (SEPS).

Another important method is the sequential living polymerization with vanadium [124] or lanthanide [125,126] catalysts, by which, for example, di- (AB-) and tri- (ABA-) block copolymers have been obtained for pairs of an α-olefin (ethylene, propylene, 1-pentene and 1-hexene) and a polar monomer (methyl methacrylate,

ε-caprolactone and tetrahydrofurane. However, the range of monomers and the polymerization conditions are generally restricted because these methods depend on polymerizations with water- and air-sensitive organometallic catalysts.

Given the difficulty in these in-situ or sequential methods, post-polymerization processes have been developed, which employ macroinitiators, macromonomers and pendant-functionalized polyolefins ("reactive polyolefins") that are to be prepared, purified and isolated before the subsequent use for final polyolefin hybrid production. Obviously, because of this additional isolation step, the post-polymerization approach is more cumbersome and sometimes more costly than the sequential synthesis, but it in turn offers an important advantage of freeing the scope of the synthesis from the serious confinement of available monomers as well as the stringent control of reaction conditions involved in the latter. These methodologies present a comprehensive scope of polyolefin hybrids, which can be classified into three general polymer structures: *block, graft and star copolymers* as shown in Figure 6.

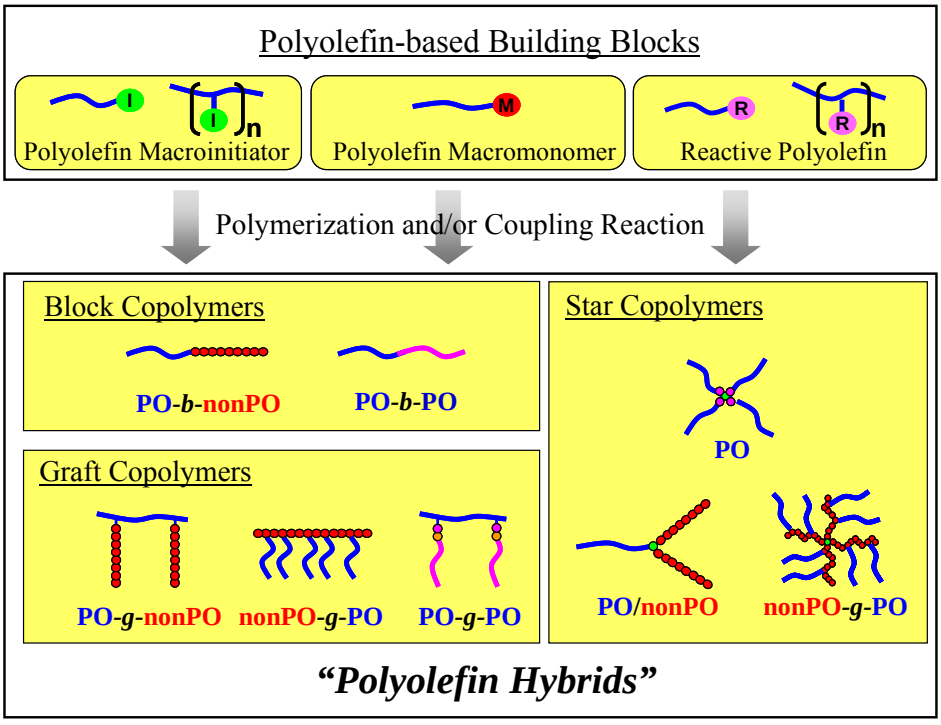

Figure 6. Creation of "*Polyolefin Hybrids*" with various topologies and compositions.

3.2.1. Polyolefin Macroinitiator

Polyolefin macroinitiator refers to a polyolefin that possesses a single or multiple initiation site(s) for living polymerization on its backbone, to be obtained by the functional-group transformation of polyolefins discussed above. A variety of polyolefin hybrids have been produced by the "macroinitiator" method, via living cationic [127,128], anionic [129-146] and radical [107,147-192] polymerizations as shown in Table 1.

Kennedy *et al.* reported that chlorobrominated poly(ethylene-*co*-propylene-*co*-1,4-hexadiene) employed as macroinitiator for cationic polymerization of styrene or isobutylene to give the corresponding graft copolymers. The methodology to synthesize polyolefin hybrids by living anionic polymerization has been also reported. For example, *p*-tolyl or styryl group containing polyolefins obtained by olefin copolymerization with *p*-methylstyrene or divinylbenzene can be converted to the macroinitiators possessing alkyllithium moieties for living anionic polymerization of styrene, methyl methacrylate or acrylonitrile to give the corresponding block and graft copolymers.

Polyolefins carrying pendant hydroxyl groups are also interesting precursors of macroinitiators. They can be synthesized by such methods as the oxidation of borane- or alkylaluminum-containing polyolefins and the coordination copolymerization of α-olefin and a hydroxylated olefin. The alcoholic functions therein are easily converted into aluminum or potassium alkoxides that, in turn, initiate living anionic polymerization of ε-caprolactone, ethylene oxide or propylene oxide.

In recent years, controlled radical polymerization (CRP) methods have extensively been developed. CRP is much expected as an attractive tool because of not only the controllability of polymerization but also the versatility of monomers and polymerization conditions. Chung *et al.* developed a peroxyborane-mediated radical polymerization using borane-containing polyolefins to give a variety of block [147-153] and graft copolymers [154-156] between polyolefins [*e.g.*, PE, PP or EPR] and polar polymers [*e.g.*, poly(methyl methacrylate)(PMMA), poly(*n*-butyl methacrylate)(PnBA), polyacrylonitrile (PAN) or polystyrene (PS)].

Nitroxide-mediated radical polymerization [193,194] is one of the most famous CRP methods and there are some reports about the synthesis of block [157,158] and graft copolymers [159-165] using alkoxyamine-containing macroinitiators. Some examples of introducing alkoxyamine moieties, such as 2,2,6,6-tetramethyl-1-piperidinyl-1-oxy (TEMPO), into a polyolefin backbone were reported. For example, Waymouth and Hawker *et al.* synthesized PP-*g*-PS graft copolymers with an alkoxyamine-functionalized PP [159].

Table 1. Overview of Polyolefin Hybrids Synthesized by Using Polyolefin Macroinitiators

	Macroinitiator (or Macro transfer agent)/catalyst	Obtained copolymers
Cationic polymerization	Chlorobrominated Nordel/alkylaluminum	Nordel-*g*-PS, Nordel-*g*-PS-*g*-PMS, Nordel-*g*-PS-*g*-PIB [127]
Anionic polymerization		
(Addition)	PP-*t*-MgBr	PP-*b*-PMMA [130,131]
	PE-*t*-MS/*sec*-BuLi, PP-*t*-MS/*sec*-BuLi	PE-*b*-PS [137], PP-*b*-PS [134]
	P(E-*co*-MS)/*sec*-BuLi	PE-*g*-PS, PE-*g*-PMS [132], PP-*g*-PBD, PP-*g*-PS
	P(P-*co*-MS)/*sec*-BuLi	PP-*g*-PMS, PP-*g*-PMMA, PP-*g*-PAN [133]
	P(E-*co*-DVB)/*sec*-BuLi, P(P-*co*-DVB)/*n*-BuLi	PE-*g*-PS [138], PP-*g*-PS [142]
	P(E-*co*-P-*co*-DVB)/*n*-BuLi, P(E-*co*-O-*co*-DVB)/*n*-BuLi	EP-*g*-PS [141], EO-*g*-PS [141]
	P(P-*co*-MS-*co*-E)/*sec*-BuLi	PP-*g*-PS [143,145]
(Ring-opening)	PE-*t*-OH/Et_3Al	PE-*b*-PLA [135]
	PE-*t*-OH/K^+, EO-*t*-OH/K^+, ES-*t*-OH/K^+	PE-*b*-PEG, EO-*b*-PEG, ES-*b*-PEG [136]
	PE-*t*-OH/$Sn(Oct)_2$	PE-*b*-PCL [139], PE-*b*-PLA [146]
	PE-*t*-OH/Et_2AlCl, PP-*t*-OH/Et_2AlCl	PE-*b*-PCL, PP-*b*-PCL [144]
	PP-*g*-OH/Et_3Al	PP-*g*-PCL [129]
	PE-*g*-OH/PZN, PE-*g*-OH/Et_3Al	PE-*g*-PPG, PE-*g*-PCL [140]
Radical polymerization		
(Borane)	PP-*t*-BR_2	PP-*b*-PMMA [147,148,150,153], PP-*b*-PEMA, PP-*b*-PMA, PP-*b*-PS [147], PP-*b*-SMA [149,151]
	PE-*t*-BR_2	PE-*b*-PMMA [107,152]
	PP-*g*-BR_2, PO-*g*-BR_2	PP-*g*-PMMA [150,155], PO-*g*-PMMA [154]
	EP-*g*-BR_2	EP-*g*-PMMA [156]
(Nitroxide)	PE-*t*-nitroxide	PE-*b*-PnBA [158]
	PP-*g*-TEMPO	PP-*g*-PS [159,160,162,164], PP-*g*-(St-*co*-BMA) [162]
	PE-*g*-TEMPO	PE-*g*-PS [161,163,164], PE-*g*-AS [161]
	EB-*g*-nitroxide	EB-*g*-PS, EB-*g*-(PS-*b*-PBD), EB-*g*-(PnBA-*b*-PS) EB-*g*-(PnBA-*b*-PBD) [165]
(RAFT)	PE-*t*-CTA, PEB-*t*-CTA	PE-*b*-PMMA [167], PEB-*b*-SMA [168]
	PP-*g*-CTA	PP-*g*-PS [169]
(Metal-catalyzed)	PEB-*t*-bromopropionate/Cu	PEB-*b*-PS, PEB-*b*-PAS, PEB-*b*-PHS [170]
	PEB-*t*-bromoisobutyrate/Cu	PEB-*b*-PMMA [174]
	HDPE film-*g*-tribromoethoxy/Ni	HDPE film-*g*-PMMA [177]
	PP film-*g*-bromide	PP film-*g*-PNIPAAm [179]
	PE-*g*-OOH/Fe-AIBN, PP-*g*-OOH/Fe-AIBN	PE-*g*-PMMA, PP-*g*-PMMA [180]
	PP-*t*-bromoisobutyrate/Cu	PP-*b*-PMMA[176, 187], PP-*b*-PnBA [176], PMMA-*b*-PP-*b*-PMMA, PS-*b*-PP-*b*-PS [192]
	PE-*t*-bromoisobutyrate/Cu	PE-*b*-PMMA [178,182], PE-*b*-PnBA[182,186,191], PE-*b*-PS [182,191], PE-*b*-PtBA [186]
	PP-*g*-chloroethylbenzene/Cu	PP-*g*-PMMA [142]
	EPDM-*g*-allylicBr/Cu	EPDM-*g*-PMMA [171]
	P(E-*co*-GMA)-*g*-chloroacetate/Cu P(E-*co*-GMA)-*g*-bromoisobutyrate/Cu	PE-*g*-PS, PE-*g*-PMMA [172]
	ES-*g*-benzylBr/Cu	ES-*g*-PS, ES-*g*-PMMA, ES-*g*-(PMMA-*b*-PS) ES-*g*-(PMMA-*b*-PHEMA), ES-*g*-(PMMA-*b*-PMA) [173]
	EVA-*g*-chloropropionate/Cu	EVA-*g*-PMMA [175]
	P(E-*co*-UnOH)-*g*-bromoisobutyrate/Cu	PE-*g*-PnBA [181,183], PE-*g*-PMMA [183]
	P(E-*co*-MS)-*g*-benzylBr/Cu	PE-*g*-PMMA, PE-*g*-PnBA [184]
	P(E-*co*-DVB)-*g*-bromoethylbenzene/Cu	PE-*g*-PMMA, PE-*g*-PS [185]
	P(P-*co*-ADMS)-*g*-chloride/Cu	PP-*g*-PMMA [188]
	P(E-*co*-BIEA)/Cu	P(E-*co*-BIEA)-*g*-PMMA [189]
	PB-*g*-bromoisobutyrate/Cu	PB-*g*-PtBA, PB-*g*-PAA [190]

Nordel: P(E-*co*-P-*co*-1,4-hexadiene) copolymer, PS: polystyrene, PMS: poly(*p*-methylstyrene), PIB: polyisobutylene, PMMA: poly(methyl methacrylate), MS: *p*-methylstyrene, PBD: poly(1,4-butadiene), PAN: polyacrylonitrile, DVB: 1,4-divinylbenzene, EP: ethylene-propylene random copolymer, EO: ethylene-octene random copolymer, PLA: polylactide, ES: ethylene-styrene random copolymer, PEG: poly(ethylene glycol), PCL: poly(ε-caprolactone), PZN: phosphazene catalyst, PPG: poly(propylene glycol), SMA: styrene-maleic anhydride copolymer, PEMA: poly(ethyl methacrylate), PMA: poly(methyl acrylate), PO: poly(1-octene), TEMPO: 2,2,6,6-tetramethyl-1-piperidinyl-1-oxy, BMA: PnBA: poly(n-butyl acrylate), AS: styrene-acrylonitrile random copolymer, EB: ethylene-1-butene random copolymer, PEB: poly(ethylene-co-butylene), CTA: chain transfer agent, PAS: poly(4-acetoxystyrene), PHS: poly(4-hydroxystyrene), PNIPAAm: poly(N-isopropylacrylamide), PtBA: poly(t-butyl acrylate), EPDM: ethylene-propylene-diene random copolymer, GMA: glycidyl methacrylate, PHEMA: poly(2-hydroxyethyl methacrylate), EVA: ethylene-vinyl acetate random copolymer, UnOH: 10-undecen-1-ol, ADMS: allyldimethylsilane, BIEA: 2-(2-bromoisobutyryloxy) ethyl acrylate, PAA: poly(acrylic acid)

Recently, reversible addition-fragmentation chain transfer (RAFT) polymerization [195-197] has been also applied to synthesize polyolefin hybrids. In the case of this method, polyolefins possessing RAFT-agent moieties including dithiocarbonate, dithiocarbamate, dithioester and trithiocarbonate act as not macroinitiator but chain transfer agent in the free-radical polymerization of polar monomers, resulting in the generation of the corresponding block [166,167] or graft [168,169] copolymers. Kawahara *et al.* reported that PE-*b*-PMMA block copolymer was synthesized by RAFT polymerization using chain transfer agent based on polyethylene, which was prepared by sequential functionalization of terminally-hydroxylated polyethylene [167].

Among CRP methods, "metal-catalyzed" living (or "atom transfer") radical polymerization, originally developed by Sawamoto and Matyjaszewski [198-200], is generally well known as one of the most attractive and convenient tools for synthesizing a variety of styrenic and/or (meth)acrylic block copolymers. The combination of this technique and the polyolefin macroinitiators realized to prepare a large number of polyolefin-based block and graft copolymers with precise control of their structure as shown in Table 1. For these, several specific halogenated structures are proposed as suitable initiators. Among them, α-haloesters are easily introduced into a polyolefin backbone, and there are many reports about the synthesis of polyolefin hybrids through the metal-catalyzed living radical polymerization with such macroinitiators. Other effective initiating groups include benzylic halide or allyl halides available for polyolefin macroinitiators.

3.2.2 Polyolefin Macromonomer

Polyolefin macromonomers are a class of polyolefins with a polymerizable chain end and useful to produce graft copolymers. Note that the "macromonomer" method leads to hybrids with polyolefin branches, just in contrast to the "macroinitiator" method, usually leading to those with a polyolefin backbone. The examples of preparing polyolefin hybrids by using polyolefin macromonomer are summarized in Table 2. For instance, polyolefin macromonomers with acryl or methacryl terminals can be employed as monomers for radical or ionic polymerization to give the graft copolymers consisting of a backbone of polar segment and one or more branches of polyolefin segment(s). Mülhaupt *et al.* employed a methacryloyl-capped polypropylene macromonomer to prepare PMMA-*g*-PP graft copolymers by conventional free radical copolymerization [201]. In this report, vinylidene-terminated PP was converted into the hydroxylated analogue (PP-*t*-OH) by hydroboration of the unsaturated group and subsequent oxidation reaction. Resulting PP-*t*-OH was allowed to react with

methacryloyl chloride to synthesize terminally-methacrylated PP. Matyjaszewski and Brookhart *et al.* reported the preparation of PnBA-*g*-PE graft copolymers using Pd-mediated olefin polymerization and controlled radical polymerization [202]. Living polymerization of ethylene with Pd α-diimine catalyst afforded highly branched PE macromonomers end-capped with methacryloyl group, which was then copolymerized with *n*-butyl acrylate by ATRP. The morphology of the resulting graft copolymers was analyzed by atomic force microscopy. Furthermore, Matyjaszewski *et al.* successfully synthesized several graft copolymers, such as PnBA-*g*-PE, poly(*t*-butyl acrylate)(PtBA)-*g*-PE, poly(acrylic acid)(PAA)-*g*-PE and PS-*g*-PE, by combination of degenerative transfer coordination polymerization and ATRP [203,204].

Table 2. Overview of Polyolefin Hybrids synthesized by Using Polyolefin Macromonomers

Synthetic method of func'd polyolefin	Macromonomer/catalyst or initiator	Obtained copolymers
Chain transfer	PP-MA/AIBN	PMMA-*g*-PP [201]
	PE-MA/Cu	PnBA-*g*-PE, PtBA-*g*-PE, PAA-*g*-PE [203]
	PE-MA/Cu	PS-*g*-PE [204]
Living polymerization	PE-MA/Cu	PnBA-*g*-PE [202]

PMMA: poly(methyl methacrylate), PnBA: poly(*n*-butyl acrylate), PtBA: poly(*t*-butyl acrylate), PAA: poly(acrylic acid)

3.2.3. Reactive Polyolefin

Reactive polyolefin having reactive functional groups is the most conventional building block to produce various copolymers with block and graft polymers as shown in Table 3. Typically, it is well known that MAH-modified polyolefins are useful as reactive polyolefin to prepare the polyolefin-based graft copolymers. For example, the coupling reactions of them with polar segments possessing some reactive functional groups give the corresponding graft copolymers, such as PE-*g*-PMMA, PP-*g*-PMMA [205], PP-*g*-polyamide [206], PP-*g*-polyester [207], PP-g-polyurethane [208] and PE-g-PEG [209]. It has been also reported that the reactive polyolefins possessing other reactive groups, such as halogen, epoxy, hydroxyl and amino groups, reacted with the end-functionalized polymers to produce PP-*b*-PCL [210], PP-*b*-PS [211], PP-*g*-PS [212] and PE-*g*-PS [213].

Table 3. Overview of Polyolefin Hybrids Synthesized by Using Reactive Polyolefins

Synthetic method of func'd polyolefin	Reactive polyolefin	Obtained copolymers
Radical graft	PP-*g*-AA, PP-*g*-MAH, PP-*g*-GMA	PP-*g*-PBT [207]
	PP-*g*-MAH	PP-*g*-PA [206], PP-*g*-PMMA [205]
	PP-*g*-MAH, PP-*g*-NH2, PP-*g*-NHR	PP-*g*-TPU [208]
Chain transfer	PP-*t*-OH, PP-*t*-NH2	PP-*b*-PCL [210]
	P(P-*co*-NB)-*t*-CHO	P(P-*co*-NB)-*b*-PS [211]
Copolymerization	P(E-*co*-MS)-*g*-MAH	P(E-*co*-MS)-*g*-PEG [209]
	P(E-*co*-GMA)	P(E-*co*-GMA)-*g*-PS [213]
	P(P-*co*-UnBr)	P(P-*co*-UnBr)-*g*-PS [212]
	P(E-*co*-MAH-*co*-MA)	P(E-*co*-MAH-*co*-MA)-*g*-PMMA [205]

AA: acrylic acid, MAH: maleic anhydride, GMA: glycidyl methacrylate, PBT: polybutylene telephtharate, PA: polyamide, PMMA: poly(methyl methacrylate), TPU: thermoplastic polyurethane, PCL: poly(ε-caprolactone), NB: norbornene, PS: polystyrene, MS: p-methystyrene, PEG: poly(ethylene glycol), UnBr: 11-bromo-1-undecene, MA: methyl acrylate

3.3. Properties and Application of Polyolefin Hybrids

In general, block and graft copolymers, where multiple polymer segments are liked together, have recently received much attention due to not only the scale of the microdomains (about tens of nanometers), their various chemical and physical properties but also the convenient size- and shape-tunability of microdomains to be achieved by simply changing their architecture and compositions [214]. Similarly, polyolefin hybrids exhibit nano-scale phase separated morphology derived from both olefinic and polar segments (Figure 7). For example, Matsugi *et al.* reported that, in PP-*b*-PMMA block copolymers, both segments were dispersed in a nanometer scale, much finer than those in PP/PMMA blends, and that its morphology varied depending on the monomer compositions [177].

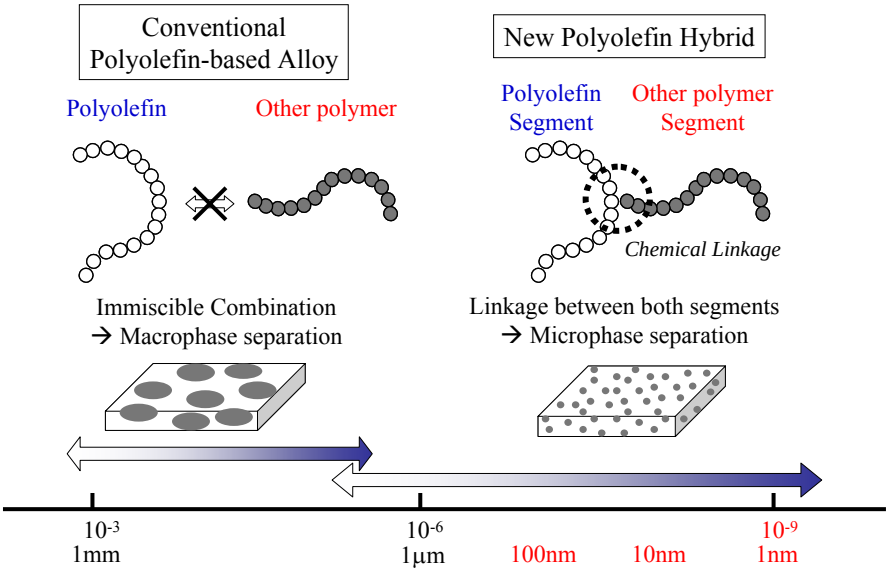

Figure 7. Opportunity for new polyolefin-based nano-structure controlled materials.

Thus, specific morphology provides polyolefin hybrids with some improved and unique properties which conventional polyolefin cannot have. Figure 8 shows the functions which could be achieved by hybridization between polyolefin and functional segments. For example, rigid segments, such as PMMA and PS, will increase the stiffness of base olefin polymer; the elastomeric and low glass-transition segments, such as EPR, EBR and PnBA, will enhance the toughness. Namely, the introduction of these segments into polyolefin is mainly expected to improve the physical properties of polyolefin and thereby to expand applications as structural materials.

In addition, some of the polar segments by radical or anionic polymerization have distinguishing characteristics, such as adhesiveness, electrical conductivity, hydrophilicity, paintability, biocompatibility, stimuli-sensitivity and so on. Therefore, polyolefins with these unique properties have long been strongly desired and expected to broaden their application in a functional materials field. Furthermore, since such polyolefin hybrids potentially improve the interfacial interaction between polyolefin and other polar materials, they are also expected to act as modifier or compatibilizer for polyolefins or polar polymers. Although there is not much report on the properties of polyolefin hybrids so far, a number of them are expected to emerge more and more with the future progress of their studies.

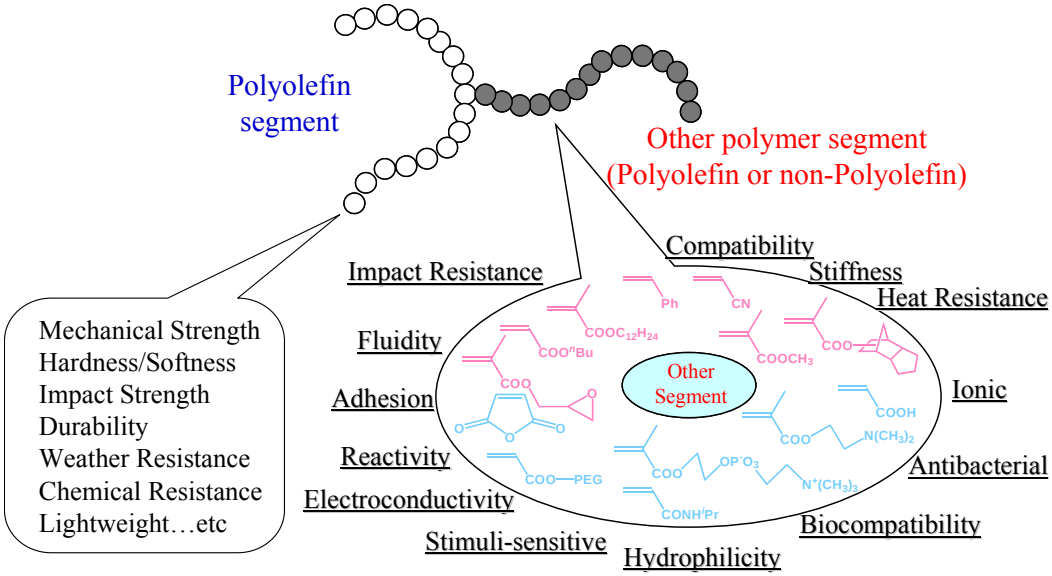

Figure 8. Various functions of polyolefin hybrids.

4. Outline of This Thesis

Under the background described above, the author has studied the polyolefin-based polymer hybrids linking other polyolefin or polar segments, so-called "Polyolefin Hybrids". This thesis thus consists of seven Chapters in three Parts, concerning the syntheses and characterization of polyolefin hybrids by a combination of functionalized polyolefins as three kinds of building blocks and controlled post-polymerization techniques (Figure 9). Furthermore, their unique and excellent properties are also discussed.

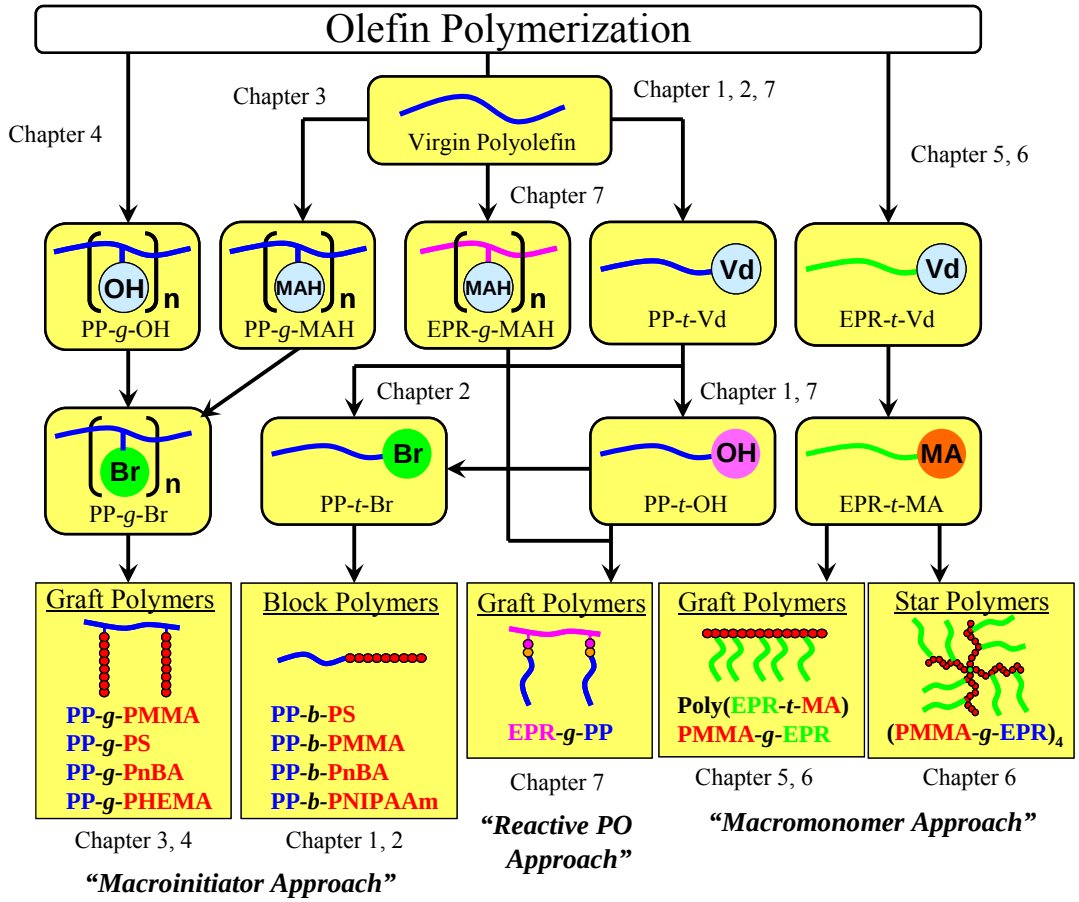

Figure 9. Overview of this thesis.

PART I concerns the synthesis and utilization of polyolefin macroinitiators.

In ***Chapter 1***, terminal-typed PP macroinitiators were prepared by a series of end functionalization of commercially-available pyrolysis PP with the vinylidene end group via hydroalumination, oxidation, and esterification. By using these PP macroinitiators, controlled radical polymerizations of MMA or *N*-isopropylacrylamide (NIPAAm) were

carried out to give PP-*b*-PMMA and PP-*b*-PNIPAAm block copolymers. From TEM observation of the block copolymers, the microphase-separation morphology at the nanometer level between PP and PNIPAAm segments was observed and its morphology was remarkably altered by the length of the attached PNIPAAm segment.

Chapter 2 includes new synthetic method of terminal-typed PP macroinitiator prepared by a direct allylic bromination of the terminally-unsaturated PP using *N*-bromosuccinimide. The brominated PP was employed as a macroinitiator for controlled radical polymerization of styrene, methyl methacrylate and *n*-butyl acrylate using a copper catalyst system. From ^{1}H NMR analysis, it was confirmed that the chain extension polymerization was certainly initiated from allylic bromide moieties with high efficiency, leading to the PP-based block copolymers. Thus obtained block copolymers demonstrated the unique thermal properties and morphological features due to the microphase separation between both segments. This new synthetic method is simpler and more facile than the other methods for synthesis of polyolefin hybrids.

In ***Chapter 3***, branch-typed PP macroinitiator was prepared by the reaction between commercially-available maleic anhydride-modified PP and ethanolamine and the subsequent reaction with 2-bromoisobutyryl bromide. Controlled radical polymerization of MMA or 2-hydroxyethyl methacrylate (HEMA) with PP macroinitiator was carried out to give the corresponding PP-PMMA or PP-PHEMA hybrids. These hybrids demonstrated microphase-separation morphology or core-shell-like morphology at the nanometer level. In addition, the PP-PHEMA hybrid showed a good affinity with water due to the hydrophilicity of the PHEMA segments.

Chapter 4 describes the evaluation of the mechanical properties of PP-based graft copolymers linking PMMA, PnBA and PS, which can be prepared by controlled radical polymerization with branch-typed PP macroinitiator derived from hydroxylated PP. The flexural and Izod impact tests revealed that the incorporation of PMMA and PS segments into PP backbone effectively enhanced stiffness and concerning PnBA segment remarkably improved toughness. This is a first report about the mechanical properties of polyolefin hybrids produced by controlled radical polymerization.

PART II concerns the synthesis and utilization of polyolefin macromonomers.

In ***Chapter 5***, methacryloyl-terminated propylene-ethylene random copolymers (PERs) were prepared by the sequential transformation of vinylidene-terminated PERs

and worked as macromonomer to give the polymacromonomer with PER branches. The obtained polymacromonomer could be successfully isolated by liquid chromatography and characterized by ^{1}H and ^{13}C NMR analyses and GPC measurement. In addition, the specific relationship between molecular weight and viscosity of the polymacromonomer was discussed. This is a first report about polyolefin-based polymacromonomer.

In ***Chapter 6***, graft and star copolymers having poly(methyl methacrylate) (PMMA) backbone and ethylene-propylene random copolymer (EPR) branches were successfully synthesized by controlled radical polymerization of EPR macromonomer and methyl methacrylate. GPC measurement and NMR analysis revealed that EPR contents and EPR branch numbers were well controlled. From transmission electron microscopy of the obtained copolymers, EPR and PMMA segments were well-dispersed each other and the morphology varied depending on the topology and composition of the copolymers. Moreover, thermal properties and compatibilizing effect of the obtained copolymers were also investigated.

PART III concerns the synthesis and utilization of reactive polyolefin.

Chapter 7 includes the synthesis and utilization of reactive polyolefin. Terminally-hydroxylated isotactic polypropylenes (PP-OHs) were synthesized via oxidation of Al-functionalized PP obtained by predominant chain transfer reaction with triethylaluminum or hydroalumination of pyrolysis PP. Thus obtained PP-OHs reacted with ethylene-propylene random copolymer possessing maleic anhydride groups (EPR-MAH) to give polymer hybrids consisting of PP and EPR segments. These polymer hybrids demonstrated unique nano-order phase separation morphology and worked as compatibilizer for PP/EPR polymer blend.

References

[1] British Patent 471 590, ICI.
[2] Ziegler, K.; Gellert, H. G.; Zosel, K.; Lehmkuhl, W.; Pfohl, W. Angew Chem 1955, 67, 424.
[3] Ziegler, K.; Holzkamp, E.; Breil, H.; Martin, H. Angew Chem 1955, 67, 541-547.
[4] Natta, G. J Polym Sci 1955, 16, 143-154.
[5] Natta, G. J Am Chem Soc 1955, 77, 1707-1708.
[6] Natta, G.; Pino, P.; Mazzanti, G. Chim Ind (Milan) 1955, 37, 927.
[7] Kashiwa, N.; Tokuzumi, T.; Fujimura, H. U.S. Patent, 3642746(1968).
[8] Luciani, L.; Kashiwa, N.; Barbe, P. C.; Toyota, A. Japanese Patent, Kokai, 52-151691(1975).
[9] Spitz, R.; Bobichon, C.; Guyot, A. Macromol Chem 1989, 190, 707-716.
[10] Forte, M. C.; Boutinho, F. M. B. Eur Polym J 1996, 32, 605-611.
[11] Natta, G. Chim Ind (Milan) 1957, 39, 653.
[12] Sinn, H.; Kaminsky, W. Adv Organomet Chem 1980, 18, 99-149.
[13] Sinn, H.; Kaminsky, W.; Vollmer, H. J.; Woldt, R. Angew Chem Int Ed Engl 1980, 19, 390-392.
[14] Johnson, L. K.; Killian, C. M.; Brookhart, M. S. J Am Chem Soc 1995, 117, 6414-6415.
[15] Saito, J.; Mitani, M.; Mohri, J.; Yoshida, Y.; Matsui, S.; Ishii, S.; Kojoh, S.; Kashiwa, N.; Fujita, T. Angew Chem Int Ed 2001, 40, 2918-2920.
[16] Kojoh, S.; Matsugi, T.; Saito, J.; Mitani, M.; Fujita, T.; Kashiwa, N. Chem Lett 2001, 822-823.
[17] Ono, S. S.; Matsugi, T.; Matsuoka, O.; Kojoh, S.; Fujita, T.; Kashiwa, N.; Yamamoto, S. Chem Lett 2003, 1182-1183.
[18] Matsugi, T.; Matsui, S.; Kojoh, S.; Takagi, Y.; Inoue, Y.; Nakano, T.; Fujita, T.; Kashiwa, N. Macromolecules 2002, 35, 4880-4887.
[19] Mitani, M.; Mohri, J.; Yoshida, Y.; Saito, J.; Ishii, S.; Tsuru, K.; Matsui, S.; Furuyama, R.; Nakano, T.; Tanaka, H.; Kojoh, S.; Matsugi, T.; Kashiwa, N.; Fujita, T. J Am Chem Soc 2002, 124, 3327-3336.
[20] Weiser, M. –S,; Thomann, Y.; Heinz, L. –C.; Pasch, H.; Mülhaupt, R. Polymer 2006, 47, 45054512.
[21] Furuyama, R.; Mitani, M.; Mohri, J.; Mori, R.; Tanaka, H.; Fujita, T. Macromolecules 2005, 38, 1546-1552.
[22] Ruokolainen, J.; Mezzenga, R.; Fredrickson, G. H.; Kramer, E. J.; Hustad, P. D.;

Coates G.W.; Macromolecules 2005, 38, 851-860.
[23] Tian, J.; Hustad, P. D.; Coates, G. W. J Am Chem Soc 2001, 123, 5134-5135.
[24] Junghanns, V. E.; Gumboldt, A.; Bier, G. Maklomol Chem 1962, 58, 18-42.
[25] Verstrate, G. W.; Cozewith, C.; Pacansky, T. J.; Davis, W. M.; Rangarajan, P. US patent 6,110,880 (2000).
[26] Arriola, D. J.; Carnahan, E. M.; Hustad, P. D.; Kuhlman, R. L.; Wenzel, T. T. Science 2006, 312, 714-719.
[27] Wang, H. P.; Khariwala, D. U.; Cheung, W.; Chum, S. P.; Hiltner, A.; Baer, E. Macromolecules 2007, 40, 2852-2862.
[28] Hustad, P. D.; Kuhkman, R. L.; Arriola, D. J.; Carnahan, E. M.; Wenzel, T. T. Macromolecules 2007, 40, 7061-7064.
[29] Shan, C. L. P.; Hazliu, L. G. Macromol Symp 2007, 257, 80-93.
[30] Khariwala, D. U.; Taha, A.; Chum, S. P.; Hiltner, A.; Baer, E. Polymer 2008, 49, 1365-1375.
[31] Patent WO90/07526 (1990), Mitsui Chemicals.
[32] Yan, D.; Wang, W. J.; Zhu, S. Polymer 1999, 40, 1737-1744.
[33] Kashiwa, N.; Kojoh, S.; Matsuo, M.; Takahashi, M.; Tsutsui, T.; Fujita, T. ACS Polymeric Materials: Sci. & Eng., 2001, 84, 112-113.
[34] Yamaguchi, M.; Wagner, M. H. Polymer 2006, 47, 3629-3635.
[35] Shiono, T.; Azad, S. M.; Ikeda, T. Macromolecules 1999, 32, 5723-5727.
[36] Langston, J. A.; Colby, R. H.; Chung, T. C. M.; Shimizu, F.; Suzuki, T.; Aoki, M. Macromolecules 2007, 40, 2712-2720.
[37] Guan, Z.; Cotts, P. M.; McCord, E. F.; McLain, S. J. Science 1999, 283, 2059-2062.
[38] Ye, Z.; Zhu, S. Macromolecules 2003, 36, 2194-2197.
[39] Ye, Z.; AlObaidi, F.; Zhu, S. Macromol Chem Phys 2004, 205, 897-906.
[40] Yanjarappa, M. J.; Sivaram, S. Prog Polym Sci 2002, 27, 1347-1398.
[41] Mehta, I. K.; Kumar, S.; Chauhan, G. S.; Misra, B. N. J Appl Polym Sci 1990, 41, 1171-1180.
[42] Singh, R. P. Prog Polym Sci 1992, 17, 251-281.
[43] Vito, G. D.; Lanzetta, N.; Maglio, G.; Malinconico, M.; Musto, P.; Palumbo, R. J Polym Sci Polym Chem Ed 1984, 22, 1335-1347.
[44] Greco, R.; Maglio, G.; Musto, P. V. J Appl Polym Sci 1987, 33, 2513-2527.
[45] Ruggeri, G.; Aglietto, M.; Petragnani, A.; Ciardelli, F. Eur Polym J 1983, 19, 863-866.
[46] Cartier, H.; Hu, G. -H. J Polym Sci Part A: Polym Chem 1998, 36, 1053-1063.

[47] Zhang, X.; Yin, Z.; Li, L.; Yin, J. J Appl Polym Sci 1996, 61, 2253-2257.
[48] Gallucci, R. R.; Going, R. C. J Appl Polym Sci 1982, 27, 425-437.
[49] Ho, R. M.; Su, A. C.; Wu, C. H.; Chen, S. I. Polymer 1993, 34, 3264-3269.
[50] Sun, Y. –J.; Hu, G. –H.; Lambla, M. J Appl Polm Sci 1995, 57, 1043-1054.
[51] Moad, G. Prog Polym Sci 1999, 24, 81-142.
[52] Rätzsch, M.; Arnold, M.; Borsig, E.; Bucka, H.; Reichelt, N. Prog Polym Sci 2002, 27, 1195-1282.
[53] Yang, L.; Zhang, F.; Endo, T.; Hirotsu, T. Macromolecules 2003, 36, 4709-4718.
[54] Ramakrishnan, S.; Berluche, E.; Chung, T. C. Macromolecules 1990, 23, 378-382.
[55] Chung, T. C.; Rhubright, D. Macromolecules 1991, 24, 970-972.
[56] Kesti, M. R.; Coates, G. W.; Waymouth, R. M. J Am Chem Soc 1992, 114, 9679-9680.
[57] Chung, T. C.; Rhubright, D. Macromolecules 1993, 26, 3019-3025.
[58] Wilén, C. –E.; Näsman, J. H. Macromolecules 1994, 27, 4051-4057.
[59] Aaltonen, P.; Löfgren, B. Macromolecules 1995, 28, 5353-5357.
[60] Chung, T. C.; Lu, H. L.; Li, C. L. Polym Int 1995, 37, 197-205.
[61] Aaltonen, P; Fink, G. Macromolecules 1996, 29, 5255-5260.
[62] Wilén, C. –E.; Luttikhedde, H.; Hjertberg, T.; Näsman, J. H. Macromolecules 1996, 29, 8569-8575.
[63] Aaltonen, P.; Löfgren, B. Eur Polym J 1997, 33, 1187-1190.
[64] Tsuchida, A.; Bolln, C.; Sernetz, F. G.; Frey, H.; Mülhaupt, R. Macromolecules 1997, 30, 2818-2824.
[65] Bruzaud, S.; Cramail, H.; Duvignac, L.; Defieux, A. Macromol Chem Phys 1997, 198, 291-303.
[66] Schneider, M. J.; Schäfer, R.; Mülhaupt, R. Polymer 1997, 38, 2455-2459.
[67] Hakala, K.; Löfgren, B.; Helaja, T. Eur Polym J 1998, 34, 1093-1097.
[68] Stehling, U. M.; Stein, K. M.; Kesti, M. R.; Waymouth, R. M. Macromolecules 1998, 31, 2019-2027.
[69] Goretzki, R.; Fink, G. Macromol Rapid Commun 1998, 19, 511-515.
[70] Stehling, U. M.; Stein, K. M.; Fischer, D.; Waymouth, R. M. Macromolecules 1999, 32, 14-20.
[71] Goretzki, R.; Fink, G. Macromol Chem Phys 1999, 200, 881-886.
[72] Marques, M. M.; Correia, S. G.; Ascenso, J. R.; Ribeiro, A. F. G.; Gomes, P. T.; Dias, A. R.; Foster, P.; Rausch, M. D.; Chien, J. C. W. J Polym Sci Part A Polym Chem 1999, 37, 2457-2469.
[73] Hakala, K.; Helaja, T.; Löfgren, B. J Polym Sci Part A: Polym Chem 2000, 38,

1966-1971.

[74] Wilén, C. –E.; Auer, M.; Strandén, J.; Näsman, J. H. Macromolecules 2000, 33, 5011-5026.

[75] Kaya, A.; Jakisch, L.; Komber, H.; Pompe, G.; Pionteck, J.; Voit, B.; Schulze, U. Macromol Rapid Commun 2000, 21, 1267-1271.

[76] Imuta, J.;Toda, Y.; Kashiwa. N. Chem Lett 2001, 30, 710-711.

[77] Hagihara, H.; Murata, M.; Uozumi, T. Macromol Rapid Commun 2001, 22, 353-357.

[78] Kaya, A.; Jakisch, L.; Komber, H.; Voigt, D.; Pionteck, J.; Voit, B.; Schulze, U. Macromol Rapid Commun 2001, 22, 972-977.

[79] Imuta, J.; Kashiwa, N.; Toda, Y. J Am Chem Soc 2002, 124, 1176-1177.

[80] Imuta, J.; Toda, Y.; Matsugi, T.; Kaneko, H.; Matsuo, S.; Kojoh, S.; Kashiwa, N. Chem Lett 2003, 32, 656-657.

[81] Hagihara, H.; Tsuchihara, K.; Sugiyama, J.; Takeuchi, K.; Shiono, T. Macromolecules 2004, 37, 5145-5148.

[82] Lipponen, S.; Seppälä, J. J Polym Sci Part A: Polym Chem 2005, 43, 5597-5608.

[83] Huang, Y.; Yang, K.; Dong, J. –Y. Macromol Rapid Commun 2006, 27, 1278-1283.

[84] Cerrada, M. L.; Benavente, R.; Pérez, E.; Moniz-Santos, J,; Campos, J. M.; Ribeiro, M. R. Macromol Chem Phys 2007, 208, 841-850.

[85] Hagihara, H.; Ishihara, T.; Ban, H. T.; Shiono, T. J Polym Sci Part A: Polym Chem 2008, 46, 1738-1748.

[86] Johnson, L. K.; Mecking, S.; Brookhart, M. J Am Chem Soc 1996, 118, 267-268.

[87] Mecking,†S.; Johnson, L. K.; Wang, L.; Brookhart, M. J Am Chem Soc 1998, 120, 888-899.

[88] Correia, S. G.; Marques, M. M.; Ascenso, J. R.; Ribeiro, A. F. G.; Gomes, P. T.; Dias, A. R.; Blais, M.; Rausch, M. D.; Chien, J. C. W. J Polym Sci Part A: Polym Chem 1999, 37, 2471-2480.

[89] Marques, M. M.; Fernandes, S.; Correia, S. G.; Ascenso, J. R.; Caroço, S.; Gomes, P. T.; Mano, J.; Pereira, S. G.; Nunes, T.; Dias, A. R.; Rausch, M. D.; Chien, J. C. W. Macromol Chem Phys 2000, 201, 2464-2468.

[90] Fernandes, S.; Marques, M. M.; Correia, S. G.; Mano, J.; Chien, J. C. W. Macromol Chem Phys 2000, 201, 2566-2572.

[91] Marques, M. M.; Fernandes, S.; Correia, S. G.; Caroço, S.; Gomes, P. T.; Dias, A. R.; Mano, J.; Rausch, M. D.; Chien, J. C. W. Polym Int 2001, 50, 579-587.

[92] Chien, J. C. W.; Fernandes, S.; Correia, S. G.; Rausch, M. D.; Dickson, L. C.;

Marques, M. M. Polym Int 2002, 51, 729-737.

[93] Zhang, X.; Chen, S.; Li, H.; Zhang, Z.; Lu, Y.; Wu, C.; Hu, Y. J Polym Sci Part A: Polym Chem 2005, 43, 5944-5952.

[94] Carlini, C.; Luise, V. D.; Martinelli, M.; Galletti, A. M. R.; Sbrana, G. J polym Sci Part A: Polym 2006, 44, 620-633.

[95] Baugh, L. S.; Sissano, J. A.; Kacker, S.; Berluche, E.; Stibrany, R. T.; Schlz, D. N.; Rucker, S. P. J Polym Sci Part A: Polym Chem 2006, 44, 1817-1840.

[96] Zhang, X.; Chen, S.; Li, H.; Zhang, Z.; Lu, Y.; Wu, Chunhong, Hu, Y. 2007, 45, 59-68.

[97] Galletti, A. M. R. G.; Carlini, C.; Giaiacopi, S.; Martinelli, M.; Sbrana, G. J Polym Sci Part A: Polym Chem 2007, 45, 1134-1142.

[98] Carone, C. L. P.; Crossetti, G.; Basso, N. R. S.; Moraes, A. G. O.; Dos Santos, J. H. Z.; Bisatto, R.; Galland, G. B. J Polym Sci Part A: Polym Chem 2007, 45, 5199-5208.

[99] Skupov, K. M.; Marella, P. R.; Simard, M.; Yap, G. P. A; Allen, N.; Conner, D; Goodall, B. L.; Claverie, J. P. Macromol Rapid Commun 2007, 28, 2033-2038.

[100] Carone, C. L. P.; Bisatto, R.; Galland, G. B.; Rojas, R.; Bazan, G. J Polym Sci Part A: Polym Chem 2008, 46, 54-59. Fullana, M. J.; Miri, M. J.; Vadhavkar, S. S.; Kolhatkar, N.; Delis, A. C. J Polym Sci Part A: Polym Chem 2008, 46, 5542-5558.

[101] Shiono, T.; Soga, K. Macromolecules 1992, 25, 3356-3361.

[102] Shiono, T.; Kurosawa, H.; Soga, K. Makromol Chem 1993, 193, 2751-2761.

[103] Fu, P. F.; Marks, T. J. J Am Chem Soc 1995, 117, 10747-10748.

[104] Koo, K.; Marks, T. J. J Am Chem Soc 1998, 120, 4019-4020.

[105] Koo, K.; Fu, P. –F.; Marks, T. J. Macromolecules 1999, 32, 981-988.

[106] Koo, K.; Marks, T. J. J Am Chem Soc 1999, 121, 8791-8802.

[107] Xu, G.; Chung, T. C. J Am Chem Soc 1999, 121, 6763-6764.

[108] Xu, G.; Dong, J. Y.; Chung, T. C. Polym Prepr 2000, 41, 1926-1927.

[109] Ringelberg, S. N.; Meetsma, A.; Hessen, B.; Teuben, J. H. J Am Chem Soc 1999, 121, 6082-6083.

[110] Hessen, B.; Ringelberg, S. N.; Meppelder, G. J.; Teuben, J. H. Polym Prepr 2000, 41, 397-398.

[111] Chung, T. C.; Dong, J. Y. J Am Chem Soc 2001, 123, 4871-4876.

[112] Mülhaupt, R.; Duschek, T.; Rieger, B. Macromol Chem Macromol Symp 1991, 48/49, 317-332.

[113] Shiono, T.; Soga, K. Macromol Chem Rapid Commun 1992, 13, 371-376.

[114] Shiono, T.; Kurosawa, H.; Ishida, O.; Soga, K. Macromolecules 1993, 26, 2085-2089.
[115] Shiono, T.; Kurosawa, H.; Soga, K. Macromolecules 1994, 27, 2635-2637.
[116] Wörner, C.; Rösch, J.; Höhn, A.; Mülhaupt, R. Polym Bull 1996, 36, 303-309.
[117] Tsubaki, S.; Jin, J.; Sano, T.; Uozumi, T.; Soga, K. Macromol Chem Phys 2001, 202, 1757-1760.
[118] Schellekens, M. A. J.; Klumperman, B. J Macromol Sci Rev Macromol Chem Phys 2000, C40, 167-192.
[119] Chung, T. C. Prog Polym Sci 2002, 27, 39-85.
[120] Dong, J. –Y.; Hu, Y. Coord Chem Rev 2006, 250, 47-65.
[121] Lopez, R. G.; D'Agosto, F.; Boisson, C. Prog Polym Sci 2007, 32, 419-454.
[122] Kawahara, N.; Saito, J.; Matsuo, S.; Kaneko, H.; Matsugi, T.; Kashiwa, N. Adv Polym Sci 2008, 217, 79-119.
[123] Yamamoto, T.; Aoshima, K.; Ohmura, H.; Moriya, Y.; Suzuki, N.; Oshibe, Y. Polymer 1991, 32, 19-28.
[124] Doi, Y.; Watanabe, Y.; Ueki, S.; Soga, K. Makromol Chem Rapid Commun 2003, 4, 533-537.
[125] Yasuda, H.; Furo, M.; Yamamoto, H. Macromolecules 1992, 25, 5115-5116.
[126] Desurmont, G.; Tokimitsu, T.; Yasuda, H. Macromolecules 2000, 33, 7679-7681.
[127] Kennedy, J. P.; Vidal, A. J Polym Sci Polym Chem Ed 1975, 13, 1765-1781.
[128] Kennedy, J. P.; Vidal, A. J Polym Sci Polym Chem Ed 1975, 13, 2269-2276.
[129] Chung, T. C.; Rhubright, D. Macromolecules 1994, 27, 1313-1319.
[130] Shiono, T.; Akino, Y.; Soga, K. Macromolecules 1994, 27, 6229-6231.
[131] Shiono, T.; Akino, Y.; Soga, K. Stud Surf Sci Catal 1994, 89, 119-128.
[132] Chung, T. C.; Lu, H. L.; Ding, R. D. Macromolecules 1997, 30, 1272-1278.
[133] Lu, H. L.; Chung, T. C. J Polym Sci Part A: Polym Chem 1999, 37, 4176-4183.
[134] Chung, T. C.; Dong, J. Y. J Am Chem Soc 2001, 123, 4871-4876.
[135] Wang, Y.; Hillmyer, M. A. J Polym Sci Part A: Polym Chem 2001, 39, 2755-2766.
[136] Lu, Y.; Hu, Y.; Wang, Z. M.; Manias, E.; Chung, T. C. J Polm Sci Part A: Polym Chem 2002, 40, 3416-3425.
[137] Dong, J. Y.; Chung, T. C. Macromolecules 2002, 35, 1622-1631.
[138] Chung, T.C.; Dong, J. Y. Macromolecules 2002, 35, 2868-2870.
[139] Han, C. J.; Lee, M. S.; Byun, D. J.; Kim, S. Y. Macromolecules 2002, 35, 8923-8925.
[140] Kashiwa, N.; Matsugi, T.; Kojoh, S.; Kaneko, H.; Kawahara, N.; Matsuo, S.; Nobori, T.; Imuta, J. J Polym Sci Part A: Polym Chem 2003, 41, 3657-3666.

[141] Dong, J. Y.; Hong, H.; Chung, T. C.; Wang, H. C.; Datta, S. Macromolecules 2003, 36, 6000-6009.
[142] Zou, J.; Cao, C.; Dong, J. –Y.; Hu, Y.; Chung, T. –C. Macromol Rapid Commun 2004, 25, 1797-1804.
[143] Caporaso, L.; Iudici, N.; Oliva, L. Macromolecules 2005, 38, 4894-4900.
[144] Lu, Y; Hu, Y.; Chung, T. C. Polymer 2005, 46, 10585-10591.
[145] Caporaso, L.; Iudici, N.; Oliva, L. Macromol Symp 2006, 234, 42-50.
[146] Ring, J. O.; Thomann, R.; Mülhaupt, R.; Raquez, J. –M.; Degée, P.; Dubois, P. Macromol Chem Phys 2007, 208, 896-902.
[147] Chung, T. C.; Lu, H. L. J Mol Cat A: Chem 1997, 115, 115-127.
[148] Chung, T. C.; Lu, H. L.; Janvikul, W. Polymer 1997, 38, 1495-1502.
[149] Lu, B.; Chung, T. C. Macromolecules 1998, 31, 5943-5946.
[150] Chung, T. C.; Janvikul, W. J Organomet Chem 1999, 581, 176-187.
[151] Lu, B.; Chung, T. C. Macromolecules 1999, 32, 2525-2533.
[152] Chung, T. C.; Xu, G.; Lu, Y.; Hu, Y. Macromolecules 2001, 34, 8040-8050.
[153] Fan, G.; Dong, J. –Y.; Wang, Z.; Chung, T. C. J Polym Sci Part A: Polym Chem 2006, 44, 539-548.
[154] Chung, T. C.; Jiang, G. J. Macromolecules 1992, 25, 4816-4818.
[155] Chung, T. C.; Rhubright, D.; Jiang, G. J. Macromolecules 1993, 26, 3467-3471.
[156] Chung, T. C.; Janvikul, W.; Bernard, R.; Jiang, G. J. Macromolecules 1994, 27, 26-31.
[157] Lopez, R. G.; Boisson, C.; D'Agosto, F.; Spitz, R.; Boisson, F.; Bertin, D.; Tordo, P. Macromolecules 2004, 37, 3540-3542.
[158] Lopez, R. G.; Boisson, C.; D'Agosto, F.; Spitz, R.; Boisson, F.; Gigmes, D.; Bertin, D. J Polym Sci Part A Polym Chem 2007, 45, 2705-2718.
[159] Stehling, U. M.; Malmström, E. E.; Waymouth, R. M.; Hawker, C. J. Macromolecules 1998, 31, 4396-4398.
[160] Miwa, Y.; Yamamoto, K.; Sakaguchi, M.; Shimada, S. Macromolecules 1999, 32, 8234-8236.
[161] Baumert, M.; Heinemann, J.; Thomann, R.; Mülhaupt, R. Macromol Rapid Commun 2000, 21, 271-276.
[162] Miwa, Y.; Yamamoto, K.; Sakaguchi, M.; Shimada, S. Macromolecules 2001, 34, 2089-2094.
[163] Yamamoto, K.; Nakazono, M.; Miwa, Y.; Hara, S. Polym J 2001, 33, 862-867.
[164] Park, E. –S.; Jin, H. –J.; Lee, I. –M.; Kim, M. –N.; Lee, H. S.; Yoon, J. -S. J Appl Polym Sci 2002, 83, 1103-1111.

[165] Bowden, N. B.; Dankova, M.; Wiyatno, W.; Hawker, C. J.; Waymouth, R. M. Macromolecules 2002, 35, 9246-9248.

[166] Lopez, R. G.; Boisson, C.; D'Agosto, F.; Spitz, R.; Boisson, F.; Gigmes, D.; Bertin, D. Macromol Rapid Commun 2006, 27, 173-181.

[167] Kawahara, N.; Kojoh, S.; Matsuo, S.; Kaneko, H.; Matsugi, T.; Saito, J.; Kashiwa, N. Polym Bull 2006, 57, 805-812.

[168] De Brouwer, H.; Schellekens, M. A. J.; Klumperman, B.; Monteiro, M. J.; German, A. L. J Polym Sci Part A: Polym Chem 2000, 38, 3596-3603.

[169] Barner, L.; Zwaneveld, N.; Perera, S.; Pham, Y.; Davis, T. P. J Polym Sci Part A Polym Chem 2002, 40, 4180-4192.

[170] Jankova, K.; Kops, J.; Chen, X.; Batsberg, W. Macromol Rapid Commun 1999, 20, 219-223.

[171] Wang, X. -S.; Luo, N.; Ying, S. -K. Polymer 1999, 40, 4515-4520.

[172] Matyjaszewki, K.; Teodorescu, M.; Miller, P. J.; Peterson, M. L. J Polym Sci Part A: Polym Chem 2000, 38, 2440-2448.

[173] Liu, S.; Sen, A. Macromolecules 2001, 34, 1529-1532.

[174] Schellekens, M. A. J.; Klumperman, B.; Linde, R. v. d. Macromol Chem Phys 2001, 202, 1595-1601.

[175] Garcia, F. G.; Pinto, M. R.; Soares, B. G. Eur Polym J 2002, 38, 759-769.

[176] Matyjaszewski, K.; Saget, J.; Pyun, J.; Schlögl, M.; Rieger, B. J Macromol Sci Part A: Pure and Appl Chem 2002, 39, 901-913.

[177] Yamamoto, K.; Miwa, Y.; Tanaka, H.; Sakaguchi, M.; Shimada, S. J Polym Sci Part A: Polym Chem 2002, 40, 3350-3359.

[178] Matsugi, T.; Kojoh, S.; Kawahara, N.; Matsuo, S.; Kaneko, H.; Kashiwa, N. J Polym Sci Part A: Polym Chem 2003, 41, 3965-3973.

[179] Desai, S. M.; Solanky, S. S.; Mandale, A. B.; Rathore, K.; Singh, R. P. Polymer 2003, 44, 7645-7649.

[180] Yamamoto, K.; Tanaka, H.; Sakaguchi, M.; Shimada, S. Polymer 2003, 44, 7661-7669.

[181] Okrasa, L.; Pakula, T.; Inoue, Y.; Matyjaszewski, K. Colloid Polym Sci 2004, 282, 844-853.

[182] Inoue, Y.; Matyjaszewski, K. J Polym Sci Part A: Polym Chem 2004, 42, 496-504.

[183] Inoue, Y.; Matsugi, T.; Kashiwa, N.; Matyjaszewski, K. Macromolecules 2004, 37, 3651-3658.

[184] Hwu, J. -M.; Chang, M. -J.; Lin, J. -C.; Cheng, H, -Y.; Jiang, G. -J. J Organomet Chem 2005, 690, 6300-6308.

[185] Cao, C.; Zou, J.; Dong, J. –Y.; Hu, Y.; Chung, T. C. J Polym Sci Part A: Polym Chem 2005, 43, 429-437.
[186] Kaneyoshi, H.; Inoue, Y.; Matyjaszewski, K. Macromolecules 2005, 38, 5425-5435.
[187] Dix, A.; Ptacek, S.; Poser, S.; Arnold, M. Macromol Symp 2006, 236, 186-192.
[188] Li, H.; Zhao, H.; Zhang, X.; Lu, Y.; Hu, Y. Eur Polym J 2007, 43, 109-118.
[189] Zhang, K.; Wang, J.; Subramanian, R.; Ye, Z.; Lu, J.; Yu, Q. Macromol Rapid Commun 2007, 28, 2185-2191.
[190] Shin, J.; Chang, A. Y.; Brownell, L. V.; Racoma, I. O.; Ozawa, C. H.; Chung, H. –Y.; Peng, S.; Bae, C. J Polym Sci Part A: Polym Chem 2008, 46, 3533-3545.
[191] Zhang, K.; Ye, Z.; Subramanian, R. Macromolecules 2008, 41, 640-649.
[192] Sasaki, D.; Suzuki, Y.; Hagiwara, T.; Yano, S.; Sawaguchi, T. Polymer 2008, 49, 4094-4100.
[193] Hawker, C. J.; Bosman, A. W.; Harth, E. Chem Rev 2001, 101, 3661-3688.
[194] Studer, A.; Schulte, T. Chem Record 2005, 5, 27–35.
[195] Favier, A.; Charreyre, M.-T. Macromol Rapid Commun 2006, 27, 653–692.
[196] Perrier, S.; Takolpuckdee, P. J Polym Sci Part A: Polym Chem 2005, 43, 5347–5393.
[197] Moad, G.; Rizzardo, E.; Thang, S. H. Aust J Chem 2005, 58, 379–410.
[198] Kamigaito, M.; Ando, T.; Sawamoto, M. Chem Rev 2001, 101, 3689–3745.
[199] Matyjaszewski, K.; Xia, J. Chem Rev 2001, 101, 2921-2990.
[200] Braunecker, W. A.; Matyjaszewski, K. J Mol Catal A: Chem 2006, 254, 155–164.
[201] Duschek, T.; Mülhaupt, R. Polym Prepr 1992, 33, 170-171.
[202] Hong, S. C.; Jia, S.; Teodorescu, M.; Kowalewski, T.; Matyjaszewski, K.; Gottfried, A. C.; Brookhart, M. J Polym Sci Part A: Polym Chem 2002, 40, 2736-2749.
[203] Kaneyoshi, H.; Inoue, Y.; Matyjaszewski, K. Macromolecules 2005, 38, 5425-5435.
[204] Kaneyoshi, H.; Matyjaszewski, K. J Appl Polym Sci 2007, 105, 3-13.
[205] Robin, J. J.; Boyer, C.; Boutevin, B.; Loubat, C. Polymer 2008, 49, 4519-4528.
[206] Li, H.; Chiba, T.; Higashida, N.; Yang, Y.; Inoue, T. Polymer 1997, 38, 3921-3925.
[207] Sun, Y. –J.; Hu, G. –H.; Lambla, M.; Kotlar, H. K. Polymer 1996, 37, 4119-4127.
[208] Lu, Q. –W.; Macosko, C. W. Polymer 2004, 45, 1981-1991.
[209] Lü, Y.; Ma, Z.; Hu, Y.; Xu, G. X.; Chung, T. C. Chin Sci Bull 2003, 48, 523-525.
[210] Dong, J. Y.; Wang, Z. M.; Hong, H.; Chung, T. C. Macromolecules 2002, 35, 9352-9359.

[211] Lin, W. –F.; Hsiao, T. –J.; Tsai, J. –C.; Chung, T. –M.; Ho, R. –M. J Polym Sci, Part A: Polym Chem 2008, 46, 4843-4856.
[212] Kawahara, N.; Saito, J.; Matsuo, S.; Kaneko, H.; Matsugi, T.; Kojoh, S.; Kashiwa, N. Polym Bull 2007, 59, 177-183.
[213] Karavia, V.; Deimede, V.; Kallitsis, J. K. J Macromol Sci Part A: Pure and Appl Chem 2004, 41, 115-131.
[214] Park, C.; Yoon, J.; Thomas, E. L. Polymer 2003, 44, 6725-6760.

PART I

POLYOLEFIN MACROINITIATOR APPROACH

Chapter 1

Polypropylene-*block*-poly(methyl methacrylate) and -*block*-poly(*N*-isopropylacrylamide) Block Copolymers Prepared by Controlled Radical Polymerization with Polypropylene Macroinitiator

Abstract

Polypropylene-*block*-poly(methyl methacrylate) (PP-*b*-PMMA) and Polypropylene-*block*-poly(*N*-isopropylacrylamide) (PP-*b*-PNIPAAm) block copolymers were successfully synthesized by radical polymerizations of MMA or NIPAAm with polypropylene (PP) macroinitiators. Polypropylene macroinitiators were prepared by a series of end functionalization of pyrolysis PP via hydroalumination, oxidation and esterification reactions. The PP macroinitiators thus obtained could initiate radical polymerizations of MMA or NIPAAm by using transition metal catalyst systems, and ^{1}H NMR analysis and gel permeation chromatography measurement confirmed the formation of PP-*b*-PMMA and PP-*b*-PNIPAAm block copolymers. In addition, the length of the incorporated PMMA or PNIPAAm segments in these block copolymers was controllable by the feed ratio between the monomer and the PP macroinitiator, and their molecular weights were estimated to be 35,700 and 68,700 (PMMA) and 1,760 and 13,300 (PNIPAAm), respectively. Transmission electron microscopy of the polymers obtained by NIPAAm polymerization revealed specific morphological features that reflected the difference of PNIPAAm segment length.

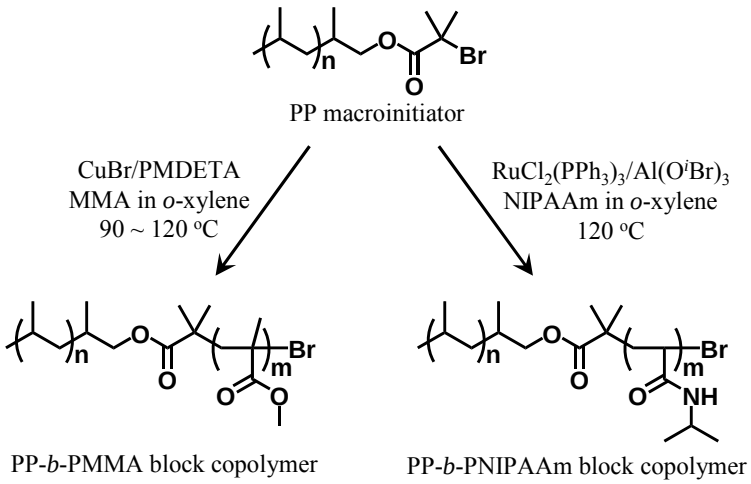

Introduction

As one of the novel polyolefin hybrids, polyolefin-based block copolymers, possessing a chemical linkage between polyolefin and polar polymer segments, have potential to improve low interfacial interactions between polyolefin and polar materials. So far, many examples for preparing them by using two types of approaches, such as a sequential living polymerization and a post-polymerization process, have been reported as mentioned in *General Introduction*. In former approach, several kinds of block copolymers were obtained by sequential living polymerization of α-olefin and polar monomers [1–3]. However, the types of monomers and the polymerization conditions are generally restricted because this method depends on a coordination polymerization with a transition metal catalyst. Then, to diversify structures and compositions of segments in block copolymers, a post-polymerization process by using polyolefin macroinitiators, which are obtained by transforming a variety of functionalized polyolefins to radical or anionic polymerization initiators, was developed as an alternative approach. To obtain the functionalized polyolefin, chain transfer reaction and olefin copolymerization with functional monomers and terminally unsaturated polyolefin have been reported as useful tools. For example, Chung *et al.* reported the syntheses of block copolymers by using borane- and *p*-methylstyrene-terminated polyolefins, which were obtained by chain transfer reaction or copolymerization, in combination with radical or anionic polymerization of methyl methacrylate (MMA) or styrene [4]. Previously, the authors reported on functionalized polyethylenes (PEs) with reactive groups such as hydroxyl or amino groups under precise control of the positions of the functional groups [5,6]. In particular, this methodology could selectively prepare the terminally-functionalized PE.

The recent development of a controlled radical polymerization has extended the possibility of synthesizing a variety of styrenic and/or (meth)acrylic block copolymers [7–9]. The combination of this technique with the functionalized polyolefin realized to prepare the well-defined polyolefin/polar polymer block copolymers. For instance, the authors have reported that the terminally-functionalized PE could be converted to a PE macroinitiator for controlled radical polymerization to give polyethylene-*block*-poly(methyl methacrylate) (PE-*b*-PMMA) block copolymer [10].

In this chapter, the authors synthesized PP macroinitiators by functionalization of the terminal vinylidene group in pyrolysis PP to produce structurally well-defined polypropylene-*block*-poly(methyl methacrylate) (PP-*b*-PMMA) and polypropylene-*block*-poly(*N*-isopropylacrylamide) (PP-*b*-PNIPAAm) block copolymers by controlled

radical polymerization. In addition, their microphase structures were investigated by transmission electron microscopy (TEM) analysis.

Experimental

General Procedures and Materials

All manipulations of air- and water-sensitive materials were performed under a dry nitrogen atmosphere in a conventional nitrogen-filled glove box. Copper bromide (CuBr), *N*,*N*,*N'*,*N''*,*N''*-pentamethyldiethylenetriamine (PMDETA), $RuCl_2(PPh_3)_3$, $Al(O\textit{i}\text{-}Pr)_3$, triethylamine and 2-Bromoisobutyryl bromide (BiBB) were purchased from Wako Pure Chemical Industries and used without further purification. MMA (Wako Pure Chemical Industries) was dried over CaH_2 and distilled *in vacuo*. NIPAAm (Wako Pure Chemical Industries) was recrystallized in hexane. *n*-Decane and *o*-xylene used as solvent were dried over Al_2O_3 and degassed by bubbling with N_2 gas. Diisobutylaluminum hydride (DIBAL-H) was purchased from Tosoh-Finechem Co. Ltd. All other chemicals were obtained commercially and used as received.

Preparation of PP Macroinitiator (PP-t-Br)

A typical process is as follows: *n*-Decane (800 mL) and pyrolysis PP containing a terminal vinylidene group (PP-*t*-Vd, 1.2 unit-Vd/chain; 93.6 g) were placed in a 1-L glass reactor equipped with a mechanical stir bar and then PP-*t*-Vd was dissolved at 110 °C for 2 h. Then, DIBAL-H (14.3 mL) was added and the mixture was maintained at 110 °C for 4 h under stirring. Dried air was then continuously fed (100 L/h) into the system at 110 °C. After 6 h, the reaction mixture was added to 2 L of acidic methanol. The polymer was collected by filtration, washed with methanol, and dried *in vacuo* at 120 °C for 10 h to give 104 g of hydroxylated PP (PP-*t*-OH, 0.63 unit-OH/chain). The PP-*t*-OH (50 g) and toluene (300 mL) thus obtained were placed in a 500-mL glass reactor equipped with a mechanical stir bar. Triethylamine (3.0 mL) and BiBB (2.5 mL) were added to the reactor and then the mixture was stirred at 80 °C for 3 h. The reaction mixture was poured into 2 L of acidic methanol. The resulting polymer was collected by filtration, washed with methanol, and dried *in vacuo* at 40 °C for 10 h to give 42 g of PP containing a terminal ester group (PP-*t*-Br, 0.46 unit-Br/chain). By selecting the pyrolysis PPs, three kinds of PP-*t*-Br with different molecular weights (PP-*t*-Br1, PP-*t*-Br2 and PP-*t*-Br3) were obtained as shown later in Table 1 and then used as a PP macroinitiator.

MMA Polymerization with PP Macroinitiator

A typical polymerization process is as follows: After PP-*t*-Br1 (0.47 g, 0.088 mmol as 2-bromoisobutyrate) was placed in a 30-mL Schlenk tube equipped with a stirring bar, *o*-xylene (1.4 mL), MMA (2.36 mL), and a solution of CuBr/PMDETA in *o*-xylene (0.106 mmol as a copper atom and 0.212 mmol as PMDETA, pretreated for 5 min. at ambient temperature) were added and the mixture was heated at 90 °C for 2.5 h. After cooling, the reaction mixture was poured into 400 mL of methanol and the white solid was collected by filtration, washed with methanol, and dried at 80 °C *in vacuo*. As shown later in Table 2, three kinds of polymers were obtained.

NIPAAm Polymerization with PP Macroinitiator

A typical polymerization process is as follows: After PP-*t*-Br2 (6.94 g, 0.20 mmol as 2-bromoisobutyrate) was placed in a 100-mL Schlenk tube equipped with a stirring bar, *o*-xylene (10 mL), NIPAAm (9.05 g), $Al(O\textit{i}\text{-}Pr)_3$ (81.7 mg), and $RuCl_2(PPh_3)_3$ (95.9 mg) were added to the tube and the mixture was heated at 120 °C for 9 h. After cooling, the reaction mixture was poured into 600 mL of acetone and the white solid was collected by filtration, washed with acetone, and dried at 120 °C *in vacuo*. As shown later in Table 3, two kinds of polymers were obtained.

Analytical Procedures

^{1}H NMR spectra were recorded on JEOL GSX-400 (400 MHz) spectrometers using 1,2-dichlorobenzene-d_4 as a solvent at 120 ^{o}C. The gel permeation chromatograms (GPC) calibrated with PP were recorded by using a Waters Alliance GPC2000 equipped with four TSKgel columns (two sets of TSKgelGMH6-HT and two sets of TSKgelGMH6-HTL) and a refractive index detector at 140 ^{o}C in 1,2-dichlorobenzene.

TEM Analysis

Ultrathin (~100 nm) sections of the polymer, which had been pressed into a sheet, were cut on a Reica Ultracut microtome equipped with a diamond knife at a low temperature and then were stained with RuO_4. TEM observations were made with a Hitachi H-7000 transmission electron microscope at an acceleration voltage of 75 kV.

Results and Discussion

Preparation of PP Macroinitiators

The synthesis of PP macroinitiator consisted of three steps (Scheme). In the first step,

PP-*t*-Vd, which possessed the vinylidene group at its chain end, was obtained by pyrolysis of PP. In the second step, the vinylidene end group was converted to the hydroxyl group by hydroalumination and oxidation to give PP-*t*-OH, according to the previous literature [11]. In the third step, the hydroxyl chain end was reacted with BiBB to produce PP-*t*-Br, which could initiate the controlled radical polymerization mediated by a transition metal catalyst. By selecting the pyrolysis conditions of PP, three kinds of PP-*t*-Br with different molecular weights, PP-*t*-Br1, PP-*t*-Br2 and PP-*t*-Br3, were obtained.

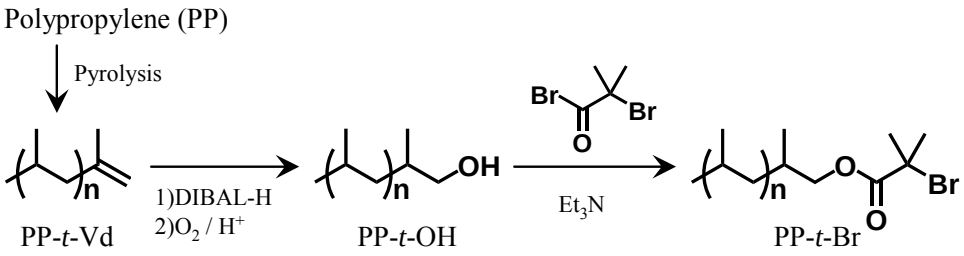

Scheme. Synthetic scheme of PP macroinitiator.

Figure 1 shows the ^{1}H NMR spectra of PP-*t*-Br3 and its precursors, PP-*t*-Vd and PP-*t*-OH. For PP-*t*-Vd (Figure 1a), two signals of δ 4.6–4.7 ppm are assigned to vinylidene (=CH_2). For PP-*t*-OH (Figure 1b), the multiple signals of δ 3.25–3.45 ppm are assigned to methylene protons (−CH_2–OH). For PP-*t*-Br3 (Figure 1c), the multiple signals of δ 3.8–4.1 ppm correspond to methylene protons (–CH_2–O–) and the single signal of δ 1.9 ppm corresponds to methyl protons (–OCOC(CH_3)$_2$Br). In addition, a small amount of methylene protons assigned to the hydroxyl group were observed. From the relative intensities of these signals, the conversion of the hydroxyl group to ester group was estimated to be about 87 %. Table 1 summarizes the preparation results of PP macroinitiators with different molecular weights. For PP-*t*-Br1 with the lowest molecular weight, the functionality of the terminal ester group was 0.98 and the overall conversion of the vinylidene group to ester group was 73 % from the number-averaged molecular weight (M_n) and the contents of the vinylidene and ester groups. On the other hand, in the case of PP-*t*-Br2 and PP-*t*-Br3 with higher molecular weight, both functionality and overall conversion were much lower than those in the case of PP-*t*-Br1. These results would be due to the difficulty of the oxidation and esterification because of their higher molecular weights. The PPs thus obtained with the terminal ester group were used as a macroinitiator for the transition metal mediated radical polymerization.

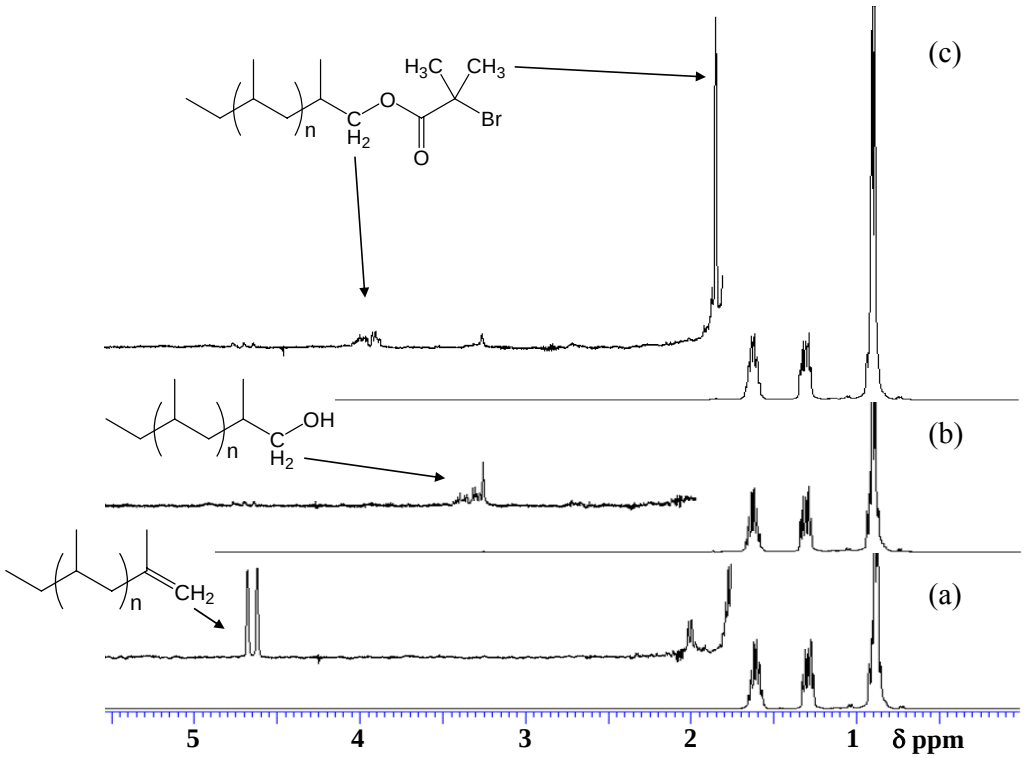

Figure 1. ^{1}H NMR spectra of (a) PP-*t*-Vd, (b) PP-*t*-OH and (c) PP-*t*-Br (400 MHz in 1,2-Dichlorobenzene-d_4 at 120 ^{o}C).

Table 1. Preparation of PP Macroinitiators

	PP-*t*-Vd			PP-*t*-Br				
Sample	M_n[a] (g mol^{-1})	M_w/M_n[a]	Vd Cont.[b] (mol%)	M_n[a] (g mol^{-1})	M_w/M_n[a]	Br Cont.[b] (mol%)	F_n[c]	Conv.[d] (%)
PP-*t*-Br1	5,980	1.79	1.1	5,270	1.47	0.80	0.98	73
PP-*t*-Br2	13,000	2.09	0.38	13,900	2.05	0.14	0.46	37
PP-*t*-Br3	17,400	2.11	0.24	17,800	2.08	0.11	0.46	46

[a] Determined by GPC calibrated with PP.
[b] Determined by ^{1}H NMR.
[c] End functionality (F_n) was calculated between the content of Br and M_n.
[d] Conversion from PP-*t*-Vd to PP-*t*-Br; calculated from the content of Vd and Br.

Radical Polymerization of MMA Initiated by PP Macroinitiator

It is well known that transition metal mediated radical polymerization realized the controlled radical polymerization of various vinyl monomers, represented by (meth)acrylates and styrenes, to give precisely controlled polymers [7,8]. In particular, in the case of using functionalized polyolefin as a macroinitiator, this polymerization system is more advantageous than anionic polymerization because of its higher polymerization temperature. The polymerization of MMA was carried out in an *o*-xylene solution by using CuBr/PMDETA as a catalyst system. Two types of PP-*t*-Br

with different molecular weights were used as macroinitiators, and polymerization with the lower molecular weight macroinitiator (PP-*t*-Br1) was carried out at 90 °C, while that with the higher molecular weight macroinitiator (PP-*t*-Br3) was carried out at 120 °C because of its poor solubility. The viscosity of the polymerization system increased with increasing time and it indicated the progress of MMA polymerization to give a PP-*b*-PMMA block copolymer with higher molecular weight compared with the macroinitiator. Table 2 summarizes the results by altering polymerization conditions in various ways. In all cases, the polymer yields were larger than the amount of macroinitiator and MMA conversions observed by GC analysis were in a range of 57–66 %. In addition, Soxhlet extraction of the obtained polymers with boiling THF confirmed that the obtained polymers contained only a small amount of homo-PMMA. These results indicate the formation of PP-*b*-PMMA block copolymer.

Table 2. Results of MMA Polymerization by using PP Macroinitiator

Run	PP Macroinitiator	(g)	(mM)	[PP-*t*-Br]/[CuBr] /[PMDETA]/[MMA] (Molar ratio)	Polymn. Temp. (°C)	Polymn. Time (h)	Yield (g)	MMA Conversion[a] (%)
1	PP-*t*-Br1	0.47	15	1 / 1.2 / 2.4 / 250	90	2.5	1.01	61
2	PP-*t*-Br3	35.9	8.0	1 / 3 / 6 / 1000	120	7.0	88.5	57
3	PP-*t*-Br3	71.8	6.6	1 / 1.5 / 3 / 500	120	2.0	132.8	66

[a] Determined by GC analysis.

Figure 2 shows the GPC traces of the obtained polymer (Run 1) and its lap samples. GPC measurements revealed that the molecular weight of the obtained polymer increased with increasing reaction time. It indicated the proceeding of the controlled radical polymerization of MMA to give a linear block copolymer. On the other hand, the molecular weight distribution of the obtained polymer was broadened with increasing reaction time and it seems that part of the starting material remained during the progress of the polymerization. Its possible explanation is that the macroinitiator used was prepared from the pyrolysis PP, which is a mixture of the polymer with the vinylidene group at both ends of its chain, at one end of its chain, and without the vinylidene group as reported previously [12], and PP without the vinylidene group cannot be converted to the macroinitiator. Therefore, the unreacted PP was observed as a shoulder in the GPC trace.

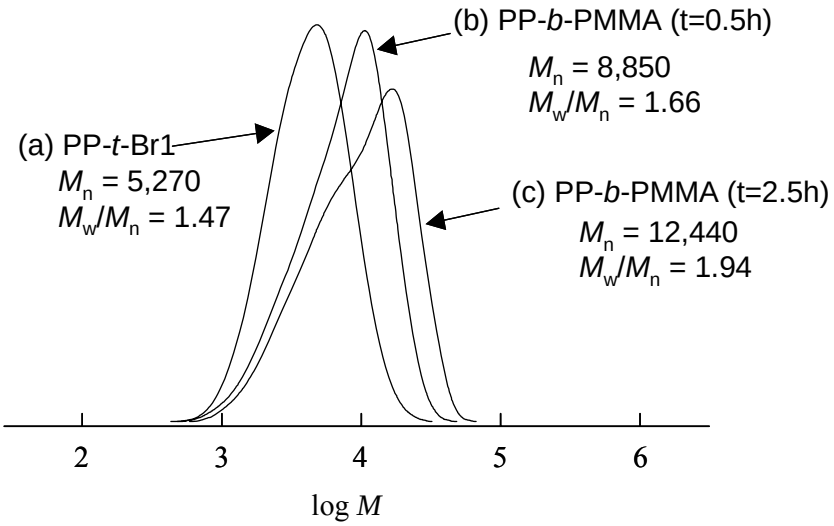

Figure 2. GPC traces of (a) PP-*t*-Br1, (b) PP-*b*-PMMA (Polymerization time = 0.5 h) and (c) PP-*b*-PMMA (Polymerization time =2.5 h) at Run 1.

Structural Analysis of the Polymer Obtained by Radical Polymerization of MMA

The obtained polymers were analyzed at 120 °C by ^{1}H NMR with 1,2-dichlorobenzene-d_4 as a solvent. Figure 3 shows the ^{1}H NMR spectra of the polymers obtained by radical polymerization of MMA with PP macroinitiator, PP-*t*-Br3 (Table 2, Runs 2 and 3). From the relative intensities between δ 3.6 ppm assigned to the methyl ester protons of the PMMA and δ 0.9–1.8 ppm assigned to the propylene unit and PMMA backbone, MMA contents in these polymers were calculated to be 48 and 64 wt%, respectively. As shown in Table 1, the functionality and M_n of PP macroinitiator (PP-*t*-Br3) were 0.46 unit-Br/chain and 17800. Assuming that the efficiency of the initiation site in this macroinitiator was almost 100 %, it is considered that these obtained polymers consisted of 54 % PP without PMMA segment and 46 % PP-*b*-PMMA block copolymer. Therefore, M_n of the attached PMMA segment in each PP-*b*-PMMA block copolymer can be estimated to be 35,700 and 68,700, respectively.

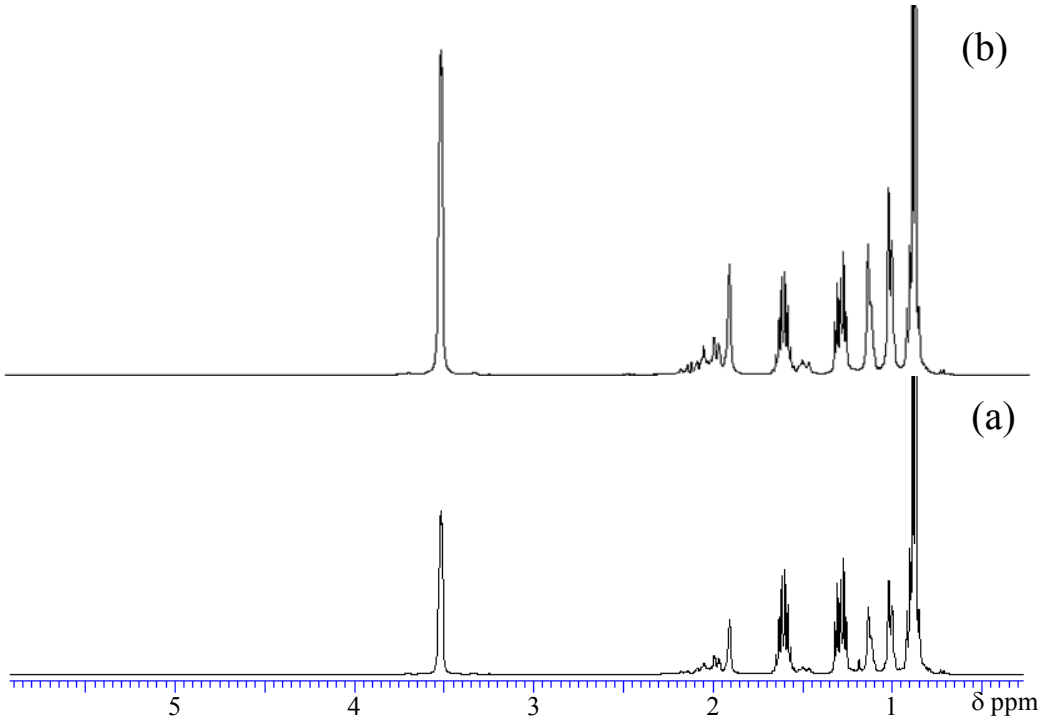

Figure 3. ^{1}H NMR spectra of PP-*b*-PMMA block copolymers with PMMA contents of (a) 48 and (b) 64 wt% (400 MHz in 1,2-Dichlorobenzene-d_4 at 120 ^{o}C).

Radical Polymerization of NIPAAm Initiated by PP Macroinitiator

The polymerization of NIPAAm initiated by PP macroinitiator (PP-*t*-Br2) was carried out at 120 °C in *o*-xylene with two commonly used catalyst systems, CuBr/PMDETA and $RuCl_2(PPh_3)_3$/Al(O*i*-Pr)$_3$. In the case of the copper catalyst system, polymerization of NIPAAm did not proceed. On the other hand, in the case of the ruthenium catalyst system, the polymerization of NIPAAm was initiated by PP macroinitiator and the content of NIPAAm in the obtained polymer could be controlled by the feed ratio between the NIPAAm monomer and the macroinitiator as shown in Table 3. One of the reasons for no polymerization in the case of the copper catalyst system is that NIPAAm interacted with the copper bromide directly and deactivated this catalyst system because of its highly active N–H bond.

Table 3. Results of NIPAAm Polymerization by using PP Macroinitiator[a]

Run	PP Macroinitiator[b] (g)	PP Macroinitiator[b] (mM)	[PP-*t*-Br]/[NIPAAm] (molar ratio)	Yield (g)	Content of NIPAAm[c] (wt%)
4	10.42	23	1 / 87	11.27	6
5	6.94	23	1/ 347	9.72	31

[a] Polymerization conditions: $[RuCl_2(PPh_3)_3]/[Al(iOPr)_3]$ = 10 / 40 mM in *o*-xylene at 120 °C for 9 h.
[b] PP-*t*-Br2 was used.
[c] Determined by ^{1}H NMR.

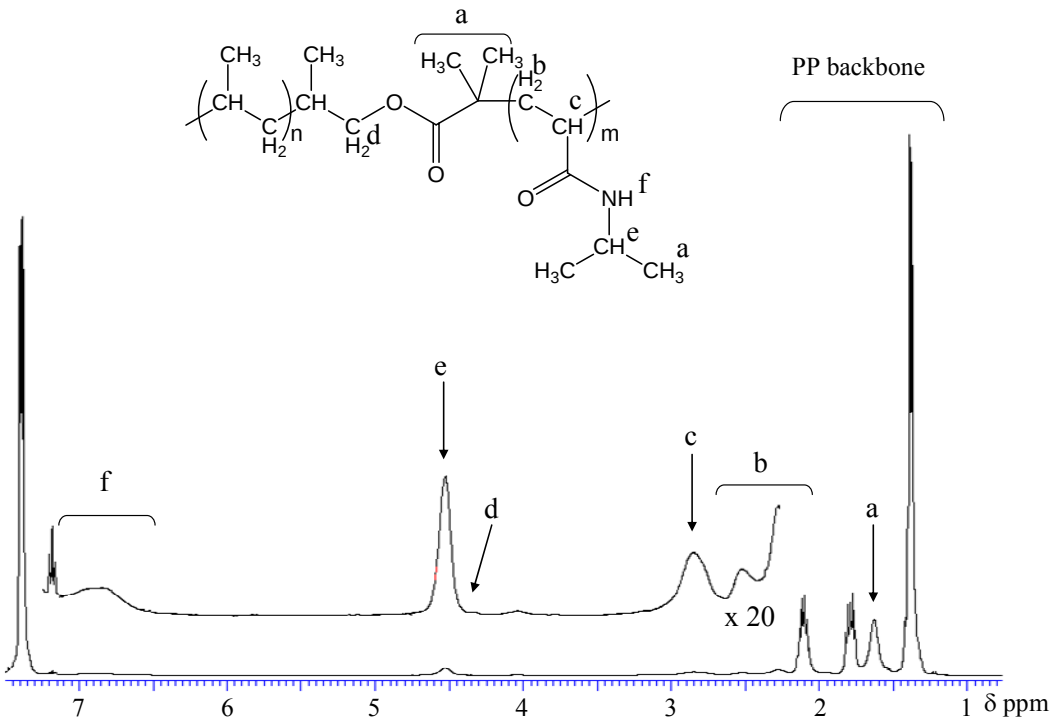

Figure 4. ^{1}H NMR spectrum of PP-*b*-PNIPAAm block copolymer (400 MHz in 1,2-Dichlorobenzene-d_4 at 120 °C).

The contents of NIPAAm in the obtained polymers were determined by ^{1}H NMR. The ^{1}H NMR spectrum of the obtained polymer (Run 5) is shown in Figure 4. In this spectrum, some specific signals were observed at δ 1.15 ppm (*a*, methyl protons of initiation site and isopropyl group of NIPAAm), δ 1.5–2.1 ppm (*b*, methylene protons of PNIPAAm backbone), δ 2.2–2.6 ppm (*c*, methyne proton of PNIPAAm backbone), δ 4.05 ppm (*e*, methyne proton of isopropyl group of NIPAAm), and δ 6.0–6.6 ppm (*f*, amine proton of NIPAAm). From the relative intensities between these signals, the contents of NIPAAm in the obtained polymers (Runs 4 and 5) were estimated to be 6 and 31 wt%, respectively. From the functionality (0.46 unit-Br/chain) and M_n (13,900) of PP macroinitiator, the obtained polymers included 46 % PP-*b*-PNIPAAm block copolymer and PNIPAAm segments attached to PP segments were estimated to have 1,760 and 13,300 of M_n, respectively.

Morphology of the Polymers Obtained by Radical Polymerization of NIPAAm

Figure 5 shows TEM micrographs of two polymers with 6 and 31 wt% NIPAAm contents. The TEM images of these polymers reveal the microphase-separation morphology at the nanometer level between the PP segment and PNIPAAm segment and the distinctive phases were observed at different NIPAAm contents. In the case of the lower NIPAAm content (6 wt%, Figure 5a), the PNIPAAm segment stained easily by RuO_4 dispersed at less than 10 nm in the PP matrix because of the short PNIPAAm segment (M_n = 1,760) compared with the PP segment (M_n = 13,900). In contrast, in the case of higher NIPAAm content (31 wt%, Figure 5b), enough long PNIPAAm segment (M_n = 13,300) easily aggregated and spherical PNIPAAm-rich domains of about 50 nm in diameter were observed in the PP matrix. These results demonstrate that the microphase morphology is controllable by changing the length of the chemically linked PNIPAAm segment in PP-*b*-PNIPAAm block copolymer.

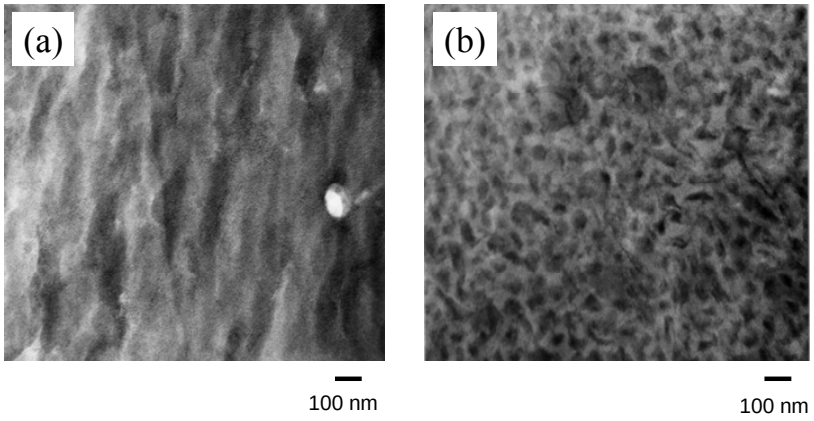

Figure 5. TEM micrographs of PP-*b*-PNIPAAm with NIPAAm contents of (a) 6 wt% (Run 4) and (b) 31 wt% (Run 5).

Conclusions

PP macroinitiators were prepared by a series of end-functionalization of pyrolysis PP with the vinylidene end group via hydroalumination, oxidation and esterification. By using these PP macroinitiators, transition-metal-mediated radical polymerizations of MMA or NIPAAm were carried out to give PP-*b*-PMMA and PP-*b*-PNIPAAm block copolymers. These structures and compositions could be confirmed by ^{1}H NMR analysis. From TEM observation of the polymers obtained by NIPAAm polymerization, the microphase-separation morphology at the nanometer level between PP and PNIPAAm segments was observed and its morphology was remarkably altered by the length of the attached PNIPAAm segment.

References

[1] Hosoda, S.; Kihara, H.; Kojima, K.; Satoh, Y.; Doi, Y. Polym J 1991, 23, 277-284.
[2] Yasuda, H.; Furo, M.; Yamamoto, H.; Nakamura, A.; Miyake, S.; Kibino, N. Macromolecules 1992, 25, 5115-5116.
[3] Desurmont, G.; Tokimitsu, T.; Yasuda, H. Macromolecules 2000, 33, 7679-7681.
[4] Chung, T.C. Prog Polym Sci 2002, 27, 39-85.
[5] Imuta, J.; Kashiwa, N.; Toda, Y. J Am Chem Soc 2002, 124, 1176-1177.
[6] Imuta, J.; Toda, Y.; Matsugi, T.; Kaneko, H.; Matsuo, S.; Kojoh, S.; Kashiwa, N. Chem Lett 2003, 32, 656-657.
[7] Matyjaszewski, K.; Xia, J. Chem Rev 2001, 101, 2921-2990.
[8] Kamigaito, M.; Ando, T.; Sawamoto, M. Chem Rev 2001, 101, 3689-3745.
[9] Hawker, C.J.; Bosman, A.W.; Harth, E. Chem Rev 2001, 101, 3661-3688.
[10] Matsugi, T.; Kojoh, S.; Kawahara, N.; Matsuo, S.; Kaneko, H.; Kashiwa, N. J Polym Sci Part A Polym Chem 2003, 41, 3965-3973.
[11] Kashiwa, N.; Kojoh, S.; Kawahara, N.; Matsuo, S.; Kaneko, H.; Matsugi, T. Macromol Symp 2003, 201, 319-326.
[12] Sawaguchi, T.; Ikemura, T.; Seno, M. Macromolecules 1995, 28, 7973-7978.

Chapter 2

Synthesis and Characterization of Polypropylene-based Block Copolymers Possessing Polar Segments via Controlled Radical Polymerization

Abstract

A new method to prepare the polypropylene (PP) macroinitiator for controlled radical polymerization was described. Bromination of terminally-unsaturated PP was carried out by using *N*-bromosuccinimide and 2,2'-azobis(isobutyronitrile) to give a brominated PP (PP-Br), which has allylic bromide moieties at or near the chain ends. Thus obtained PP-Br was successfully employed as a macroinitiator for radical polymerization of styrene, methyl methacrylate and *n*-butyl acrylate using a copper catalyst system. From ^{1}H NMR analysis, it was confirmed that the chain extension polymerization was certainly initiated from allylic bromide moieties with high efficiency, leading to the PP-based block copolymers linking the polar segment. From differential scanning calorimetry, peak melting temperature of block copolymers was higher than that of PP-Br and the obtained PP-PS block copolymers with different compositions of each segment demonstrated the unique morphological features due to the microphase separation between both segments.

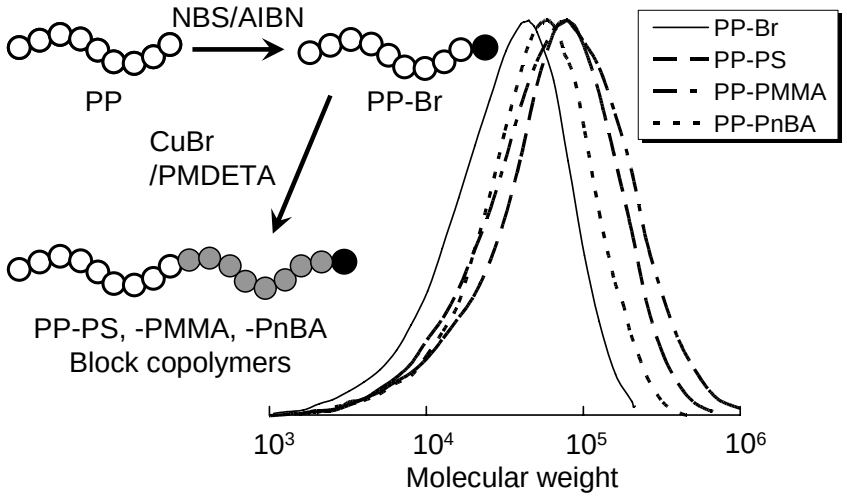

Introduction

As mentioned at *General Introduction*, in recent years several kinds of controlled radical polymerization (CRP) methods have been developed remarkably. CRP methods are very effective tool for preparing the polyolefin hybrids with well-defined structures because of not only the controllability of polymerization but also the versatility of monomers and polymerization conditions. In particular, the combination of metal-catalyzed living radical polymerization and polyolefin macroinitiators allowed the preparation of polyolefin-based block and graft copolymers with precise control of their structure [1-26]. Although this approach is excellent and useful ways, it seems arduous to prepare the functionalized polyolefins and subsequently to convert to the macroinitiators. In general, most of the functionalized polyolefins were prepared under unusual olefin polymerization conditions in the presence of specific chain transfer agents or polar monomers, which are poisonous for most olefin polymerization catalysts to retard the polymerization.

Therefore, it is very important factor how to prepare the precisely-site-selective polyolefin macroinitiators with another simple and facile way. Ying *et al.* reported a bromination of ethylene/propylene/diene terpolymer (EPDM) and the synthesis of EPDM-*g*-poly(methyl methacrylate) graft copolymers using the brominated EPDM as an initiator [24]. Sen *et al.* synthesized the polyethylene-based graft copolymers from brominated ethylene/styrene copolymer [25] and Jiang *et al.* also synthesized the PE-based graft copolymers through the bromination of ethylene/*p*-methylstyrene copolymer [26]. Furthermore, there are a few reports on the graft copolymers synthesized by CRP using commercially available polymers with initiation sites, such as poly(vinyl chloride) [27,28] and isobutene/*p*-methylstyrene/*p*-bromomethylstyrene copolymer [29]. These synthetic routes are very simple and facile, but the structure of the obtained copolymer is only graft structure and the types of applicable polyolefins are restricted to the specific copolymers derived from halogenated monomers, styrene or diene.

Alternatively, terminally-unsaturated polyolefin, which is prepared by thermal degradation of polyolefin [30,31] or chain transfer reaction with β-hydride elimination at olefin polymerization [32,33], is well known as one of the end-functionalized polyolefins and are used as building block of polyolefin-based block copolymers. However, although its production process is simple and low-cost compared with olefin copolymerization with functional monomers, introduction of the initiation site for metal-catalyzed living radical polymerization into the unsaturated bond is not easy so

far and thereby overall production process for preparing polyolefin-based block copolymers tends to be complicated [3,4,7,10,22].

In this chapter, the authors introduce a new synthetic method for the preparation of PP macroinitiators by direct bromination at the allylic position of terminally-unsaturated PP in order to prepare the PP-based copolymers linking the polar segment using metal-catalyzed living radical polymerization. And the authors discuss their structures and characteristics using several analytical studies, such as nuclear magnetic resonance (NMR), gel permeation chromatography (GPC), differential scanning calorimetry (DSC), transmission electron microscopy (TEM) and so on.

Experimental

Materials

All manipulations of air- and water-sensitive materials were performed under a dry nitrogen atmosphere in a conventional nitrogen-filled glove box. *N*-bromosuccinimide (NBS), 2,2'-azobis(isobutyronitrile) (AIBN), chlorobenzene, copper bromide (CuBr) and *N,N,N',N'',N''*-pentamethyldiethylenetriamine (PMDETA) were purchased from Wako Pure Chemical Industries and used without further purification. Styrene (St), Methyl methacrylate (MMA) and *n*-butyl acrylate (nBA) (Wako Pure Chemical Industries) were dried over CaH_2 and distilled *in vacuo*. *o*-Xylene used as a solvent were dried over Al_2O_3 and degassed by bubbling with N_2 gas. Polypropylene with terminal vinylidene group (PP-Vd) was prepared by pyrolysis of commercial PP (Prime Polypro^{TM} J106G, Prime Polymer Co., Ltd.) using the nitrogen-sealed single screw extruder at 380 ^{o}C. From ^{1}H NMR analysis, the composition of propylene and terminal vinylidene group was 99.45 and 0.55 mol-%, respectively. Number average molecular weight (M_n) and polydispersity (M_w/M_n) was 13,300 and 2.06, respectively, determined by gel permeation chromatography (GPC) using PP calibration. From the vinylidene content and M_n, an average number of terminal vinylidene group was estimated to be 1.75 units per chain.

Analytical Procedures

^{1}H NMR spectra were recorded on JEOL GSX-400 (400 MHz) spectrometers using 1,2-dichlorobenzene-d_4 as a solvent at 120 ^{o}C. The gel permeation chromatograms calibrated with PP were recorded by using a Waters Alliance GPC2000 equipped with four TSKgel columns (two sets of TSKgelGMH6-HT and two sets of TSKgelGMH6-HTL) and a refractive index detector at 140 ^{o}C in 1,2-dichlorobenzene

and those calibrated with PS standard were recorded by using a CFC T-150A (Mitsubishi Kagaku Corp.) equipped with three columns (Shodex AT-806MS) and an IR spectrometer Miran 1ACVF at 140 ^{o}C in 1,2-dichlorobenzene. Differential scanning calorimetry (DSC) was measured on a Seiko Instruments RDC220 differential scanning calorimeter. The DSC curves were recorded during the second heating cycle from 30 to 230 ^{o}C for the homo PP and brominated PP and -100 to 230 ^{o}C for the copolymers, with a heating rate of 10 ^{o}C•min^{-1}.

Bromination of Polypropylene

Chlorobenzene (800 mL) and PP with terminal vinylidene group (PP-Vd; 100 g, 13.1 mmol as a vinylidene unit) were placed in a 1-L glass reactor equipped with a mechanical stir bar and then PP-Vd was dissolved at 120 ^{o}C for 2 h under nitrogen atmosphere. After cooling to 100 ^{o}C, NBS (6.33 g, 35.6mmol) and AIBN (584.3 mg, 3.56 mmol) were added and the mixture was maintained at 100 ^{o}C for 2 h under stirring. Then, the reaction mixture was cooled to ambient temperatures under stirring and the obtained slurry was poured into acetone (1.5 L). The precipitated polymer was collected by filtration, washed with acetone and dried in vacuo at 80 ^{o}C for 10 h to give brominated PP (PP-Br; 99.5 g) as a light brown powder. M_n: 13,900, M_w/M_n: 1.9 (determined by GPC calibrated with PP). The composition of propylene and allylic bromide group was 99.59 and 0.41 mol% from ^{1}H NMR analysis.

Radical Polymerization of Polar Monomers with PP-Br

A typical polymerization process is as follows: PP-Br (10 g, 0.97 mmol as allylic bromide group), monomer (50 mL) and *o*-xylene (100 mL) were placed in a 500 mL glass reactor equipped with a mechanical stir bar and then this slurry was stirred at ambient temperatures for 2 h under nitrogen atmosphere. After adding a solution of CuBr/PMDETA in *o*-xylene (5.0 mmol as a copper atom and 10.0 mmol as PMDETA, pretreated for 5 min.), the mixture was heated to 100 ^{o}C to dissolve PP-Br and start the polymerization. Then, the reaction mixture was maintained at 100 ^{o}C for the prescribed times under stirring. The reaction mixture was cooled to ambient temperatures under stirring and the obtained slurry was poured into methanol (1.5 L). The white powder was collected by filtration, washed with methanol and dried *in vacuo* at 80 ^{o}C for 10 h. As shown later in Table 1, six kinds of copolymers were obtained.

Transmission Electron Microscopy (TEM) Observations

Ultrathin (*ca.* 100 nm) sections of the polymer, which had been pressed into a sheet, were cut on a Reica Ultracut microtome equipped with a diamond knife at a low temperature and were then stained with RuO_4. TEM observations were made with a Hitachi H-7000 transmission electron microscope at an acceleration voltage of 75 kV and at a magnification of 100,000.

Results and Discussion

Bromination Reaction

Bromination of the polypropylene with terminal vinylidene group (PP-Vd) was carried out by using NBS and AIBN in chlorobenzene at 100 °C. Figure 1 shows the ^{1}H NMR spectra of the starting PP-Vd and PP-Br. The chemical shifts at δ 4.6 – 4.7 ppm are assigned to the vinylidene protons in PP-Vd. After bromination, the vinylidene signals completely disappeared and the new signals were observed at δ 3.7 – 4.1 and 4.7 – 5.5 ppm, respectively. It is well known that in the bromination reaction of unsaturated bond using NBS, the bromine radical generated from NBS preferentially attack the allylic carbon leading to the formation of allylic bromide moieties [34].

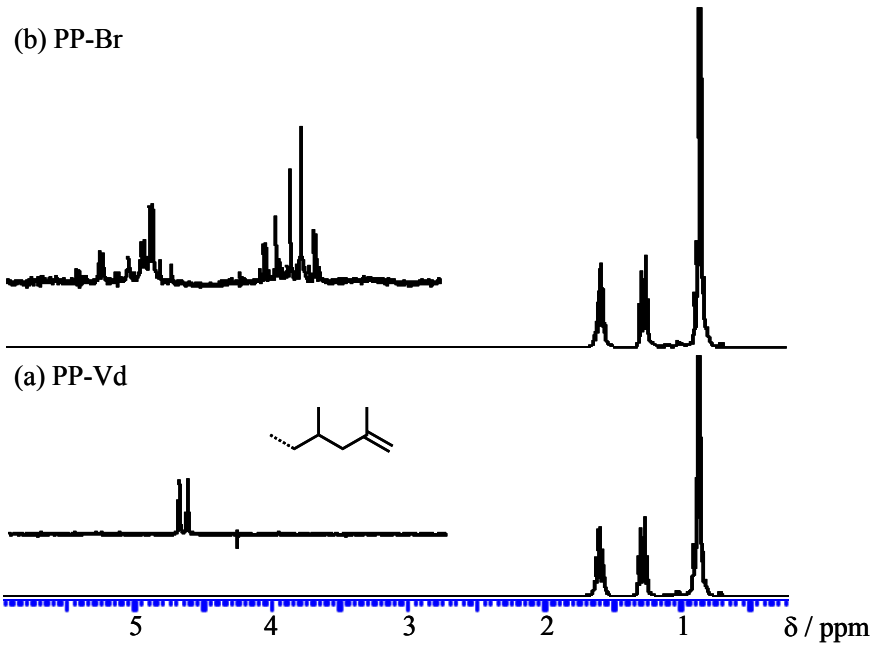

Figure 1. ^{1}H NMR spectra of (a) PP-Vd and (b) PP-Br (in 1,2-dichlorobenzene-d_4 at 120 °C).

Scheme 1 shows the plausible pathway of the bromination reaction. In the first step, the bromine radical, generated from NBS decomposition, attacks methyl or methylene carbon at the allylic position of PP-Vd to give the intermediate radicals (I and II) and their resonance forms (I'and II'). Then these intermediates are brominated by a small amount of Br_2 generated from a reaction between NBS and HBr [34], leading to three kinds of allylic bromide moieties, structure A, B and C. Figure 2 shows ^1H NMR spectrum of 3-bromo-2-methylpropene as a model compound analogous to structure A and C, in which the signals at δ 3.9 ppm can be assigned to bromomethyl group. In addition, from a study on brominated butyl rubber, it is reported that the chemical shifts of the bromomethyl and bromomethylene groups adjacent to unsaturated bond are δ 4.04 – 4.08 and 4.34 ppm, respectively [35]. Therefore, structure A and C possessing bromomethyl group are considered to be the major brominated structure in the obtained PP-Br.

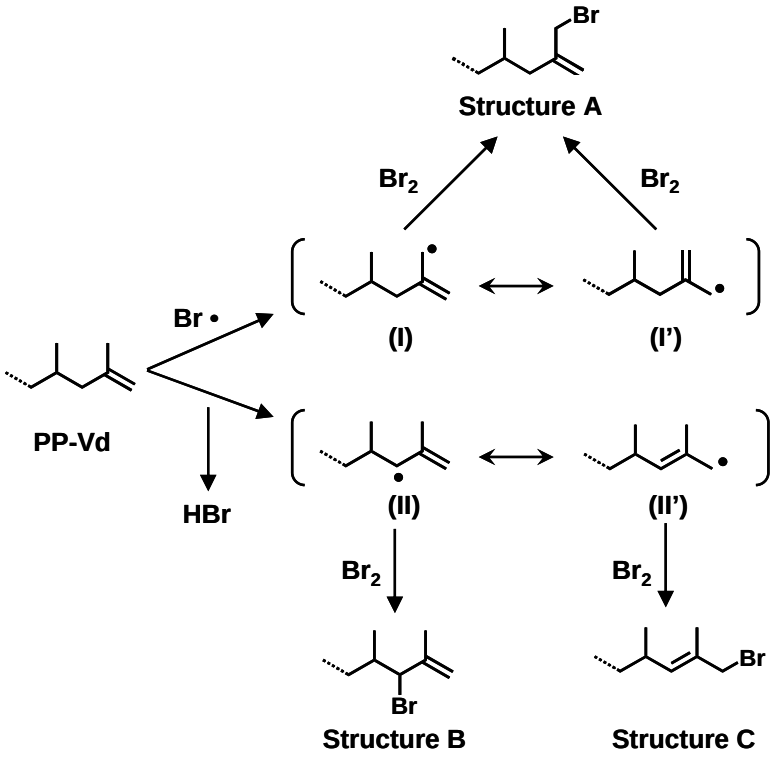

Scheme 1. Plausible structures of the allylic bromide moieties.

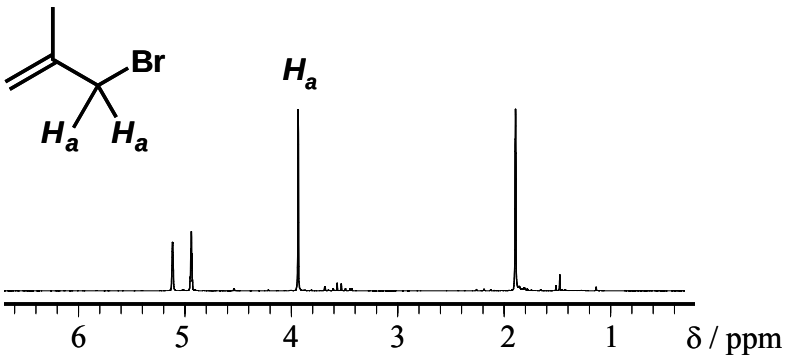

Figure 2. ^{1}H NMR spectrum of 3-bromo-2-methylpropene (in 1,2-dichlorobenzene-d_4 at 25 ^{o}C).

From the relative peak integrations of propylene units observed at δ 0.7 – 1.7 ppm and bromomethyl units at δ 3.7 – 4.1 ppm attributed to the allylic bromide moieties, the total contents of allylic bromide moieties in PP-Br are estimated to be 0.41 mol%. Although the signals assigned to the bromomethylene unit in structure B were also observed at δ 4.2 – 4.4 ppm, their peak intensity was so small that those signals were excepted from the calculation of the content. From the difference between the amounts of vinylidene units in the starting PP-Vd (0.55 mol%) and the allylic bromide moieties (0.41 mol%), about 75 % of the allylic positions in PP-Vd were brominated into the allylic bromide moieties and the other 25 % were supposedly isomerized to isobutenyl unit (-CH=C(CH$_3$)$_2$) due to the presence of HBr generated from the reaction between PP and bromine radical. In ^{1}H NMR analysis, the chemical shift of isobutenyl unit is observed at lower field than that of vinylidene unit [36,37] and therefore its signals would overlap with those of the allylic bromide moieties. Since the number average molecular weight (M_n) was nearly constant throughout the bromination reaction, it was confirmed that undesirable side reactions such as cross-linking and chain scission hardly occurred under this reaction condition. The average number of the allylic bromide moieties in PP-Br was estimated to be 1.35 units per chain calculated from the M_n (13,900 calibrated with PP) and the content of allylic bromide moieties. These results show that PP-Br is possibly a mixture of the structures possessing one or two allylic bromide moieties per chain and these moieties would be located at or near the chain ends of PP backbone.

Radical Polymerization

The radical polymerization of St, MMA and nBA with PP-Br as a macroinitiator was carried out using CuBr/PMDETA catalyst system in *o*-xylene solution at 100 °C as shown in Scheme 2. The viscosity of the polymerization mixture increased over time, suggesting the progress of polymerization and the formation of the polymer with higher molecular weight compared with PP-Br macroinitiator. In the case of the styrene polymerization, the polymerization was stopped at 1, 2, 4 and 7 h to obtain the polymers with variable compositions. The polymerization conditions and results are summarized in Table 1. In all cases, the polymer yields were larger than the amount of the PP-Br macroinitiator. In order to remove the homopolymer of polar monomer supposed to be generated by thermal polymerization, the obtained polymers were treated by Soxhlet extraction with boiling acetone. For all of the obtained polymers, the major portion was insoluble in boiling acetone, indicating that the amount of homopolymer as a by-product was very small and most of the consumed monomer was introduced into the PP backbone to form the polymer hybrids linking between PP and polar segments.

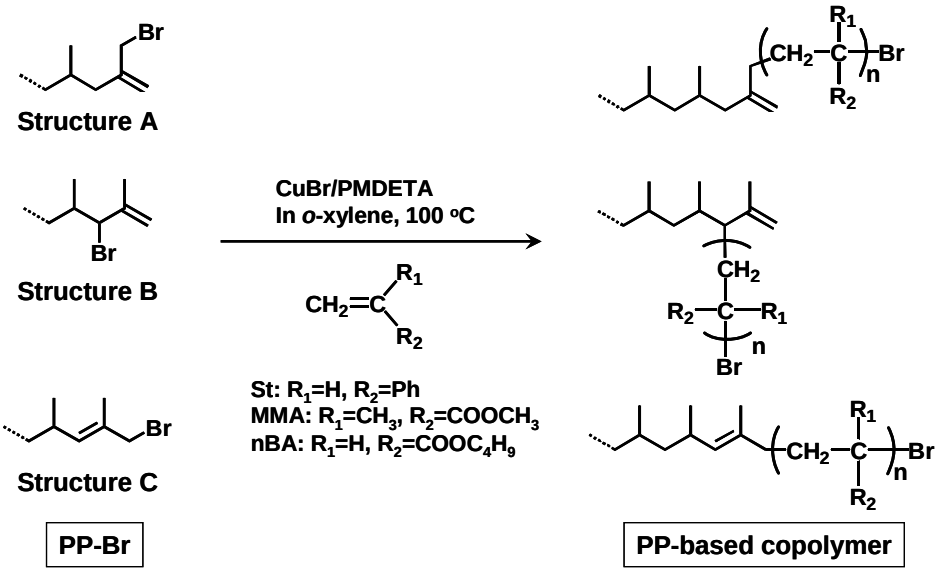

Scheme 2. Radical polymerization with PP-Br macroinitiator.

Table 1. Summary of Radical Polymerizations with PP-Br.

Run	Monomer	Time (h)	Yield (g)	Acetone Insoluble[a] (wt%)	Composition (wt%)[b]		M_n[c] (g mol^{-1})	M_w/M_n[c]
					^{1}H NMR	Gravimetrically		
PP-Vd							19,300	2.07
PP-Br							20,400	2.12
1	St	1	13.1	98.3	24.4	22.5	26,400	2.05
2	St	2	15.2	98.1	35.1	32.7	29,400	2.09
3	St	4	19.4	96.8	48.3	46.7	32,700	2.35
4	St	7	23.2	97.2	56.3	55.6	35,400	2.72
5	MMA	1	24.0	93.9	55.8	55.7	38,200	3.09
6	nBA	1	18.9	89.7	43.2	41.1	30,500	2.23

T = 100 °C; *o*-xylene 100 mL; monomer 50 mL; PP-Br 10 g (0.97 mmol-Br); CuBr 5.00 mmol; PMDETA 5.00 mmol

[a] Determined by Soxhlet extraction in boiling acetone for 9h.

[b] Content of polar segment in the obtained copolymer.

[c] Determined by GPC at 140 °C calibrated with PS standard.

The purified copolymers were analyzed by ^{1}H NMR at 120 °C in 1,1,2,2-tetrachloroethane-d_2 (for PS) or 1,2-dichlorobenzene-d_4 (for PMMA and PnBA) as a solvent. The ^{1}H NMR spectra of some purified copolymers (Run 3, 5 and 6 in Table 1) were shown in Figure 3. In Figure 3a the aromatic and aliphatic proton signals of PS segments were observed at δ 6.4 – 7.2 and 1.4 – 2.2 ppm, respectively. Figure 3b and 3c also revealed some additional signals assigned to PMMA (δ 3.6 and δ 1.0 – 2.4 ppm) and PnBA (δ 4.05 and 1.0 – 2.7 ppm), respectively. From the ratio of the integrated intensities between PP and polar segments, the content of the polar segments in these copolymers can be calculated as shown in Table 1. In all cases, the contents of polar segments determined by ^{1}H NMR agreed well with those calculated gravimetrically from Equation (1).

$$\text{Contents of polar segments (wt-\%)} = 1 - m_0 / (m \times x) \times 100 \qquad \text{Equation (1)}$$

Where m_0 = amount of PP-Br introduced (10 g); m = amount of the obtained polymer; x = weight fraction of acetone insoluble fraction by Soxhlet extraction.

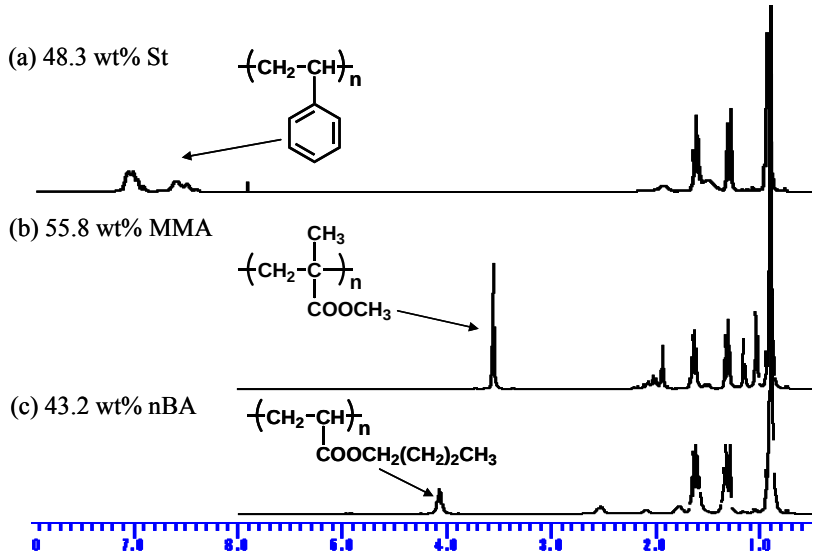

Figure 3. ^{1}H NMR spectra of (a) PP-PS (in 1,1,2,2-tetrachloroethane-d_2), (b) PP-PMMA and (c) PP-PnBA copolymers (in 1,2-dichlorobenzene-d_4) at 120 ^{o}C.

Molecular weight of each purified PP-PS copolymer was measured by GPC and calibrated with PS standard. For comparison, GPC data of PP-Vd and PP-Br calibrated with PS standard were measured again. The GPC traces of the purified PP-PS copolymers are shown in Figure 4. In all cases, the GPC curves showed monomodal molecular weight distributions and a high-molecular-weight tailing was not observed, suggesting no radical coupling under these polymerization conditions. The peak maximum of the GPC curves gradually shifted to the higher molecular weight region as the monomer conversion increased, which indicated the successful chain extension from the PP-Br macroinitiator.

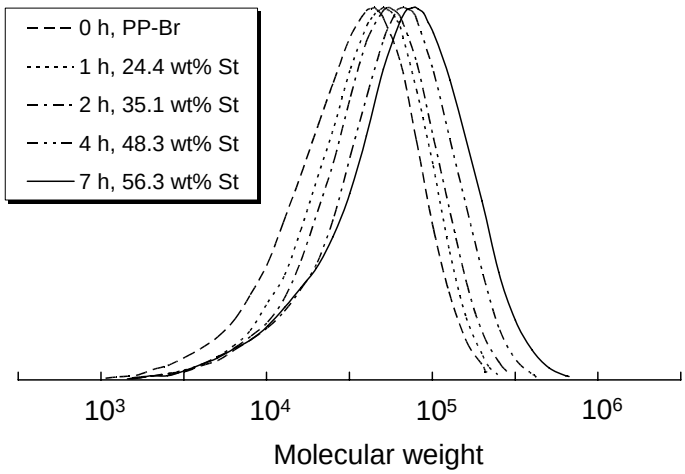

Figure 4. GPC traces of PP-PS copolymers with different polymerization time.

Figure 5 shows the magnification of the ^{1}H NMR spectra for the macroinitiator and the obtained polymers (Run 4, 5 and 6 in Table 1) in the range of δ 3.0 – 5.5 ppm. After St or MMA polymerization, the signals at δ 3.7 – 4.4 ppm (–C*H*$_2$Br and >C*H*Br) completely disappeared. This result indicates that the chain extension polymerization of these monomers was likely to be initiated from the allylic bromide moieties, leading to the block copolymer consisting of PP and polar segments. If the polymerization occurred at all of the allylic bromide moieties, the resulting polymer was supposed to be a mixture of AB and ABA block copolymers and show the bimodal GPC trace (end-functionality of the macroinitiator: 1.35 units per chain as mentioned previously). However, since each obtained copolymer has a monomodal distribution as shown in Figure 4, the initiation efficiency of the macroinitiator is estimated to be not so much high as ABA triblock copolymer can be clearly observed in GPC trace. In the case of nBA polymerization, it was difficult to confirm whether the allylic bromide moieties were completely consumed owing to the signal-overlapping around δ 4.0 ppm, but the changes of the signals at δ 4.7 – 5.5 ppm before and after polymerization suggests that the chain extension polymerization proceeded as in the case of St or MMA polymerization.

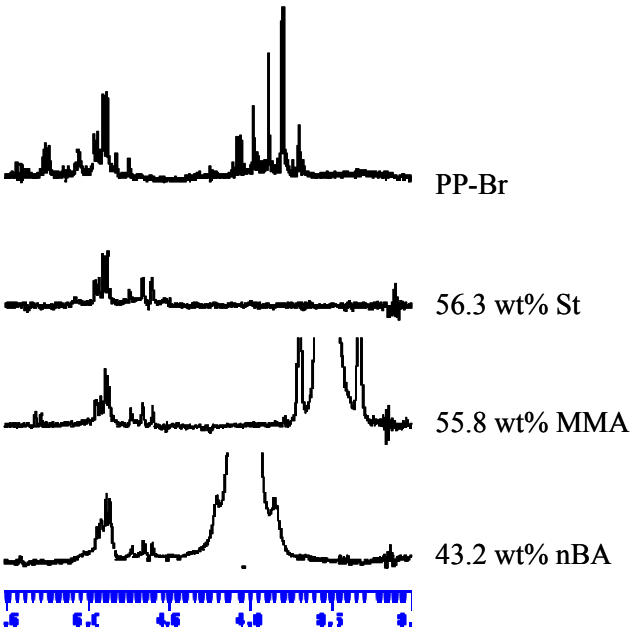

Figure 5. Magnified ^{1}H NMR spectra of the macroinitiator and the obtained copolymers.

In Figure 6, the number average molecular weight (M_n) and polydispersity (M_w/M_n) of the PP-PS block copolymers determined by GPC measurements were plotted with the increase of polymer yield. In the early stage of the polymerization (until 2 h of polymerization), M_n increased linearly along with the increase of polymer yield and the M_w/M_n values were maintained around 2.0. However, the increase of M_n slowed down and M_w/M_n gradually increased with the further progress of polymerization. Such phenomena are likely caused by the termination of propagating radicals. The first order kinetic plots of the styrene polymerization are shown in Figure 7. While the kinetic plots showed linear increase of the conversion over time to 4 h, the polymerization rate after 7 h became slightly slower, indicating that the concentration of propagating radicals decreased. In addition, the decrease of the polymerization rate might occur due to the higher viscosity of the polymerization system.

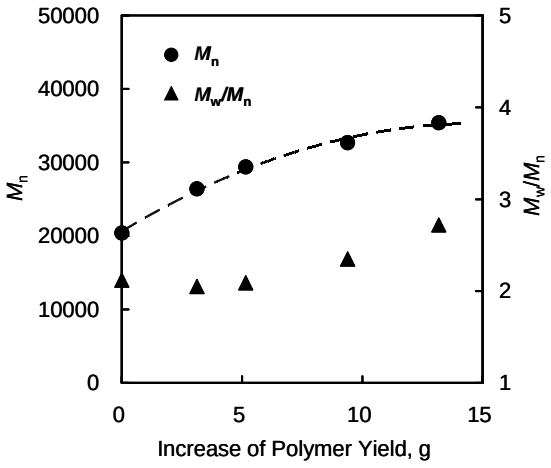

Figure 6. Dependence of number average molecular weight and polydispersity for PP-PS block copolymers with the increase of polymer yield.

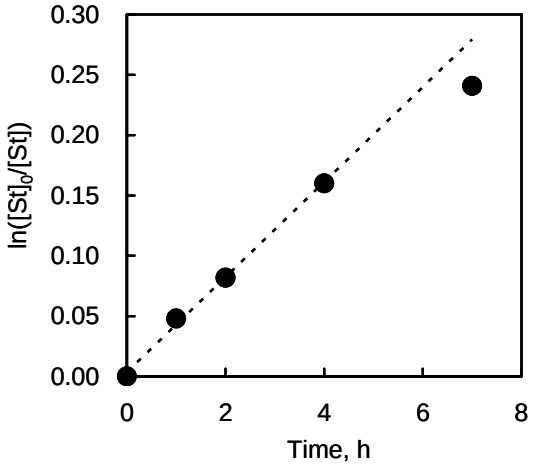

Figure 7. Kinetic plot for the polymerization of styrene initiated by PP-Br.

Figure 8 presents GPC traces of the other block copolymers linking PMMA and PnBA segments. In both cases, the molecular weight obviously increased, suggesting the occurrence of chain extension. In the case of MMA polymerization, the polydispersity of the copolymer was larger than that of PP-PS block copolymer in spite of the similar contents of polar segment. This result would imply the poor initiation efficiency of the allylic bromide moieties for metal-catalyzed CRP of MMA because of the slow addition of allyl radical to MMA as reported by Matyjaszewski *et al* [38]. On the other hand, in the polymerization of nBA, the molecular weight distribution was maintained constant, suggesting that well-controlled polymerization would be achieved.

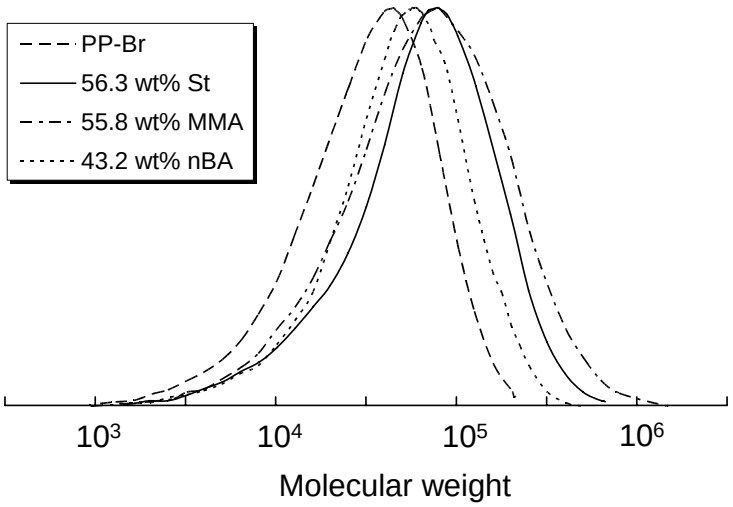

Figure 8. GPC traces of block copolymers with different polar segments.

One of the interesting features of the CRP technique is that the initiation site at the propagating chain end is maintained and can be employed for a next polymerization cycle to yield multi-block copolymers. In this work, the second cycle polymerization of nBA using PP-PS block copolymer containing 48.3 wt-% of styrene (Run 3 in Table 1) was carried out. From ^{1}H NMR analysis of the copolymer purified by Soxhlet extraction, the composition of the copolymer (propylene/styrene/*n*-butyl acrylate) was determined to be 45/41/14 wt-% (Figure 9). This result suggests the possibility of the generation of PP-PS-PnBA triblock copolymer.

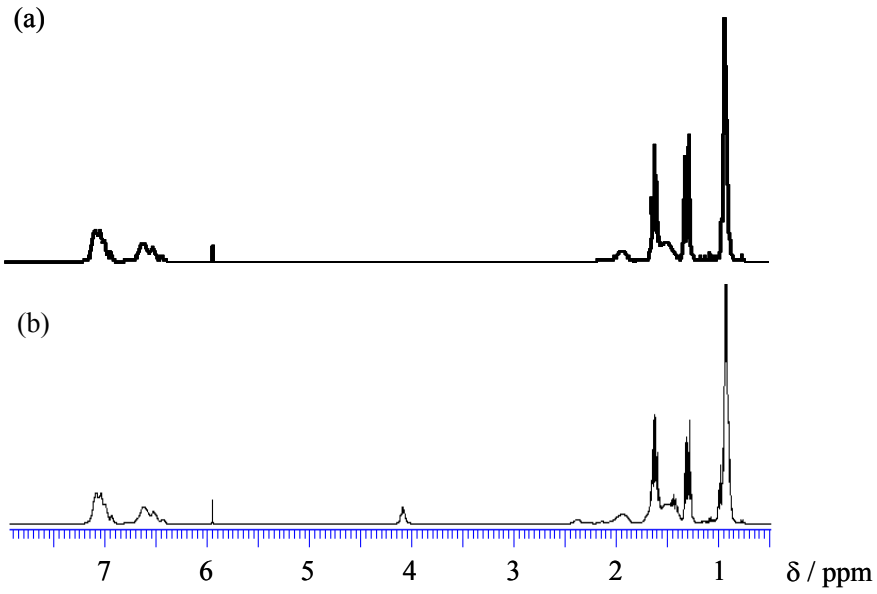

Figure 9. ^{1}H NMR spectra of PP-PS block copolymers (a) before and (b) after nBA polymerization.

Thermal Properties of Block Copolymers

Table 2 shows the thermal properties of brominated PP and the obtained block copolymers determined by DSC analysis. The peak melting temperature (T_m) and the heat of fusion (ΔH_{whole}) were apparently changed after block copolymerization. For block copolymers, T_m values clearly increased in comparison with PP-Br. Particularly, in the case of PP-PS block copolymer, it was observed that the increase of T_m value depended on the styrene content. On the other hand, ΔH_{whole} values gradually decreased with increasing contents of the polar monomers. To estimate the net heat of fusion for the PP part, ΔH_{whole} values can be normalized by the fraction of PP segment in the block copolymer (ΔH_{PP} in Table 2). The obtained ΔH_{PP} values were constant around 100 $J \bullet g^{-1}$ independent of the type and contents of polar monomers. These results indicate that the polar segments did not disturb the crystallization of the PP segment but rather would tend to accelerate the nucleation of the PP segment due to the microphase separation between PP and polar segments.

Table 2. Thermal Properties of PP-Br and PP-based Block Copolymers

Run	Sample	Composition[a] (wt%)	T_m[b] (^oC)	ΔH_{whole}[b] ($J \cdot g^{-1}$)	ΔH_{PP}[b] ($J \cdot g^{-1}$)
	PP-Br		142.6	89.2	
1	PP-PS	24.4	146.8	77.0	101.9
2	PP-PS	35.1	148.1	63.2	97.3
3	PP-PS	48.3	148.9	54.2	104.8
4	PP-PS	56.3	147.9	44.5	101.8
5	PP-PMMA	55.8	148.2	37.7	85.3
6	PP-PnBA	43.2	145.8	55.2	93.9

[a] Content of polar segment in the block copolymers.
[b] Determined by DSC.

TEM Observation

Figure 10 shows TEM micrographs of PP-PS block copolymers. The TEM images of these copolymers revealed the microphase-separation morphology at the nanometer level between PP and PS segments and the distinctive morphologies were observed at different styrene contents. Figure 10(a) mainly shows the spherical microdomains stained by RuO_4 as the minor component (PS) in a PP matrix, while Figure 10(b) represents the alternating lamellar structure of the two components. This morphological transition would occur due to the difference of the compositions. When the molecular weight of the PS segment is much lower than that of the PP segment, the interface

formed between both segments could become a stable curved interface, leading to the spherical morphology. On the other hand, when the molecular weight of the PS segment gets higher to some extent, the interface would tend to be flat and then the morphology changes to the lamellar structure. In the case of much higher styrene contents, it was observed that the lamellar thickness of PS segments increased and the lamellar morphology gradually deformed because of increasing the molecular weight of PS segment as shown in Figure 10(c) and 10(d). In addition, these morphological changes might be caused by the broadened polydispersity or composition distribution as polymerization progresses.

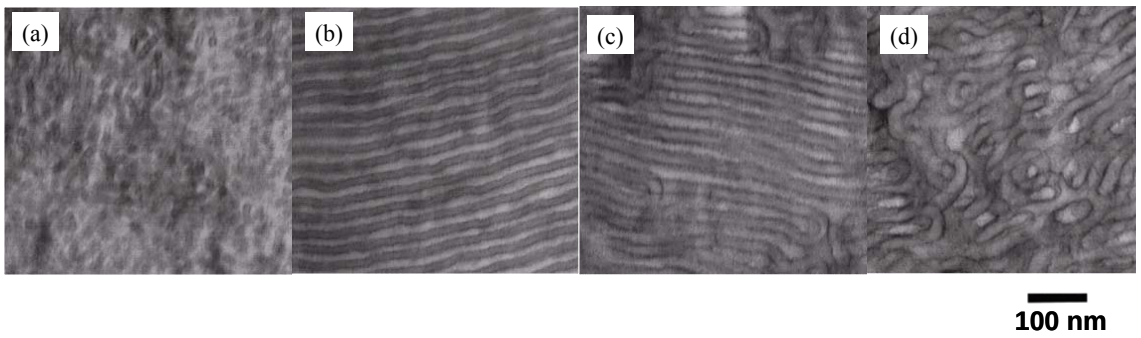

Figure 10. TEM micrographs of the PP-PS block copolymers with styrene contents of (a) 24.4 wt%, (b) 35.1 wt%, (c) 48.3 wt% and (d) 56.3 wt%.

Conclusions

We have described the efficient synthesis of the polypropylene-based block copolymers via controlled radical polymerization. This includes the first example of PP macroinitiator prepared by a direct allylic bromination of terminally-unsaturated PP. The brominated PP was successfully employed as a macroinitiator for controlled radical polymerization of typical polar monomers, such as styrene, methyl methacrylate and *n*-butyl acrylate. From ^{1}H NMR analysis of the brominated PP and the resulting block polymers, the allylic bromide moieties located at or near the chain ends likely initiated the radical polymerization with high initiation efficiency to give the block copolymers consisting of PP and polar segments. From GPC measurements, successful chain extensions from the brominated PP were achieved and block copolymers having polar segments of controlled molecular weight were conveniently synthesized. Furthermore, thus obtained PP-based block copolymers demonstrated the unique thermal properties and morphologies due to the microphase separation between both segments. This new synthetic method is simpler and more facile than the other methods for the synthesis of

polyolefin hybrids and seems attractive for not only academic research, but also for industrial use.

References

[1] Matyjaszewki, K.; Teodorescu, M.; Miller, P. J.; Peterson, M. L. J Polym Sci Part A: Polym Chem 2000, 38, 2440-2448.

[2] Schellekens, M. A. J.; Klumperman, B.; Linde, R. v. d. Macromol Chem Phys 2001, 202, 1595-1601.

[3] Matyjaszewski, K.; Saget, J.; Pyun, J.; Schlögl, M.; Rieger, B. J Macromol Sci Part A: Pure and Appl Chem 2002, 39, 901-913.

[4] Inoue, Y.; Matyjaszewski, K. J Polym Sci Part A: Polym Chem 2004, 42, 496-504.

[5] Inoue, Y.; Matsugi, T.; Kashiwa, N.; Matyjaszewski, K. Macromolecules 2004, 37, 3651-3658.

[6] Kaneyoshi, H.; Inoue, Y.; Matyjaszewski, K. Macromolecules 2005, 38, 5425-5435.

[7] Dix, A.; Ptacek, S.; Poser, S.; Arnold, M. Macromol Symp 2006, 236, 186-192.

[8] Matsugi, T.; Kojoh, S.; Kawahara, N.; Matsuo, S.; Kaneko, H.; Kashiwa, N. J Polym Sci Part A: Polym Chem 2003, 41, 3965-3973.

[9] Kaneko, H.; Matsuo, S.; Kawahara, N.; Saito, J.; Matsugi, T.; Kashiwa, N. Macromol Symp 2007, 260, 9-14.

[10] Kaneko, H.; Matsugi, T.; Kawahara, N.; Matsuo, S.; Kojoh, S.; Kashiwa, N. Kinet Catal 2006, 47, 227-233.

[11] Jankova, K.; Kops, J.; Chen, X.; Batsberg, W. Macromol Rapid Commun 1999, 20, 219-223.

[12] Garcia, F. G.; Pinto, M. R.; Soares, B. G. Eur Polym J 2002, 38, 759-769.

[13] Yamamoto, K.; Miwa, Y.; Tanaka, H.; Sakaguchi, M.; Shimada, S. J Polym Sci Part A: Polym Chem 2002, 40, 3350-3359.

[14] Desai, S. M.; Solanky, S. S.; Mandale, A. B.; Rathore, K.; Singh, R. P. Polymer 2003, 44, 7645-7649.

[15] Yamamoto, K.; Tanaka, H.; Sakaguchi, M.; Shimada, S. Polymer 2003, 44, 7661-7669.

[16] Okrasa, L.; Pakula, T.; Inoue, Y.; Matyjaszewski, K. Colloid Polym Sci 2004, 282, 844-853.

[17] Cao, C.; Zou, J.; Dong, J. –Y.; Hu, Y.; Chung, T. C. J Polym Sci Part A: Polym Chem 2005, 43, 429-437.

[18] Li, H.; Zhao, H.; Zhang, X.; Lu, Y.; Hu, Y. Eur Polym J 2007, 43, 109-118.

[19] Zhang, K.; Wang, J.; Subramanian, R.; Ye, Z.; Lu, J.; Yu, Q. Macromol Rapid Commun 2007, 28, 2185-2191.
[20] Shin, J.; Chang, A. Y.; Brownell, L. V.; Racoma, I. O.; Ozawa, C. H.; Chung, H. –Y.; Peng, S.; Bae, C. J Polym Sci Part A: Polym Chem 2008, 46, 3533-3545.
[21] Zhang, K.; Ye, Z.; Subramanian, R. Macromolecules 2008, 41, 640-649.
[22] Sasaki, D.; Suzuki, Y.; Hagiwara, T.; Yano, S.; Sawaguchi, T. Polymer 2008, 49, 4094-4100.
[23] Kaneko, H.; Saito, J.; Kawahara, N.; Matsuo, S.; Matsugi, T.; Kashiwa, N. Polymer 2008, 49, 4576-4584.
[24] Wang, X. -S.; Luo, N.; Ying, S. -K. Polymer 1999, 40, 4515-4520.
[25] Liu, S.; Sen, A. Macromolecules 2001, 34, 1529-1532.
[26] Hwu, J. -M.; Chang, M. -J.; Lin, J. -C.; Cheng, H, -Y.; Jiang, G. -J. J Organomet Chem 2005, 690, 6300-6308.
[27] Percec, V.; Asgarzadeh, F. J Polym Sci Part A: Polym Chem 2001, 39, 1120-1135.
[28] Percec, V.; Cappotto, A.; Barboiu, B. Macromol Chem Phys 2002, 203, 1674-1683.
[29] Hong, S. C.; Pakula, T.; Matyjaszewski, K. Macromol Chem Phys 2001, 202, 3392-3402.
[30] Sawaguchi, T.; Ikemura, T.; Seno, M. Macromolecules 1995, 28, 7973-7978.
[31] Sawaguchi, T.; Seno, M. Polym J 1996, 28, 817-820.
[32] Resconi, L.; Piemontesi, F.; Franciscono, G.; Abis, L.; Fiorani, T. J Am Chem Soc 1992, 114, 1025-1032.
[33] Kawahara, N.; Kojoh, S.; Matsuo, S.; Kaneko, H.; Matsugi, T.; Toda, Y.; Mizuno, A.; Kashiwa, N. Polymer 2004, 45, 2883-2888.
[34] March, J. In Advanced Organic Chemistry: Reactions, Mechanisms, and Structure, 4th Ed.; J. Wiley & Sons, Inc.; 1992, pp 694-695.
[35] Cheng, D. M.; Gardner, I. J.; Wang, H. C.; Frederick, C. B.; Dekmezian, A. H. Rubber Chem. Technol. 1990, 63, 265-275.
[36] Resconi, L.; Piemontesi, F.; Camurati, I.; Sudmeijer, O.; Nifant'ev, I. E.; Ivchenko, P. V.; Kuz'mina, L. G. J Am Chem Soc 1998, 120, 2308-2321.
[37] Carvill, A.; Zetta, L.; Zannoni, G.; Sacchi, M. C. Macromolecules 1998, 31, 3783-3789.
[38] Jakubowski, W.; Tsarevsky, N. V.; Higashihara, T.; Faust, R.; Matyjaszewski, K. Macromolecules 2008, 41, 2318-2323.

Chapter 3

Synthesis and Characterization of Polypropylene-based Polymer Hybrids Linking Poly(methyl methacrylate) and Poly(2-hydroxyethyl methacrylate)

Abstract

Isotactic polypropylene-based polymer hybrids linking poly(methyl methacrylate) (PMMA) and poly(2-hydroxyethyl methacrylate) (PHEMA) were successfully synthesized by a graft copolymerization from maleic anhydride-modified polypropylene (PP-MAH). PP-MAH reacted with ethanolamine to produce a hydroxyl group containing polypropylene (PP-OH) and the thus obtained PP-OH was treated with 2-bromoisobutyryl bromide and converted to a 2-bromoisobutyryl group-containing polypropylene (PP-Br). The metal-catalyzed radical polymerization of MMA with PP-Br was performed using a copper catalyst system in *o*-xylene solution at 100 °C to give the PP-based polymer hybrids linking PMMA segments (PP-PMMA hybrids). Thus obtained PP-PMMA hybrids demonstrated higher melting temperature than PP-Br and microphase-separation morphology at the nanometer level owing to the chemical linkage between both segments. On the other hand, the polymer hybrids linking PHEMA segment (PP-PHEMA hybrids) were also obtained by the radical polymerization of HEMA with PP-Br in *o*-xylene slurry at 25 °C. TEM observation suggested that the polymerization mainly initiated on the surface of the PP-Br powder, led to the peculiar core-shell-like morphology. These PP-PHEMA hybrid powders showed a good affinity with water due to the hydrophilicity of the PHEMA segments.

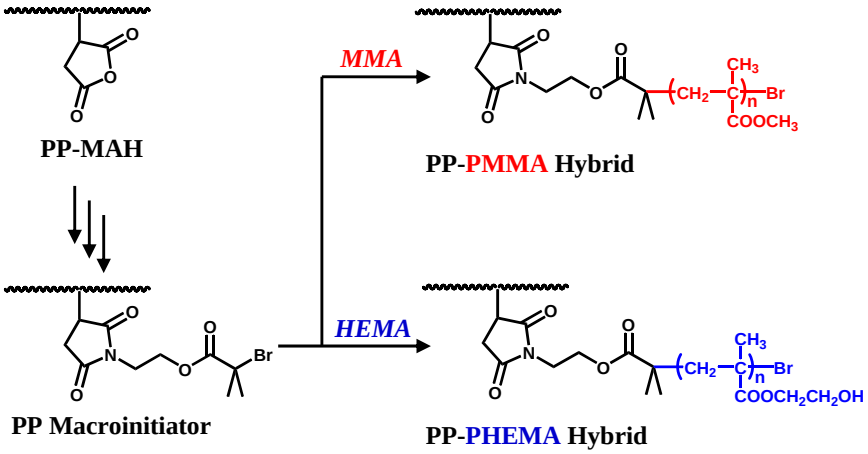

Introduction

As mentioned in *General Introduction*, one of the synthetic methods for the polyolefin hybrids is a post-polymerization process with polyolefin macroinitiators, which are obtained by transforming a variety of functionalized polyolefins to radical, anionic or cationic polymerization initiators. To prepare the functionalized polyolefin, several kinds of methods using chain transfer reaction at olefin polymerization, olefin copolymerization with polar monomers and chemical modification of terminally unsaturated polyolefin have been reported. In *Chapter 1* and *2*, the polyolefin-based block copolymers were successfully prepared by the end-functionalization of the terminally unsaturated polyolefins and subsequent metal-catalyzed living radical polymerization. This chapter is aimed at the polyolefin-based graft copolymers, which have a polyolefin backbone and some polymer branches. Previously, the authors reported on the functionalized polyethylene (PE) with reactive groups such as hydroxyl [1] or amino [2] groups under precise control of the positions of the functional groups. In particular, this methodology can selectively prepare both the terminally functionalized PE and the functionalized branch-grafted PE. Their reactive groups can be easily converted to initiation sites for the various polymerization systems, such as metal-catalyzed radical polymerization, reversible addition-fragmentation chain transfer (RAFT) polymerization and ring-opening anionic polymerization. Of these site-selective functionalized polyolefins, the functionalized branch-grafted PE gave a variety of graft copolymers such as PE-*g*-PMMA, PE-*g*-poly(*n*-butyl acrylate) [3], PE-*g*-poly(propylene glycol), PE-*g*-poly(ε-caprolactone) [4]. In addition, there are some examples of the polyolefin-based graft copolymers produced by radical or anionic polymerization with functionalized polyolefin [5-7]. These functionalization methods of polyolefin, however, need unusual olefin polymerization conditions in the presence of polar monomers, which are poisonous for most olefin polymerization catalysts to retard the polymerization. Therefore, the type of polyolefins and the polymerization conditions are generally restricted.

Alternatively, it has been well known that some commercially available functionalized polyolefins are produced by a direct copolymerization or a radical grafting method. Many types of ethylene copolymers with polar monomers, such as vinyl acetate, ethyl acrylate, glycidyl methacrylate and so on, are produced by direct radical copolymerization under a high pressure process. Chemical modification is one of the useful approaches to preparing the polyolefin macroinitiators. For example, Matyjaszewski *et al.* reported that PE macroinitiators prepared from commercially

available poly(ethylene-*co*-glycidyl methacrylate) initiated atom transfer radical polymerization of St and MMA, leading to the corresponding PE-*g*-polystyrene and PE-*g*-PMMA [8].

On the other hand, the radical grafting of polar monomers on polyolefins is also an important method for preparing functionalized polyolefins and the incorporation of many kinds of polar monomers, such as methacrylates, acrylates, styrene and so on, has been reported [9,10]. Maleic anhydride-modified polyolefin (PO-MAH) is well known as a commercially available functionalized polyolefin and many types of PO-MAH with various MAH-contents, molecular weights and olefin compositions have been industrially produced. Compared with the direct copolymerization method, this method has the advantage in that it can provide not only ethylenic but also propylenic and higher α-olefinic polymers. Because of its accessibility and high reactivity, PO-MAHs are widely used for various purposes such as additives, adhesives, coatings and compatibilizers for polymer blends. Furthermore, they can be also used as a building block for the PO-based graft copolymers. For example, coupling reactions of them with the other polymer chains possessing some reactive functional groups give the corresponding graft copolymers, such as polyolefin-polyamide [11], polyolefin-polyester [12] and polyolefin-polyurethane [13]. However, there are few reports on graft copolymers syntheses via the graft copolymerization using macroinitiators derived from PO-MAHs [14].

In this article, the authors herein introduce the PP-based polymer hybrids linking PMMA or poly(2-hydroxyethyl methacrylate) (PHEMA) using a new synthetic method through a combination of PP-MAH and metal-catalyzed radical polymerization. In addition, the authors also discuss their unique characteristics and properties demonstrated by thermal analysis and transmission electron microscopy (TEM) observation.

Experimental

General Procedures and Materials

All manipulations of air- and water-sensitive materials were preformed under a dry nitrogen atmosphere in a conventional nitrogen-filled glove box. CuBr, *N,N,N',N'',N''*-pentamethyldiethylenetriamine (PMDETA), ethanolamine, triethylamine and 2-bromoisobutyryl bromide (BiBB) were purchased from Wako Pure Chemical Industries and used without further purification. MMA and HEMA (Wako Pure Chemical Industries) were dried over CaH_2 and distilled *in vacuo*. *o*-Xylene used as a

solvent were dried over Al_2O_3 and degassed by bubbling with N_2 gas. Maleic anhydride-modified polypropylene (PP-MAH) was prepared in the conventional way [15]. From GPC measurement and ^1H NMR analysis, the number average molecular weight of the obtained PP-MAH was 33,000 and the content of MAH was 0.14 mol% as shown later in Table 1.

Preparation of PP Macroinitiator (PP-Br)

A typical process is as follows: *o*-Xylene (700 mL) and PP-MAH (75 g, 2.5 mmol-MAH) were placed in a 1-L glass reactor equipped with a mechanical stir bar and then PP-MAH was dissolved at 120 ^oC for 3 h under a nitrogen atmosphere. Then, ethanolamine (200 mL, 3.3 mmol) was added and the mixture was maintained at 120 ^oC for 6 h under stirring. The reaction mixture was poured into 2 L of acetone. The precipitated polymer was collected by filtration, washed with acetone and dried *in vacuo* at 80 ^oC for 10 h to give 75.1 g of hydroxyl group containing PP (PP-OH) as a white powder. Thus obtained PP-OH (71 g) and toluene (700 mL) were placed in a 1-L glass reactor equipped with a mechanical stir bar and then PP-OH was dissolved at 105 ^oC for 2 h under a nitrogen atmosphere. Triethylamine (8.1 mL, 54.4 mmol) and BiBB (6.7 mL, 54.4 mmol) were added to the reactor and the mixture was stirred at 105 ^oC for 2 h. The reaction mixture was poured into 2 L of methanol. The resulting polymer was collected by filtration, washed with methanol and dried *in vacuo* at 80 ^oC for 10 h to give 71 g of 2-bromoisobutyryl group containing PP (PP-Br).

MMA Polymerization with PP Macroinitiator

A typical polymerization process (for PP-PMMA1 in Table 2) is as follows: PP-Br (15 g, 0.47 mmol as 2-bromoisobutyryl group) and *o*-xylene (100 mL) were placed in a 500-mL glass reactor equipped with a mechanical stir bar and then PP-Br was dissolved at 100 ^oC for 2 h under nitrogen atmosphere. Then, MMA (3.8 mL) and a solution of CuBr/PMDETA in *o*-xylene (0.89 mmol as a copper atom and 1.78 mmol as PMDETA, pretreated for 5 min. at ambient temperature) were added to the reactor and the mixture was maintained at 100 ^oC for 4 h under stirring. After adding 200 mL of toluene and cooling, the reaction mixture was poured into 1.5 L of methanol and the white solid was collected by filtration, washed with methanol and dried *in vacuo* at 80 ^oC for 10 h. As shown later in Table 2, three kinds of polymers were obtained.

HEMA Polymerization with PP Macroinitiator

A typical polymerization process (for PP-PHEMA1 in Table 5) is as follows: PP-Br

(15 g, 0.47 mmol as 2-bromoisobutyryl group) and *o*-xylene (250 mL) were placed in a 500-mL glass reactor equipped with a mechanical stir bar and PP-Br was dissolved at 130 ^{o}C for 1 h under nitrogen atmosphere. Then the obtained solution was cooled to 25 ^{o}C for 2 h under stirring to give the slurry of the precipitated PP-Br in *o*-xylene. HEMA (4.3 mL) and a solution of CuBr/PMDETA in *o*-xylene (0.89 mmol as a copper atom and 1.78 mmol as PMDETA, pretreated for 5 min. at ambient temperature) were added to the reactor and the mixture was maintained at 25 ^{o}C for 4 h under stirring. Then, the resulting slurry was poured into 1.5 L of methanol and the white solid was collected by filtration, washed with methanol and dried *in vacuo* at 80 ^{o}C for 10 h. As shown later in Table 5, two kinds of polymers were obtained.

Preparation of the Blended Polymers

A typical procedure is as follows: The polymers (*ca.* 1 g as a total amount) and *o*-xylene (30 mL) were added to a 100-mL glass reactor equipped with a magnetic stir bar and were stirred at 130 ^{o}C until the polymer mixture was homogeneous (*ca.* 2 h). The blended polymer was precipitated into cold methanol (400 mL) and then dried *in vacuo* at 80 ^{o}C for 10 h.

Analytical Procedures

^{1}H NMR spectra were recorded on JEOL GSX-400 (400 MHz) spectrometers using 1,2-dichlorobenzene-d_4 as a solvent at 120 ^{o}C. The gel permeation chromatograms (GPC) calibrated with PP were recorded by using a Waters Alliance GPC2000 equipped with four TSKgel columns (two sets of TSKgelGMH6-HT and two sets of TSKgelGMH6-HTL) and a refractive index detector at 140 ^{o}C in 1,2-dichlorobenzene and those calibrated with PS standard were recorded by using a CFC T-150A (Mitsubishi Kagaku Corp.) equipped with three columns (Shodex AT-806MS) and an IR spectrometer Miran 1ACVF at 140 ^{o}C in 1,2-dichlorobenzene. Elemental analysis for CHN was carried out on a Perkin-Elmer 2400II type analyzer and that for O was carried out on an Elementar vario EL III type analyzer. Attenuated total reflection infrared (ATR/IR) spectra were recorded on a Varian FTS-6000 FT-IR spectrometer over a spectral range from 4000 to 400 cm^{-1} at a resolution of 2 cm^{-1} (32 cumulative scans). A thin film for IR analysis was prepared by a compression molding at 250 ^{o}C. For a determination of bromine content in PP-Br, PP-Br was pretreated by oxygen flask combustion method to be analyzed using a Dionex DX-500 ion chromatography system consisting of two columns (IonPac AS12A and IonPac AG12A) and a suppressed conductivity detector. The peak melting temperature of the polymers was measured by

using Seiko Instruments RDC220 differential scanning calorimeter. The DSC curves were recorded during the second heating cycle from 30 to 200 ^{o}C, with a heating rate of 10 ^{o}C/min.

Transmission Electron Microscopy (TEM) Observations

Ultrathin (*ca.* 100 nm) sections of the polymer, which had been pressed into a sheet, were cut on a Reica Ultracut microtome equipped with a diamond knife at a low temperature and were then stained with RuO_4. TEM observations were made with a Hitachi H-7000 transmission electron microscope at an acceleration voltage of 75 kV and at a magnification of 5,000, 20,000 and 100,000.

Results and Discussion

Synthesis of PP Macroinitiators

The synthetic route of PP macroinitiators is shown in Scheme 1. In the first step, the succinic anhydride (SA) group grafted in PP-MAH reacted with excess ethanolamine to give the PP with *N*-(2-hydroxyethyl)succinimide group (PP-OH). The reaction was performed in *o*-xylene solution at 120 ^{o}C. In the second step, the PP-OH reacted with 2-bromoisobutyryl bromide to produce PP-Br, which has 2-bromoisobutyryl groups as an initiation site for the metal-catalyzed radical polymerization. In general, the bromination reaction is preferably performed under mild conditions to avoid any side reactions. However, in the case of crystalline polyolefin such as polyethylene and polypropylene, high temperature and long holding time are often needed to complete the reaction owing to low solubility and low hydroxyl-group concentration [3,16,17]. Therefore, in this case the reaction was carried out in toluene solution at 105 ^{o}C through the addition of an excess amount of 2-bromoisobutyryl bromide and triethylamine.

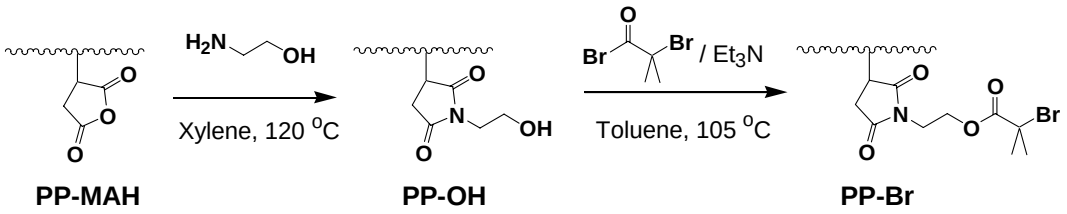

Scheme 1. Synthesis of PP-Br.

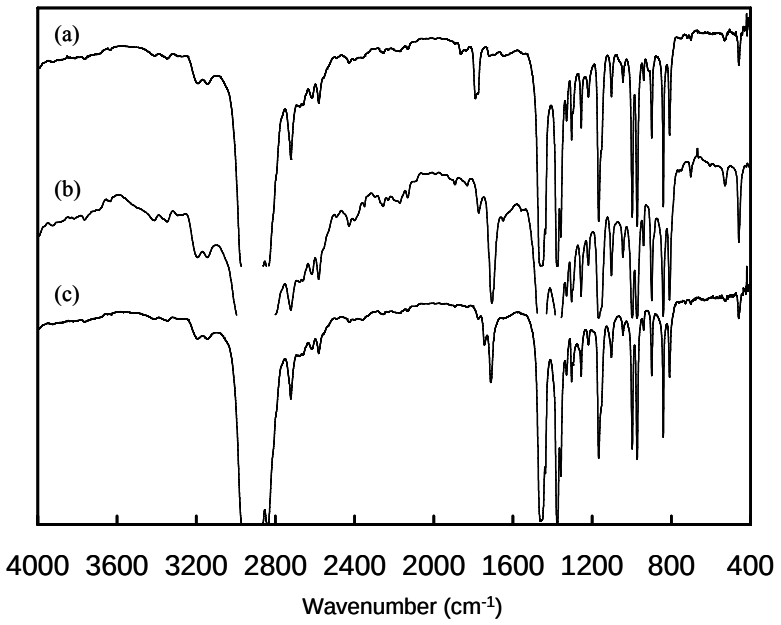

Figure 1. IR spectra of (a) PP-MAH, (b) PP-OH and (c) PP-Br.

Figure 1 shows the IR spectra of PP-Br and its precursors, PP-MAH and PP-OH. In Figure 1(a), the absorption bands for C=O stretching vibration of SA group were observed around 1800 cm^{-1}. After a reaction with ethanolamine, the absorption bands for C=O stretching vibration at 1770 and 1700 cm^{-1} appeared as shown in Figure 1(b). These absorption bands would be able to be assigned to a succinimide group, suggesting that SA group predominantly reacted with amino group rather than hydroxyl group of ethanolamine. In Figure 1(c), new absorption bands for C=O stretching vibration of an ester group at 1740 cm^{-1} were observed in addition to the succinimide group. These results of IR analysis obviously indicate a successful progress of the expected functionalization reactions as shown in Scheme 1.

Figure 2 shows ^{1}H NMR spectra of PP-Br and its precursors, PP-MAH and PP-OH. For PP-MAH (Figure 2(a)), the broad and multiple signals of δ 2.5-3.25 ppm would be assigned to the protons of the SA ring (-CH_2-CH<) and the signals of the PP backbone were observed at δ 0.7-2.0 ppm. For PP-OH (Figure 2(b)), two broad signals of δ 3.60 and 3.65 ppm correspond to two kinds of methylene protons (>N-CH_2-CH_2-OH) and the signals of the SA ring observed in Figure 2(a) slightly shifted to the higher magnetic field (δ 2.4-3.05 ppm), which would show the SA group was converted to the succinimide group by a reaction with ethanolamine. The relative intensities of the signals at 3.65, 3.60 and 2.4-3.05 ppm were roughly estimated to be 2/2/3, respectively, indicating the existence of the *N*-(2-hydroxyethyl) succinimide group. For PP-Br

(Figure 2(c)), in addition to the signals of the succinimide ring, the signals of methylene protons (>N-CH_2-CH_2-OCO-) and methyl protons (-OCOC(CH_3)$_2$Br) were observed at 4.25, 3.70 and 1.85 ppm, respectively. Because the resolution of ^{1}H NMR spectrum for PP-Br was not enough to determine the content of 2-bromoisobutyrate group, a bromine content in PP-Br was analyzed by ion chromatography and estimated to be 0.25 wt%. Assuming all of the detected bromine atoms attributes to 2-bromoisobutyrate group, its content can be calculated to be 0.13 mol%, indicating that more than 90 % of SA groups in the starting PP-MAH were converted into the 2-bromoisobutyrate group. These functionalization results were summarized in Table 1. It can be seen that molecular weight and molecular weight distribution of PP-OH and PP-Br were higher than those of PP-MAH. One of the reasons for these results might be because the coupling reaction between PP-OH and PP-MAH occurred to give the higher molecular weight component. However, both samples completely dissolve in toluene at 110 ^{o}C and therefore, such portion would be vanishingly small. From the number average molecular weight of the obtained PP-Br, the average number of the 2-bromoisobutyrate group in PP-Br can be estimated to be 1.1 units per chain. Namely, all of the PP backbones averagely have one initiation site. The thus-obtained PP-Br was used as a macroinitiator for the metal-catalyzed radical polymerization.

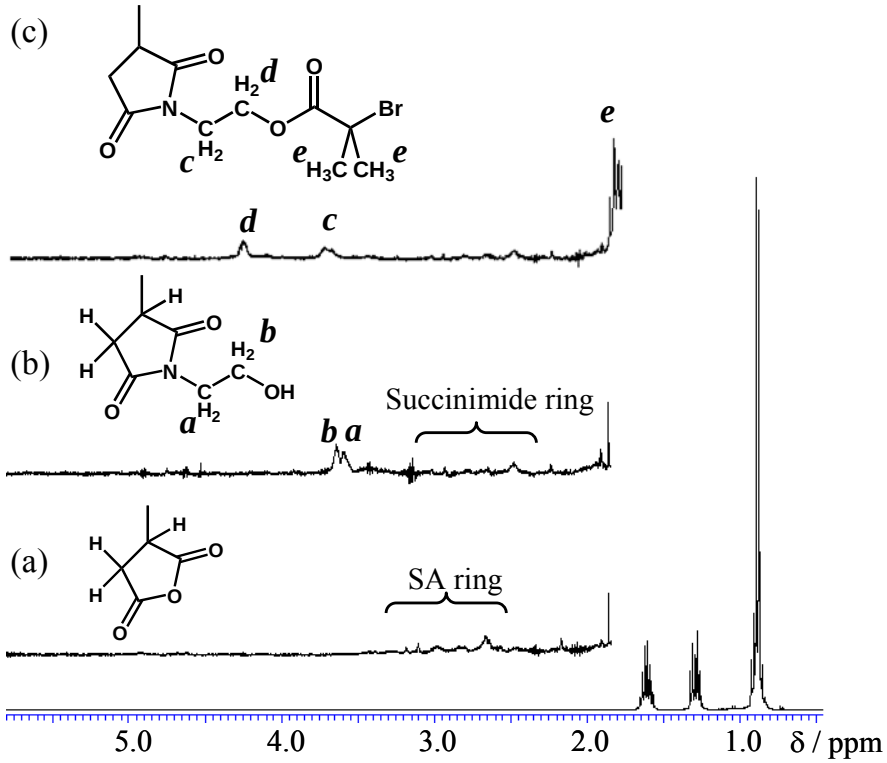

Figure 2. ^{1}H NMR spectra of (a) PP-MAH, (b) PP-OH and (c) PP-Br (400 MHz in 1,2-dichlorobenzene-d_4 at 120 ^{o}C).

Table 1. Summary of Functionalization of PP

Sample	Content of Functional Group	M_w[c] (g mol^{-1})	M_n[c] (g mol^{-1})	M_w/M_n[c]	Functionality[d] (unit/chain)
PP-MAH	MAH, 0.14 mol%[a]	95,700	33,000	2.9	1.1
PP-OH	OH, 0.13 mol%[a]	139,000	36,900	3.8	1.2
PP-Br	Br, 0.25 wt% [b]	114,000	33,600	3.4	1.1

[a] Determined by ^{1}H NMR.
[b] Determined by ion chromatography.
[c] Measured at 140 °C in 1,2-dichlorobenzene with PP calibration.
[d] Calculated from content of functional group and M_n.

Table 2. Summary of MMA Polymerization[a]

Sample	PP-Br[d] (g)	MMA (mL)	CuBr (mmol)	Yield (g)	THF Insoluble Part[e] (wt%)	MMA Content[f] (mol%)	MMA Content[f] (wt%)
PP-PMMA1	15.0	3.8	0.89	16.0	98.4	2.9	6.6
PP-PMMA2	15.0	9.5	0.89	18.3	97.6	8.4	17.9
PP-PMMA3	15.0	53.2	0.89	30.0	96.7	25.9	45.5
PP-PMMA4[b]	3.0	10.6	0.18	2.9	-	n.d.	n.d.
PP-PMMA5[c]	3.0	10.6	0	3.1	93.0	n.d.	n.d.

[a] Polymerization conditions: $[PP\text{-}Br]_0/[CuBr]_0/[PMDETA]_0$ = 1/1.9/3.8 (molar ratio) in 100 mL of *o*-xylene at 100 °C for 4h.
[b] PP-OH was used in place of PP-Br. Polymerization conditions: $[CuBr]_0/[PMDETA]_0$ = 1/2 (molar ratio) in 20 mL of *o*-xylene at 100 °C for 4h.
[c] Polymerization conditions: $[PP\text{-}Br]_0/[CuBr]_0/[PMDETA]_0$ = 1/0/0 (molar ratio) in 20 mL of *o*-xylene at 100 °C for 4h.
[d] 0.031 mmol of Br/g of polymer.
[e] Determined by Soxhlet extraction in boiling THF for 9h.
[f] Determined by ^{1}H NMR for THF insoluble part. n.d. = not determined.

Radical Polymerization of MMA Initiated by PP Macroinitiator

It is well known that the metal-catalyzed radical polymerization realized controlled polymerization of various vinyl monomers, represented by (meth)acrylates and styrenes, to give the precisely-controlled polymers [18,19]. In particular, it is an effective method for the syntheses of block and graft copolymers using macroinitiators. We applied this method to create the polymer hybrids linking between PO and polar polymers. The polymerization of MMA with a PP macroinitiator was carried out in an *o*-xylene solution using CuBr/PMDETA as a catalyst system. Table 2 summarizes the results by altering polymerization conditions. Because of high molecular weight of PP macroinitiator, a significant amount of *o*-xylene was needed to dissolve the PP macroinitiator and reduce the viscosity in the early stage of polymerization, resulting in very low concentration of initiation sites in this polymerization system. Therefore, the

excess amount of catalyst had to be used for achieving sufficient initiation and propagation rate as shown in Table 2. In the case of PP-PMMA1, 2 and 3, the viscosity of the polymerization system increased as polymerization time increased and this suggested the progress of MMA polymerization to give a polymer with higher molecular weight compared with the starting PP macroinitiator. The polymerization was stopped by cooling of the reactor with an ice bath. The resulting mixture was poured into methanol and the precipitated polymer was collected by filtration. To remove the homo-PMMA produced by thermal polymerization, the obtained polymers were purified by the Soxhlet extraction with boiling THF. In each sample, the extracted fraction was only a small amount, suggesting that most of the consumed monomer was grafted onto the PP backbone. In contrast, when PP-OH was used as a macroinitiator in place of PP-Br (PP-PMMA4), the polymer yield did not increase. In addition, the graft polymerization did not proceed in the absence of catalyst (PP-PMMA5).

The obtained copolymers purified by Soxhlet extraction were analyzed at 120 °C by ^{1}H NMR in 1, 2-dichlorobenzene-d_4 as a solvent. Figure 3 shows the ^{1}H NMR spectra of the purified copolymers. From the ratio of two integrated intensities between δ 3.52 ppm assigned to the methyl ester protons of the PMMA segment and δ 0.8 – 2.3 ppm assigned to the propylene unit and PMMA backbone, each copolymer contained 6.6, 17.9 and 45.5 wt% of PMMA segment, respectively.

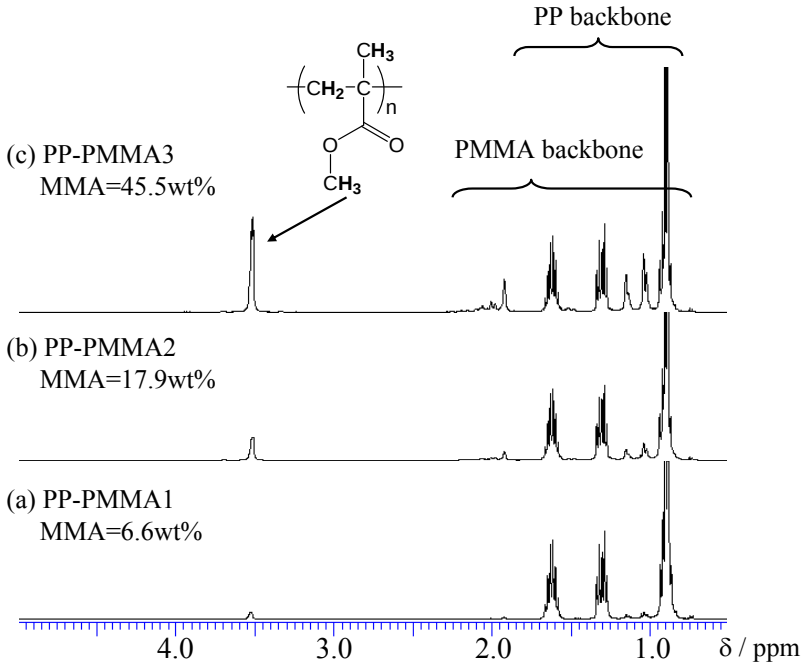

Figure 3. ^{1}H NMR spectra of the polymer hybrids, (a) PP-PMMA1, (b) PP-PMMA2 and (c) PP-PMMA3 (400 MHz, in 1,2-Dichlorobenzene-d_4 at 120 °C).

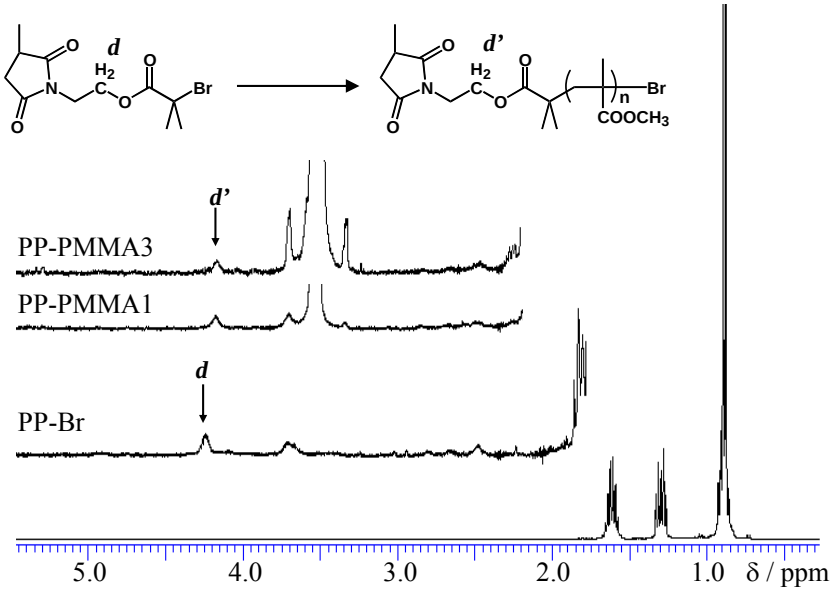

Figure 4. Evolution of the ^{1}H NMR signals of the initiating species during the polymerization of MMA with PP-Br (400 MHz, in 1,2-Dichlorobenzene-d_4 at 120 ^{o}C).

Furthermore, the signals of methylene protons adjacent to the ester group (-CH_2-OCO-) were shifted to the slightly higher magnetic field in comparison with the PP-Br as shown in Figure 4. This indicates that the polymerization would be initiated at the 2-bromoisobutyryl group in the PP-Br and its initiation efficiency may be nearly complete [20]. The GPC traces of PP-Br and purified polymers are shown in Figure 5. Since GPC curves were maintained monomodal molecular weight distribution after MMA polymerization, the obtained polymers had almost no PMMA homopolymers with extremely high molecular weight, which might be generated by thermal polymerization at 100 ^{o}C. The peak top of the GPC curve gradually shifted to higher molecular weight region as the MMA content increased, which indicated the successful graft copolymerization onto the PP-Br macroinitiator. The data derived from GPC measurement are shown in Table 3. The weight average molecular weight of PP-PMMA copolymers obviously increased with increasing MMA content. However, the number average molecular weight of PP-PMMA1 and PP-PMMA2 was lower than that of PP-Br and the molecular weight distribution of PP-PMMA copolymer was significantly broadened. Although these phenomena would suggest the poorly-controlled polymerization of MMA owing to high polymerization temperature, at least it was confirmed that the PP-based polymer hybrids linking PMMA segment (PP-PMMA hybrid) were obtained by MMA polymerization with PP-Br and the resulting polymers mainly consist of the PP-*g*-PMMA graft copolymer.

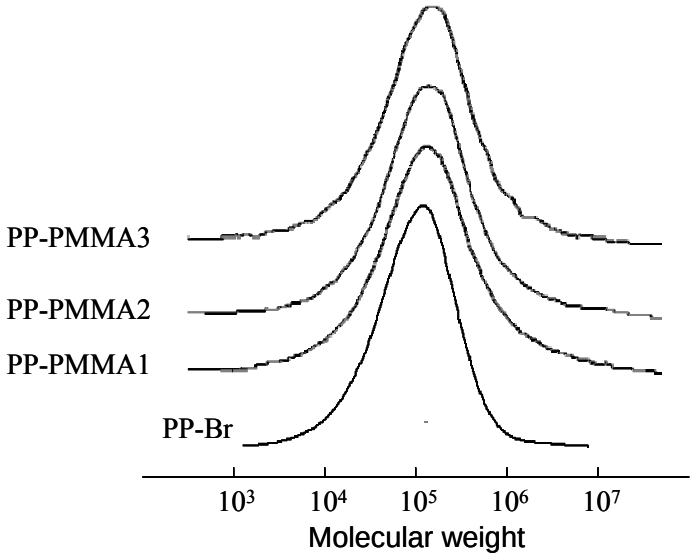

Figure 5. GPC traces of PP-Br before and after MMA polymerization.

Table 3. GPC Data of PP-Br before and after MMA Polymerization[a]

Sample	M_w (g mol^{-1})	M_n (g mol^{-1})	M_w/M_n
PP-Br	168,000	48,600	3.4
PP-PMMA1	416,000	42,400	9.8
PP-PMMA2	671,000	47,700	14.1
PP-PMMA3	714,000	49,000	14.6

[a] Measured at 140 ^{o}C in 1,2-dichlorobenzene with PS calibration.

Table 4 summarizes the DSC results of PP macroinitiator and the obtained PP-PMMA hybrids. The thermogram of each sample was recorded in the second heating run at 10 ^{o}C / min to eliminate the thermal history. In all samples, it is clear that the peak melting temperatures (T_m) at around 160 ^{o}C show the PP segments in the backbone and heat of fusion (ΔH) gradually decreased with increasing MMA content of the hybrid. The relative crystallinity, which is calculated by the ΔH of the hybrid divided by the ΔH of the PP-Br and the wt% of PP in the hybrid, can be used to estimate the crystallinity of the PP part in the hybrid compared to the PP-Br [11]. In spite of increase of the MMA content, the relative crystallinities of the PP part in the hybrids are nearly constant. This result suggests that PMMA segments grafted on the PP backbone would not disturb the crystallization of PP segments at least within 45.5 wt% of MMA content.

Table 4. Summary of DSC Results for PP-Br and PP-PMMA Hybrids

Sample	MMA Content[a] (wt%)	T_m[b] (°C)	ΔH[b] (J/g)	Relative Crystallinity of PP Part[c] (%)
PP-Br	0	157.1	91.5	100
PP-PMMA1	6.6	160.0	83.7	98
PP-PMMA2	17.9	159.2, 146.5	75.9	101
PP-PMMA3	45.5	162.2, 148.2	54.0	108

[a] Determined by ^{1}H NMR for THF insoluble part.
[b] Observed by DSC measurement.
[c] Relative crystallinity (%) = [$\Delta H_{PP\text{-}PMMA}$ / ($\Delta H_{PP\text{-}Br}$ x weight ratio of PP in the PP-PMMA hybrid)] × 100.

Morphology of PP-PMMA Hybrids

The morphology of these PP-PMMA hybrids was observed by TEM, as shown in Figure 6. Despite the different MMA contents, the microphase-separation morphology at the nanometer level between the PP phase (stained by RuO_4) and the PMMA phase (unstained by RuO_4) was observed in all samples, indicating the chemical linkage between both segments. In the cases of the low and middle MMA contents (6.6 and 17.9 wt%, Figure 6(a) and 6(b)), both phases finely dispersed and the distinction as to which phase was matrix was impossible. On the other hand, in the case of higher MMA content (45.5 wt%, Figure 6(c)) the PMMA domains were partially observed. It is thought that these domains form by the aggregation of the longer PMMA segments grafted on PP backbone.

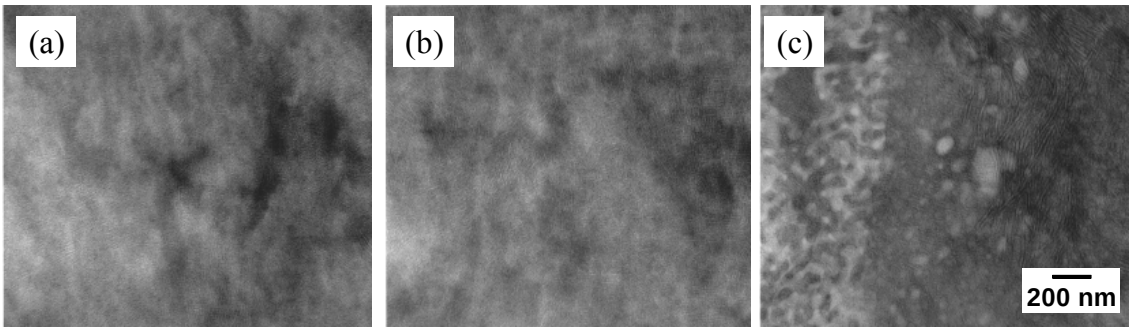

Figure 6. TEM images of the PP-PMMA hybrids with different MMA contents, (a) 6.6 wt%, (b) 17.9 wt% and (c) 45.5 wt%.

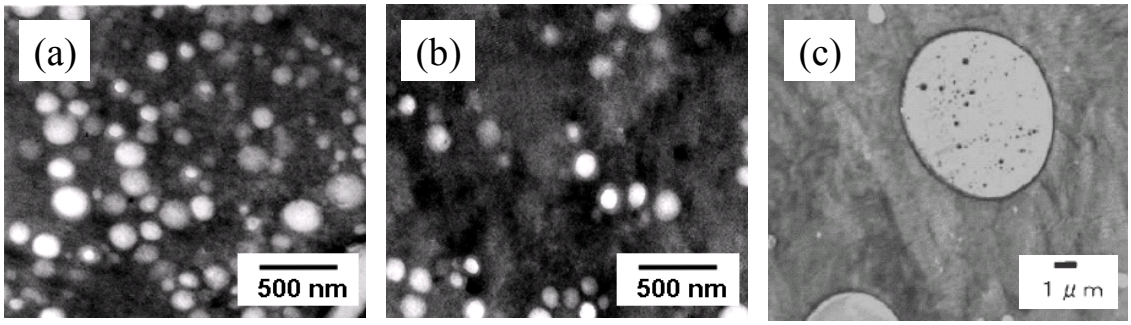

Figure 7. TEM images of homo-PP/homo-PMMA blended polymer adding the PP-PMMA hybrid with MMA contents of (a) 6.6 wt% and (b) 45.5 wt% (PP/PMMA/PP-PMMA hybrid = 70/30/10 w/w/w) and (c) homo-PP/homo-PMMA blended polymer without the PP-PMMA hybrid (PP/PMMA = 70/30 w/w).

Compatibility of PP-PMMA Hybrids for PP/PMMA Blend

Because the polymer hybrids obtained in this study consist of two segments with a different nature, such as PP and PMMA, they can be expected to work as a compatibilizer for improving the interfacial interactions between blended polymers. To evaluate this effectiveness, each PP-PMMA hybrid was added to homo-PP / homo-PMMA blended system in an *o*-xylene solution at 130 ^{o}C. For comparison, a blended sample without the hybrid was also prepared. Figure 7 shows the TEM images of the blended polymers with the hybrid and the optical micrograph of the blended polymer without the hybrid. The blended polymers with the hybrid (Figure 7(a) and 7(b)) showed a morphology in which the size of the dispersed domains was significantly smaller than that of the blended polymer without the hybrid (Figure 7(c)). In addition, the morphologies between two kinds of blended polymers with the hybrids were almost the same. It would seem that these polymer hybrids effectively work as a compatibilizer for PP / PMMA blended polymer and the compatibility of the PP-PMMA hybrid is independent of its MMA content at least in a range of 6.6 – 45.5 wt%.

Figure 8 shows the DSC thermograms of PP and PP / PMMA blended polymers without and with the PP-PMMA hybrids. In cooling thermograms as shown in Figure 8(a), the peak crystallization temperature of the PP / PMMA blended polymer (116.5 ^{o}C) was higher than that of only PP (114.3 ^{o}C) and the addition of PP-PMMA1 and PP-PMMA3 remarkably increased the peak crystallization temperature (121.7 ^{o}C and 122.7 ^{o}C, respectively). In addition, the peak melting temperature as shown in Figure 8(b) also showed the same tendency of the peak crystallization temperature and particularly, the hybrid with higher MMA content (PP-PMMA3, 45.5 wt%) was very effective for the increasing the melting temperature. These phenomena show that the well-dispersed PMMA domains also worked as efficient nucleating agents for the

crystallization of PP matrix like inorganic nanoparticle, clay and organic salts [22-24].

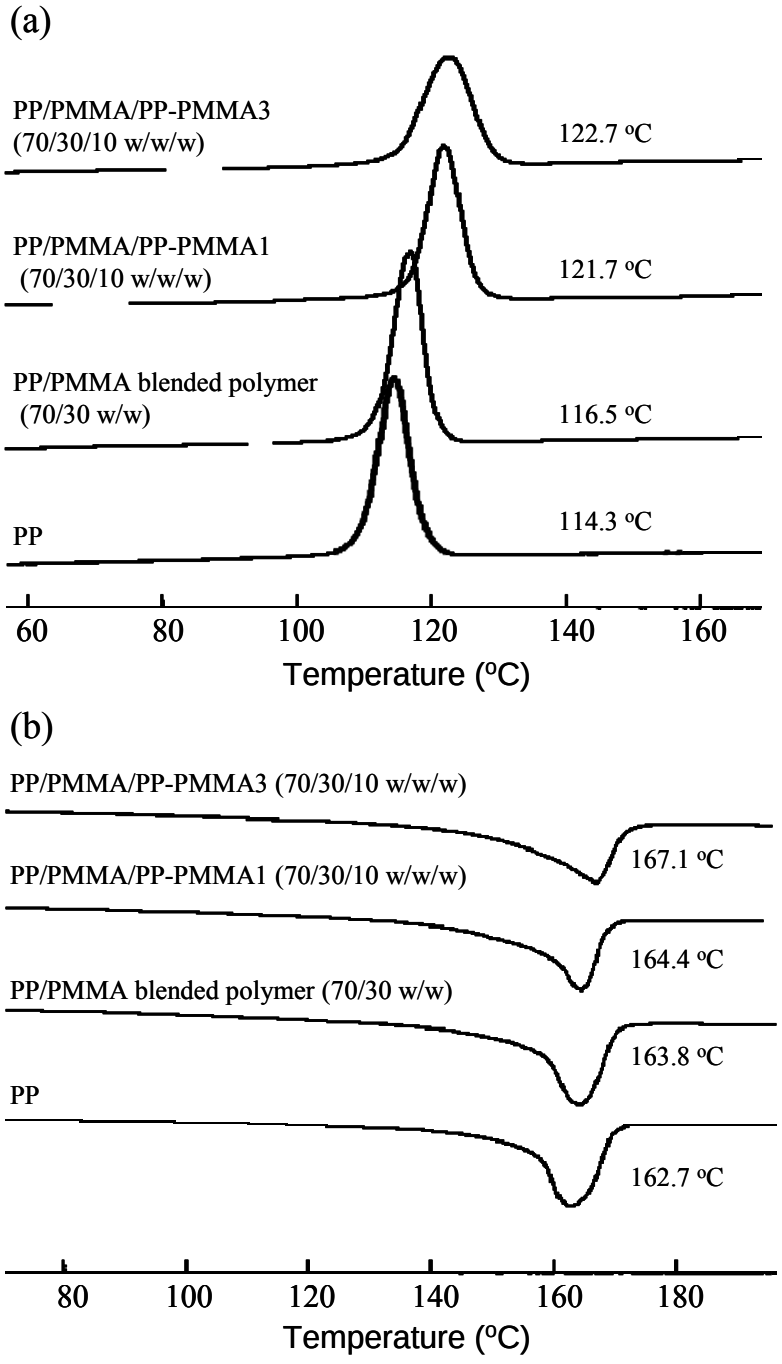

Figure 8. DSC cooling thermograms (a) and heating thermograms (b) for PP and PP/PMMA blended polymers without and with the PP-PMMA hybrids.

Table 5. Summary of HEMA Polymerization[a]

Sample	PP-Br[d] (g)	HEMA (mL)	CuBr (mmol)	Yield (g)	DMF Insoluble Part[e] (wt%)	HEMA Content[f] (wt%)
PP-PHEMA1	15.0	4.3	0.89	18.8	95.4	26.5
PP-PHEMA2	15.0	16.7	0.89	31.5	96.0	60.0
PP-PHEMA3[b]	3.0	3.3	0.18	2.9	-	n.d.
PP-PHEMA4[c]	3.0	3.3	0	2.9	-	n.d.

[a] Polymerization conditions: $[PP\text{-}Br]_0/[CuBr]_0/[PMDETA]_0 = 1/1.9/3.8$ (molar ratio) in 250 mL of *o*-xylene at 25 °C for 4h.
[b] PP-OH was used in place of PP-Br. Polymerization conditions: $[CuBr]_0/[PMDETA]_0 = 1/2$ (molar ratio) in 50 mL of *o*-xylene at 25 °C for 4h.
[c] Polymerization conditions: $[PP\text{-}Br]_0/[CuBr]_0/[PMDETA]_0 = 1/0/0$ (molar ratio) in 50 mL of *o*-xylene at 25 °C for 4h.
[d] 0.031 mmol of Br/g of polymer.
[e] Determined by Soxhlet extraction in boiling DMF for 12 h.
[f] Determined by elemental analysis for DMF insoluble part. n.d. = not determined.

Radical Polymerization of HEMA Initiated by PP Macroinitiator

2-Hydroxyethyl methacrylate (HEMA) is one of the typical methacrylate monomers possessing a functional group and it is well known that its homopolymer (PHEMA) has hydrophilicity. Therefore, the polymer hybrid combining PO with PHEMA is expected to be a new PO-based material with a hydrophilic nature. We successfully obtained the PP-based polymer hybrids linking PHEMA segments through the metal-catalyzed radical polymerization using a PP macroinitiator (PP-Br) for the first time. The polymerization of HEMA initiated by PP-Br was carried out at 25 °C in *o*-xylene with a CuBr/PMDETA catalyst system. Table 5 shows the result of HEMA polymerization. Although the PP macroinitiator did not dissolve into *o*-xylene under this condition, the polymerization of HEMA proceeded easily and most of the monomer was consumed in only four hours. On the other hand, PP-OH did not initiate the polymerization and the polymerization without catalyst did not proceed as in the case of MMA (PP-PHEMA3 and 4). To remove the homopolymer (PHEMA) produced by the thermal polymerization, the obtained polymers were purified by the Soxhlet extraction with boiling DMF, which is a good solvent for PHEMA and a poor solvent for PP. In the case of PP-PHEMA1 and 2, the extracted fraction was less than 5 wt% of the obtained polymer, indicating the graft polymerization of HEMA proceeded efficiently.

Since the obtained polymers were rigid and brittle, it was so difficult to prepare the thin and transparent film for normal FT-IR analysis. Then, the existence of PHEMA segment in these polymers was confirmed by the attenuated total reflection infrared (ATR/IR) analysis of the molded press sheet as shown in Figure 9. In these spectra, the

absorption bands for C=O stretching vibration centered at 1727 cm^{-1} and O-H stretching vibration at 3600 – 3200 cm^{-1} show the existence of PHEMA segment and the absorption band at 3000 – 2800 cm^{-1} can be assigned to C-H stretching vibration of PP segment. We tried to determine the HEMA contents in these purified polymers by using ^{1}H NMR, however, selecting a good solvent for both PP and PHEMA segments was difficult so that their monomer compositions could not be determined by ^{1}H NMR. Instead, elemental analysis was used for the determination of monomer composition. As shown in Table 6, the oxygen content in these obtained polymers was higher than that in PP-Br, suggesting the introduction of PHEMA segment and the formation of the PP-PHEMA hybrid. From the contents of each element, the HEMA contents of PP-PHMEA1 and PP-PHEMA2 were estimated to be 26.5 and 60.0 wt%, respectively.

Table 7 summarizes the DSC results of the purified PP-PHEMA hybrids. As is the case with the PP-PMMA polymer hybrids, the peak melting temperature of the PP-PHEMA hybrid was higher than that of PP-Br and the heat of fusion gradually decreased with increased HEMA content. On the other hand, the relative crystallinity of the PP part did not decrease in spite of the higher HEMA content as the PP-PMMA hybrids.

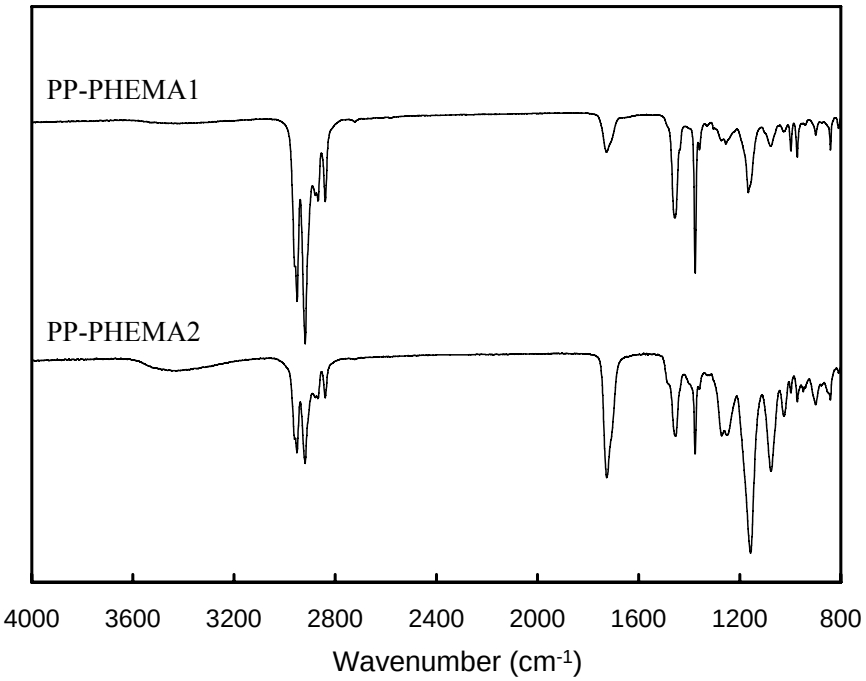

Figure 9. ATR/IR spectra of PP-PHEMA hybrids with different HEMA contents.

Table 6. Elemental Analysis Data for PP-Br and PP-PHEMA Hybrids

	C/H/N/O	
Sample	Found	Calc'd
PP-Br	84.9/14.2/<0.3/0.6	-
PP-PHEMA1	77.1/12.4/<0.3/10.2	77.1/12.5/0.2/10.2 (as HEMA cont.: 26.5 wt%)
PP-PHEMA2	67.0/10.4/<0.3/22.3	67.2/10.3/0.1/22.4 (as HEMA cont.: 60.0 wt%)

Table 7. Summary of DSC Results for PP-PHEMA Hybrids

Sample	HEMA Content[a] (wt%)	T_m[b] (^oC)	ΔH[b] (J/g)	Relative Crystallinity of PP Part[c] (%)
PP-Br	0	157.1	91.5	100
PP-PHEMA1	26.5	160.6	71.7	107
PP-PHEMA2	60.0	159.4	36.1	99

[a] Determined by elemental analysis for DMF insoluble part.
[b] Observed by DSC measurement.
[c] Relative crystallinity (%) = [$\Delta H_{PP\text{-}PHEMA}$ / ($\Delta H_{PP\text{-}Br}$ x weight ratio of PP in the PP-PHEMA hybrid)] x 100.

TEM Observation of the PP-PHEMA Hybrid Powder

Figure 10 shows TEM micrographs of the cross-section of the PP-PHEMA hybrid powders with 26.5 and 60.0 wt% of HEMA contents. The TEM images at a magnification of 5,000 times (Figure 10(A) and 10(B)) reveal that the obtained powders consisted of two phases with a different brightness. Since the PHEMA segment is more easily stained by RuO_4 than the PP segment, it is considered that the interior of the particle is the PP-rich phase and the surface of the powder is the PHEMA-rich phase. From the observation at high magnification as shown in Figure 10(C) and 10(D), the thickness of the surface layer of each powder is estimated to be about 80 and 300 nm, respectively. Because these values of thickness were too small for the HEMA content, it can be suggested that the PHEMA chain grows not only on the surface of the PP powder but also under the surface of the PP powder, probably at the amorphous part, to give a peculiar core-shell-like morphology.

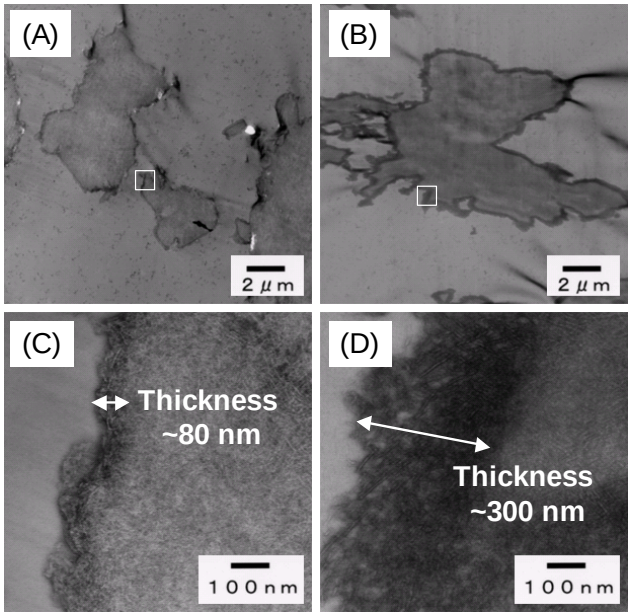

Figure 10. TEM images of the cross section of the PP-PHEMA hybrid powders: (A) PP-PHEMA1 and (B) PP-PHEMA2 at a magnification of 5,000 times and (C) PP-PHEMA1 and (D) PP-PHEMA2 at a magnification of 100,000 times.

Hydrophilicity of the PP-PHEMA Hybrids

Figure 11 shows the behavior of PP-Br and polymer hybrids in water. In the case of PP-Br and the PP-PHEMA hybrid with lower HEMA content (Figure 11(A) and 11(B)), the polymer powder floated on water. On the other hand, the PP-PHEMA hybrid powders with higher HEMA content (60.0 wt%, in Figure 11(C)) were well suspended in water. These phenomena clearly demonstrate that the PHEMA segment was properly grafted on the surface of the PP powder, which led to an increase in the affinity with water because of its hydrophilicity. Alternatively, the densities of the PP and PHEMA segments were determined to be 0.91 and 1.27 g/cm^3, respectively [25]. Therefore, this distinctive behavior might be due to not only the hydrophilicity but also the density among each graft copolymer.

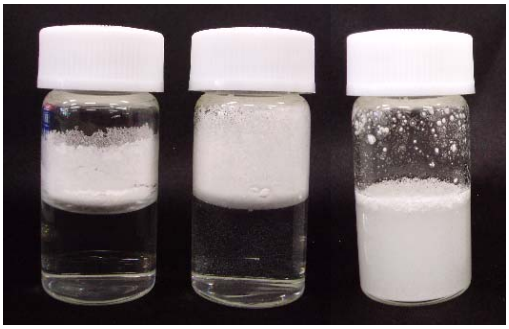

(A) (B) (C)

Figure 11. Pictures of (A) PP-Br and PP-PHEMA hybrids with HEMA contents of (B) 26.5 and (C) 60.0 wt% in water.

Conclusions

PP macroinitiator was prepared by the reaction between maleic anhydride-modified PP and ethanolamine and the subsequent reaction with 2-bromoisobutyryl bromide. The obtained PP macroinitiator was successfully employed for the radical polymerization of MMA and HEMA using a CuBr/PMDETA catalyst system to give the corresponding polymer hybrids. In the case of MMA polymerization, the polymerization proceeded in a solution condition and the MMA content of the obtained polymers was confirmed to be in the range of 6.6 – 45.5 wt% by ^{1}H NMR analysis. From TEM observation of these polymer hybrids, the PP and PMMA segments finely dispersed at the nanometer level and these hybrids worked as a good compatibilizer for the PP / PMMA polymer blend. In the case of HEMA polymerization, the polymerization proceeded in slurry conditions resulting in the polymer hybrids with 26.5 and 60.0 wt% of HEMA contents. TEM micrographs of the cross-section of the obtained PP-PHEMA hybrid powder revealed a core-shell structure consisting of a PP-rich core and a PHEMA-rich shell. In addition, the core-shell hybrid with higher HEMA content showed an affinity for water because of the modification of the PP powder surface by the incorporation of the PHEMA segment. The introduction of PMMA and PHEMA segments into PP improved its low interfacial interaction with polar polymers or water and thus obtained PP hybrids are expected to be used as not only compatibilizer and modifier but also the other new applications such as antistatic agent, antifog additive, aqueous coating and aqueous emulsion. Thus, the polymer hybrids by chemical linkage between PP and the other polymers are useful as a new material possessing unique and improved properties reflecting the kind and content of the grafted polar segments.

References

[1] Imuta, J.; Kashiwa, N.; Toda, Y. J Am Chem Soc 2002, 124, 1176-1177.

[2] Imuta, J.; Toda, Y.; Matsugi, T.; Kaneko, H.; Matsuo, S.; Kojoh, S.; Kashiwa, N. Chem Lett 2003, 32, 656-657.

[3] Inoue, Y.; Matsugi, T.; Kashiwa, N.; Matyjaszewski, K. Macromolecules 2004, 37, 3651-3658.

[4] Kashiwa, N.; Matsugi, T.; Kojoh, S.; Kaneko, H.; Kawahara, N.; Matsuo, S.; Nobori, T.; Imuta, J. J Polym Sci Part A: Polym Chem 2003, 41, 3657-3666.

[5] Stehling, U.M.; Malmström, E. E.; Waymouth, R. M.; Hawker, C. J. Macromolecules 1998, 31, 4396-4398.

[6] Liu, S.; Sen, A. Macromolecules 2001, 34, 1529-1532.
[7] Caporaso, L.; Iudici, N.; Oliva, L. Macromol Symp 2006, 234, 42-50.
[8] Matyjaszewski, K.; Teodorescu, M.; Miller, P. J.; Peterson, M. L. J Polym Sci Part A: Polym Chem 2000, 38, 2440-2448.
[9] Moad, G. Prog Polym Sci 1999, 24, 81–142.
[10] Rätzsch, M.; Arnold, M.; Borsig, E.; Bucka, H.; Reichelt, N. Prog Polym Sci 2002, 27, 1195-1282.
[11] Li, H.; Chiba, T.; Higashida, N.; Yang, Y.; Inoue, T. Polymer 1997, 38, 3921-3925.
[12] Sun, Y. –J.; Hu, G. –H.; Lambla, M.; Kotlar, H. K. Polymer 1996, 37, 4119–4127.
[13] Lu, Q. –W.; Macosko, C.W.; Polymer, 45, 1981-1991.
[14] Steinert, V.; Reinhardt, S.; Werner, K. J Polym Sci Part A: Polym Chem 1999, 37, 2045-2054.
[15] Minoura, Y.; Ueda, M.; Mizunuma, S.; Oba, M. J Appl Polym Sci 1969, 13, 1625-1640.
[16] Matsugi, T.; Kojoh, S.; Kawahara, N.; Matsuo, S.; Kaneko, H,; Kashiwa N. J Polym Sci Part A: Polym Chem 2003, 41, 3965-3973.
[17] Kaneyoshi, H.; Matyjaszewski, K. J Appl Polym Sci 2007, 105, 3-13.
[18] Matyjaszewski, K.; Xia, J. Chem Rev 2001, 101, 2921-2990.
[19] Kamigaito, M.; Ando, T.; Sawamoto, M. Chem Rev 2001, 101, 3689-3745.
[20] Lutz, J. –F.; Matyjaszewski, K. J Polym Sci Part A: Polym Chem 2005, 43, 897-910.
[21] Chung, T. C.; Rhubright, D. Macromolecules 1994, 27, 1313-1319.
[22] Naffakh, M.; Martín, Z.; Fanegasn, N.; Gómez, M. A.; Jiménez, I. J Polym Sci Part B: Polym Phys 2007, 45, 2309-2321.
[23] Wu, J.; Wu, T:; Chen, W.; Tsai, S.; Kuo, W. J Polym Sci Part B: Polym Phys 2005, 43, 3242-3254.
[24] Zhang, Y.; Xin, Z. J Appl Polym Sci 2006, 100, 4868-4874.
[25] Habsuda, J.; Simon, G. P.; Cheng, Y. B.; Hewitt, D. G.; Diggins, D. R.; Toh, H.; Cser, F. Polymer 2002, 43, 4627-4638.

Chapter 4

Synthesis and Mechanical Properties of Polypropylene-based Polymer Hybrids via Controlled Radical Polymerization

Abstract

Isotactic polypropylene-based graft copolymers linking poly(methyl methacrylate), poly(*n*-butyl acrylate) and polystyrene were successfully synthesized by a controlled radical polymerization with isotactic polypropylene (PP) macroinitiator. The hydroxylated PP, prepared by propylene/10-undecen-1-ol copolymerization with a metallocene/methylaluminoxane/triisobutylaluminum catalyst system, was treated with 2-bromoisobutyryl bromide to produce a Br-group containing PP (PP-*g*-Br). The resulting PP-*g*-Br could initiate controlled radical polymerization of methyl methacrylate, *n*-butyl acrylate and styrene by using a copper catalyst system, leading to a variety of PP-based graft copolymers with a different content of the corresponding polar segment. These graft copolymers demonstrated unique mechanical properties dependent upon the kind and content of the grafted polar segment.

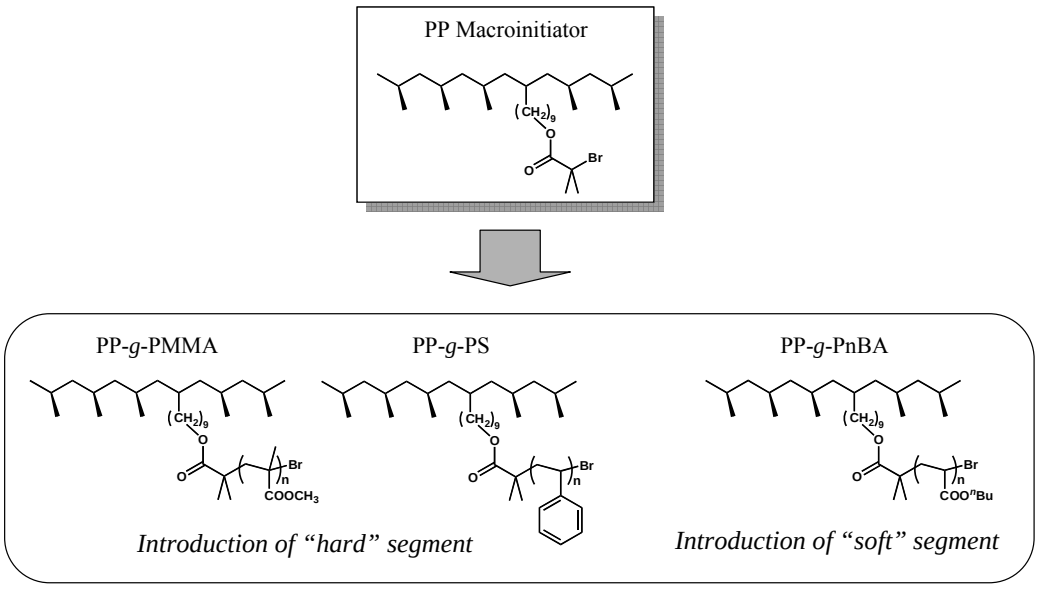

Introduction

Isotactic polypropylene (PP) is one of the most widespread commodity plastics due to its outstanding combination of cost performance and excellent physical properties. Its blending with other polymers can be expected to broaden its property range and applications in highly profitable fields. However, in many cases their simple physical blend tends to bring out the poor properties rather than the improved properties because of incompatibility. To overcome this problem, a combination of PP and other polymers by chemical linkage has been attracting a lot of attention as a new polymer hybrid between immiscible segments such as crystalline/amorphous, polar/nonpolar or hydrophilic/hydrophobic segments. Such new polymer hybrid can be used as a compatibilizer for the polymer blends. For example, Chung *et al.* reported that PP-based block or graft copolymers, such as PP-*g*-poly(methyl methacrylate) [1] and PP-*g*-poly(ε-caprolactone) [2], could be prepared by using borane-contained PP in combination with radical or ring-opening anionic polymerization of polar monomers and then used as a compatibilizer for PP-based polymer blends. Previously, by a combination of the polyethylene (PE) macroinitiator derived from the hydroxylated PE and these polymerization systems, the authors successfully synthesized PE-based block or graft copolymers, such as PE-*b*-poly(methyl methacrylate) [3], PE-*g*-poly(propylene glycol) and PE-*g*-poly(ε-caprolactone) [4]. These copolymers demonstrated nano-order phase separation morphology, due to the chemical linkage between PE and polar segments, to work as a good compatibilizer for the immiscible polymer blends.

On the other hand, these new polymer hybrids based on polyolefins are expected not only to work as a compatibilizer but also to have unique and improved properties. In this chapter, the authors focus on PP-based polymer hybrids, which can be produced by controlled radical polymerization with a PP macroinitiator derived from the hydroxylated PP, and evaluated the mechanical properties of such new polymer hybrids themselves. For example, the authors introduce synthesis and properties of PP-*g*-poly(methyl methacrylate) (PP-*g*-PMMA), PP-*g*-polystyrene (PP-*g*-PS) and PP-*g*-poly(*n*-butyl acrylate) (PP-*g*-PnBA) graft copolymers.

Experimental

General Procedures and Materials

All manipulations of air- and water-sensitive materials were performed under dry N_2 atmosphere in a conventional N_2-filled glove box. Copper bromide (CuBr),

N,*N*,*N'*,*N''*,*N''*-pentamethyldiethylenetriamine (PMDETA), 2-bromoisobutyryl bromide (BiBB), methyl methacrylate (MMA), Styrene (St) and *n*-butyl acrylate (nBA) were purchased from Wako Pure Chemical Industries and used without further purification. Propylene was obtained from Mitsui Chemicals. Methylaluminoxane (MAO) was purchased from Albemarle as 1.2 M toluene solution with the remaining trimethylaluminum and evaporated *in vacuo* before use. Toluene and *n*-hexane used as a solvent were dried over Al_2O_3 and degassed by bubbling with N_2 gas.

Preparation of Hydroxylated PP (PP-g-OH)

Toluene (800 mL) was introduced to a N_2-purged 1-L glass reactor equipped with a mechanical stir bar, a temperature probe and a condenser and stirred vigorously. The reactor was kept at 40 ^oC with an oil bath and then triisobutylaluminum (3.3 mmol) and 10-undecen-1-ol (3.0 mmol) were added. After 10 min, dimethylsilylenebis(2-methyl-4-phenyl-1-indenyl)zirconium dichloride (0.002 mmol) and 1.31 M toluene solution of MAO (1.0 mmol) were introduced into the reactor and immediately the feeding of propylene gas was started. After adding isobutyl alcohol, the polymerization mixture was poured into acidic methanol. The polymer was collected by filtration, washed with methanol and dried *in vacuo* at 80 ^oC for 10 h to give PP-*g*-OH (19 g; number-average molecular weight (M_n) = 54,600, melting temperature (T_m) = 153 ^oC, 0.14 mol% of hydroxyl group according to ^1H NMR measurements). By repeating this procedure, a sufficient amount of PP-*g*-OH for this study was obtained.

Preparation of PP Macroinitiator (PP-g-Br)

PP-*g*-OH (150 g), BiBB (10.9 mL) and *n*-hexane (1500 mL) were introduced into a N_2-purged 2-L glass reactor equipped with a mechanical stir bar and then were stirred vigorously at 60 ^oC for 3 h. The reaction mixture was cooled to 25 ^oC and poured into 2 L of acetone. The resulting polymer was collected by filtration, washed with acetone and dried *in vacuo* at 80 ^oC for 10 h.

Radical Polymerization with PP Macroinitiator

A typical polymerization process is as follows: PP-*g*-Br (100 g) and MMA (800 mL) were placed in a 1-L glass reactor equipped with a mechanical stir bar and then N_2 gas was fed into the reactor at 90 ^oC. A solution of CuBr/PMDETA in toluene (0.69 mmol as a copper atom and 1.38 mmol as PMDETA, pretreated for 5 min. at ambient temperature) was added to the reactor and the mixture was maintained at 90 ^oC for 30 min under stirring. The polymerization was stopped by cooling the mixture in an ice

bath and then quenched by the addition of methanol. The resulting mixture was filtered and the obtained powdery polymer was washed by methanol and then dried *in vacuo* at 80 °C for 10 h.

Polymer Characterization Methods

^{1}H NMR spectra were recorded on JEOL GSX-270 or GSX-400 spectrometers using 1,2-dichlorobenzene-d_4 or 1,1,2,2-tetrachloroethane-d_2 as a solvent at 120 °C. For the measurements of mechanical properties, 40 g of the obtained copolymer and 0.04 g of the antioxidant (Irganox 1010, Ciba-Geigy Corporation) were blended and then kneaded by a labo plastomill at 200 °C. After 5 min of kneading, the specimens were prepared by compression molding at 200 °C for 5 min in a laboratory press. The flexural strength and modulus were measured according to ASTM D 790 and the Izod impact strength was measured at 23 °C according to ASTM D 256.

Results and Discussion

Preparation of PP Macroinitiator

The synthetic route of PP macroinitiator is shown in Scheme 1. In the first step, PP-*g*-OH possessing hydroxyl groups at the side-chain ends was successfully obtained through the copolymerization of propylene with aluminum-capped 10-undecen-1-ol by using a metallocene catalyst system. In the second step, the hydroxyl groups in PP-*g*-OH were reacted with BiBB to produce 2-bromoisobutyrate group containing PP (PP-*g*-Br), which could initiate the controlled radical polymerization.

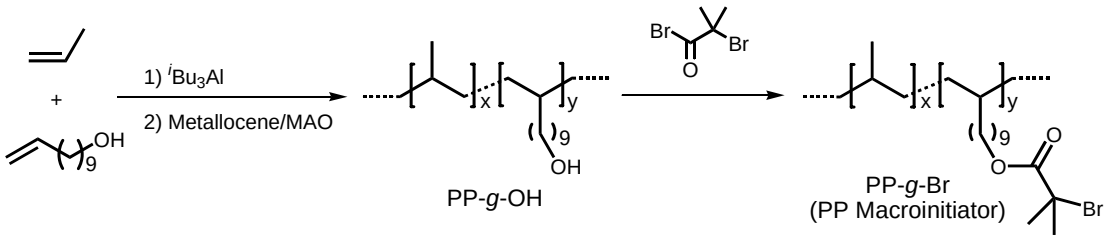

Scheme 1. Synthetic route for preparing PP-*g*-Br.

Figure 1 shows the ^{1}H NMR spectra of PP-*g*-OH and PP-*g*-Br. For PP-*g*-OH (Figure 1(a)), the triplet signals of δ 3.5 ppm are assigned to methylene protons (-CH_2-OH). For PP-*g*-Br (Figure 1(b)), other triplet signals of δ 4.1 ppm correspond to methylene protons (-CH_2-OCO-) and the single signal of δ 1.8 ppm corresponds to methyl protons

(-OCOC(CH_3)$_2$Br). On the other hand, no signals at δ 3.5 ppm were detected and this indicates almost all of the hydroxyl groups in PP-*g*-OH were converted to the 2-bromoisobutyrate groups. From the relative intensities of the signals between PP backbone and 2-bromoisobutyrate groups, the content of 2-bromoisobutyrate group was calculated to be 0.14 mol%. From the number-average molecular weight of the obtained PP-*g*-Br (54,600), the average number of the 2-bromoisobutyrate groups as the initiation site can be estimated to be 1.9 units per chain. Thus-obtained PP-*g*-Br was used as a macroinitiator for the controlled radical polymerization.

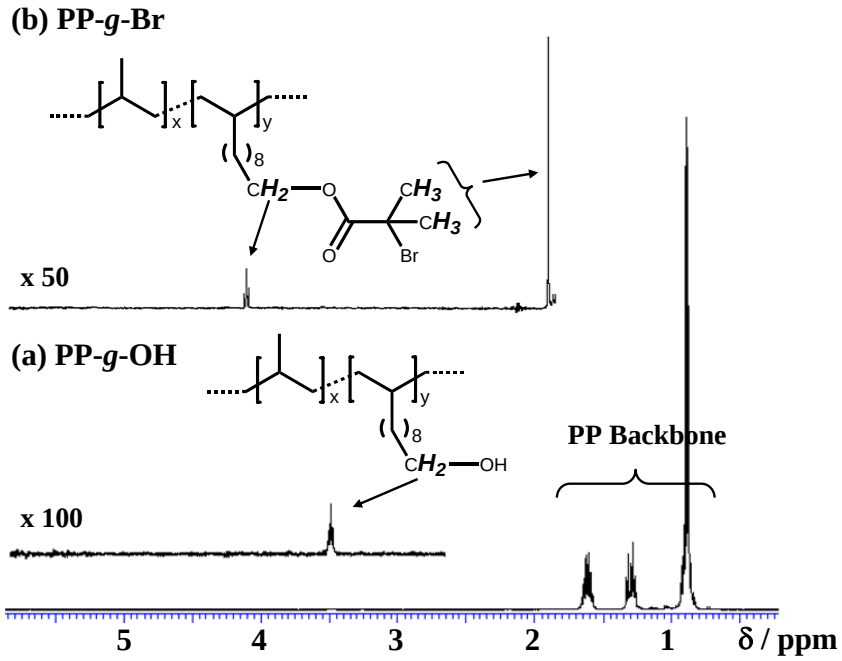

Figure 1. ^{1}H NMR spectra of (a) PP-*g*-OH and (b) PP-*g*-Br (400 MHz in 1,2-dichlorobenzene-d_4 at 120 ^{o}C).

Radical Polymerization of Polar Monomers Initiated by PP Macroinitiator

It is well known that transition metal catalyzed radical polymerization results in the controlled radical polymerization of various vinyl monomers, represented by (meth)acrylates and styrenes, to produce precisely controlled polymers [5,6]. In particular, it is a very effective method for the synthesis of block and graft copolymers when using macroinitiators. We applied this method to create the polymer hybrids based on polyolefins. The radical polymerization for three kinds of polar monomers, such as MMA, St and nBA, with the obtained PP-*g*-Br as a PP macroinitiator were carried out using a CuBr/PMDETA catalyst system. The molar ratios of each monomer to the initiation site in the PP macroinitiator were set at 2181, 1272 and 1627, respectively and

the molar ratio of CuBr to the initiation site was set at 0.2 for MMA and nBA polymerization and 0.5 for St polymerization. Polymerization temperature was controlled in the range of 50 – 90 ^{o}C and polymerization time was set in the range of 15 – 240 min to give polymer hybrids with different polar monomer contents. Since PP-*g*-Br was not dissolved at these polymerization conditions, the polymerization proceeded at a slurry state. To remove the homopolymer of the polar monomer contained in the obtained polymer, the polymers were purified by the Soxhlet extraction with boiling THF. In each sample, the amount of the extracted homopolymer was only little, and therefore, most of the consumed monomer was obviously grafted onto the PP backbone. This result indicates that the formation of the graft copolymers consisted of PP backbone and polar polymer branches, such as PP-*g*-PMMA, PP-*g*-PS and PP-*g*-PnBA. Table 1 summarizes the results by altering the polymerization conditions. The purified copolymers were analyzed by ^{1}H NMR at 120 ^{o}C in 1,1,2,2-tetrachloroethane-d_2 as a solvent. Figure 2 shows the ^{1}H NMR spectra of some purified copolymers. From the ratio of the integrated intensities between both signals assigned to propylene and polar monomer units, the content of the polar segments in the graft copolymers could be calculated as shown in Table 1.

Table 1. Summary of Radical Polymerization[a]

Run	Monomer	Polymn. Temp. (^{o}C)	Polymn Time (min)	Monomer Conversion[b] (%)	Polar Monomer Contents[c] (wt%)
1	MMA	90	30	11.1	46.9
2	MMA	70	40	6.4	34.0
3	MMA	70	15	2.9	18.6
4	MMA	50	15	0.1	0.7
5	St	90	240	17.5	46.6
6	St	90	120	2.6	11.6
7	St	90	60	2.2	9.9
8	nBA	90	60	6.1	32.8
9	nBA	70	30	1.8	12.4
10	nBA	50	30	0.03	0.3

[a] MMA polymerization: PP-*g*-Br 100 g, MMA 800 mL, $[CuBr]_0/[PMDETA]_0$ = 0.858/1.72 mM.
St polymerization: PP-*g*-Br 100 g, St 500 mL, Anisole 500 mL, $[CuBr]_0/[PMDETA]_0$ = 1.72/3.43 mM.
nBA polymerization: PP-*g*-Br 100 g, nBA 800 mL, $[CuBr]_0/[PMDETA]_0$ = 0.858/1.72 mM.
[b] Calculated from polymer yield.
[c] Determined by ^{1}H NMR.

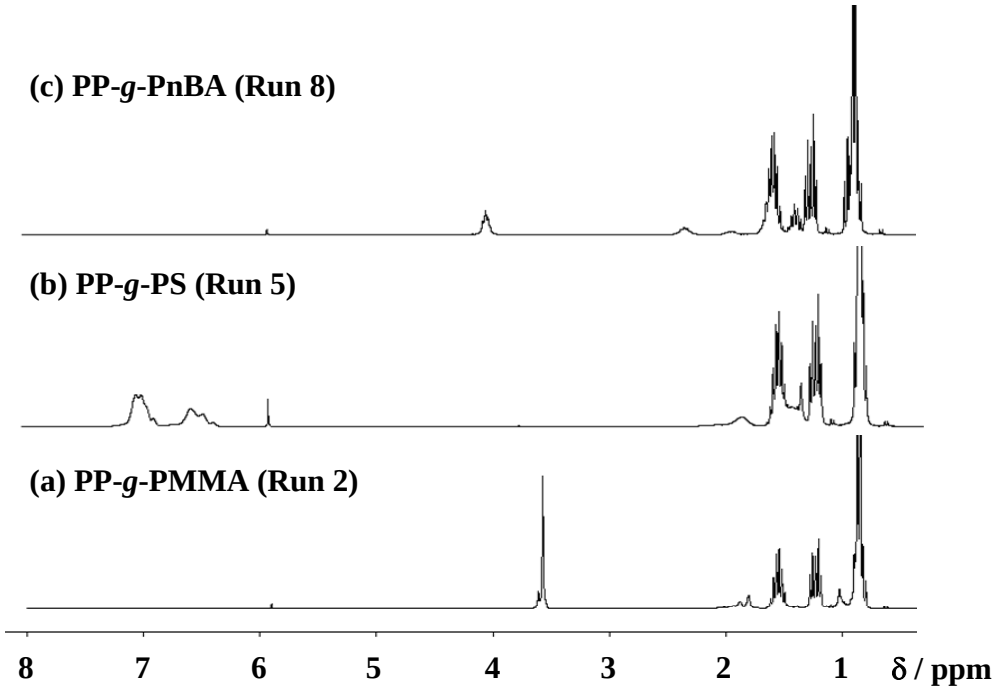

Figure 2. ^{1}H NMR spectra of (a) PP-*g*-PMMA, (b) PP-*g*-PS and (c) PP-*g*-PnBA graft copolymers (270 MHz, in 1,1,2,2-tetrachloroetane-d_2 at 120 ^{o}C).

Mechanical Properties of Graft Copolymers

The obtained copolymers were kneaded at 200 ^{o}C for 5 min by labo plastomill and then the specimens were prepared by compression molding at 200 ^{o}C for 5 min. Mechanical properties of these copolymers were characterized by flexural modulus, flexural strength and Izod impact strength measurements. As was expected, the mechanical properties were influenced by the kind and content of the grafted polar segments. Figure 3(a) shows a plot of the flexural modulus *versus* the content of the polar segment. For PP-*g*-PMMA and PP-*g*-PS, the flexural modulus clearly increased in comparison with the base polymer (PP-*g*-OH) and the increase of the flexural modulus depended on the content of the grafted segment. On the other hand, for PP-*g*-PnBA the flexural modulus considerably decreased with the increase of PnBA content because of its softness. Figure 3(b) shows a plot of the flexural strength *versus* the content of the polar segment. As in the case of the flexural modulus, the flexural strength has also been expected to increase by the grafting of PMMA and PS segment and decrease by PnBA segment. However, the flexural strength of PP-*g*-PS copolymers gradually decreased with the increase of PS content. This demonstrates that the balance of the

mechanical properties for these new graft copolymers can be controlled by the kind of grafting polar segment. Furthermore, since the flexural strength of the physical blended sample of PP-*g*-OH and PMMA (weight ratio = 70/30) was much lower than that of the obtained PP-*g*-PMMA graft copolymers, it was confirmed that the chemical linkage between both segments significantly contributes to the enhancement of the mechanical properties. Finally, the result of Izod impact test is shown in Figure 4. The Izod impact strength was remarkably improved by the incorporation of the PnBA segment, indicating the function of the PnBA segment as an impact modifier of PP.

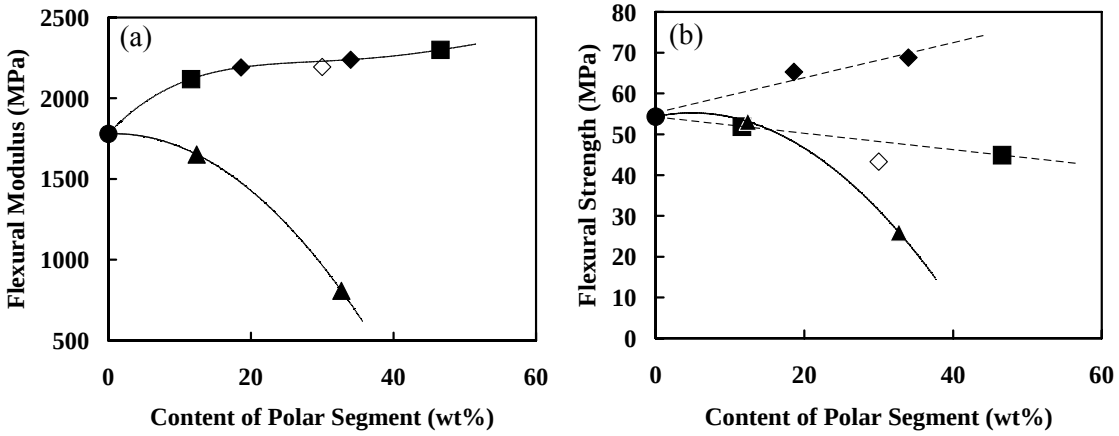

Figure 3. Plot of (a) flexural modulus and (b) flexural strength versus content of polar segment (◆ : PP-g-PMMA, ■ : PP-g-PS, ▲ : PP-g-PnBA, ● : PP-g-OH, ◇ : PP-g-OH/PMMA (7/3) Blend).

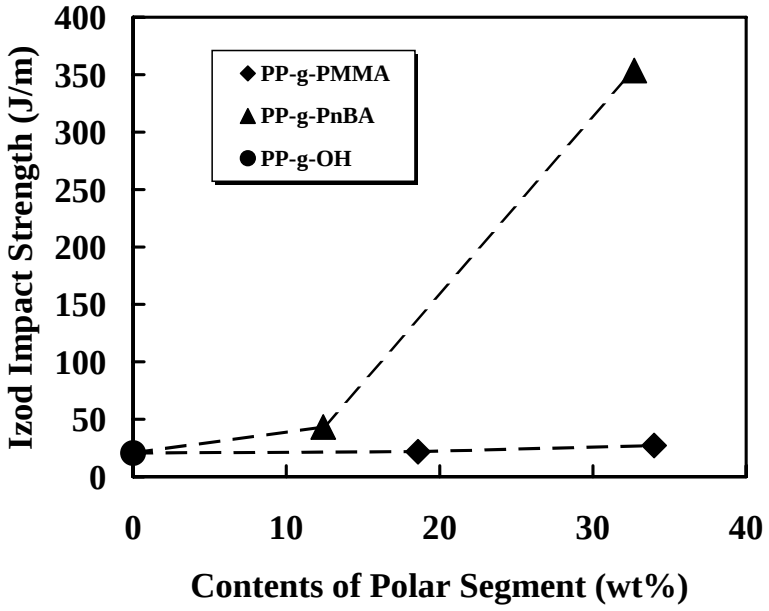

Figure 4. Plot of Izod impact strength *versus* content of polar segment.

Conclusion

PP macroinitiator was prepared by a metallocene-catalyzed copolymerization of propylene/10-undecen-1-ol and subsequent reaction with 2-bromoisobutyryl bromide. The radical polymerization of MMA, St and nBA with the obtained PP macroinitiator using a CuBr/PMDETA catalyst system resulted in most of the consumed monomer being grafted onto the PP backbone following a Soxhlet extraction test. The content of the polar segments in the obtained graft copolymers were controlled in the range of 11.6 – 46.6 wt%. The flexural and Izod impact tests revealed that the incorporation of PMMA and PS into the PP backbone effectively enhanced stiffness and concerning PnBA remarkably improved toughness. Thus, the polymer hybrids by chemical linkage between PP and other polymers are useful as a new material possessing unique and improved mechanical properties reflecting the kind and content of the grafted polar segments.

References

[1] Chung, T. C.; Rhubright, D.; Jiang, G. J. Macromolecules 1993, 26, 3467-3471.
[2] Chung, T. C.; Rhubright, D. Macromolecules 1994, 27, 1313-1319.
[3] Matsugi, T.; Kojoh, S.; Kawahara, N.; Matsuo, S.; Kaneko, H.; Kashiwa, N. J Polym Sci Part A: Polym Chem 2003, 41, 3965-3973.
[4] Kashiwa, N.; Matsugi, T.; Kojoh, S.; Kaneko, H.; Kawahara, N.; Matsuo, S.; Nobori, T.; Imuta, J. J Polym Sci Part A: Polym Chem 2003, 41, 3657-3666.
[5] Matyjaszewski, K.; Xia, J. Chem Rev 2001, 101, 2921-2990.
[6] Kamigaito, M.; Ando, T.; Sawamoto, M. Chem Rev 2001, 101, 3689-3745.

PART II

POLYOLEFIN MACROMONOMER APPROACH

Chapter 5

Polymacromonomers with Polyolefin Branches Synthesized by Free-radical Homopolymerization of Polyolefin Macromonomer with a Methacryloyl End Group

Abstract

Polymacromonomers with polyolefin branches were successfully synthesized by free-radical homopolymerization of polyolefin macromonomer with a methacryloyl end group. Propylene-ethylene random copolymer (PER) with a vinylidene end group was prepared by polymerization using a metallocene catalyst. Then, the unsaturated end group was converted to a hydroxyl end group via hydroalumination and oxidation. The PER with the hydroxyl end group was easily reacted with methacryloyl chloride to produce methacryloyl-terminated PER (PER macromonomer; PERM). The free-radical polymerization of thus-obtained PERM was done using 2,2'-azobis(isobutyronitrile) (AIBN) as a free-radical initiator. From NMR analyses, the obtained polymers were identified as poly(PERM). Based on gel permeation chromatography (GPC), the estimated degree of polymerization (D_p) of these polymers were about 30. Thus, new class of polymacromonomers with polyolefin branches was synthesized.

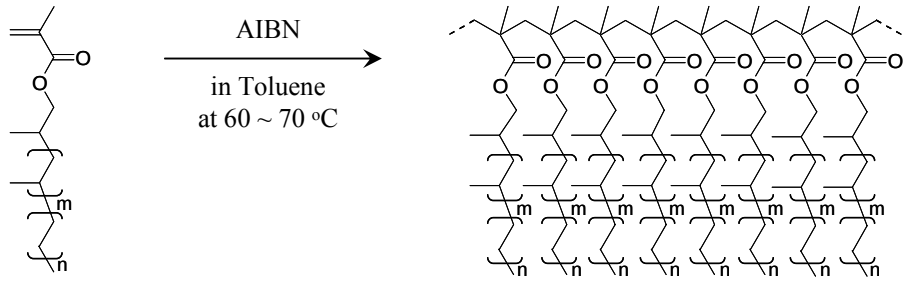

PER macromonomer

Poly(PER macromonomer)

Introduction

Macromonomers, which consist of a macromolecular segment and a polymerizable chain end segment, are useful as a starting material for producing new polymer architectures. Homopolymerization and copolymerization of macromonomer yield various polymers that have unique topologies and properties. For example, polymacromonomers, which are produced by homopolymerization of macromonomer, can have unique molecular morphologies ranging from star-shaped spheres to rodlike cylinders by controlling the degree of polymerization (D_p) of the backbone and the length of the branch chains [1-5]. However, previous studies on macromonomers have been limited to polymers obtained by radical, cationic, and anionic polymerizations, such as polymethacrylate, polystyrene, and poly(ethylene oxide).

Synthesis and copolymerization of macromonomer possessing a polyolefin segment obtained by coordination polymerization have also been reported. For example, Mülhaupt *et al.* reported the synthesis of methacryloyl-terminated polypropylene via vinylidene-terminated polypropylene obtained by metallocene-catalyzed polymerization and the free-radical copolymerization of this polyolefin macromonomer with methyl methacrylate [6]. Matyjaszewski *et al.* reported the synthesis of methacryloyl-terminated polyethylene obtained by Pd-mediated living polymerization and the copolymerization of this polyethylene macromonomer with *n*-butyl acrylate by atom transfer radical polymerization [7]. However, there have been no reports on homopolymerization of polyolefin macromonomer to give a graft copolymer consisting of polar polymer backbone and polyolefin branches.

In this chapter, the authors focused on the macromonomers based on lower molecular weight PER as a polyolefin segment. These PER macromonomers (PERMs) were expected to have the advantage of facile homopolymerization because those have low viscosity and are easily soluble by many hydrocarbon solvents. By using such new class of polyolefin macromonomers obtained by the functionalization of vinylidene-terminated PER, we successfully synthesized polymacromonomers possessing polyolefin branches by the free-radical homopolymerization. Furthermore, the nature of the obtained polymacromonomer that consisted of a polymethacrylate backbone and PER branch chains was investigated. This is a first report of a polyolefin-based polymacromonomer with unique polymer architecture.

Experimental

Materials

Dicyclopentadienylzirconium dichloride (Cp_2ZrCl_2), Bis(1,3-dimethylcyclopentadienyl)zirconium dichloride ($(1,3\text{-}Me_2Cp)_2ZrCl_2$), methacryloyl chloride, triethylamine, and AIBN were commercially obtained and used without further purification. Ethylene was purchased from Sumitomo Seika Co., Ltd., and propylene was obtained from Mitsui Chemicals, Inc. Methylaluminoxane (MAO) was purchased from Albemarle as a 1.2M toluene solution, and the trimethylaluminum, which is considered an impurity was evaporated in vacuo prior to use. Diisobutylaluminum hydride (DIBAL-H) was purchased from Tosoh-Finechem Co. Ltd. All other chemicals were obtained commercially and used as received.

Preparation of PER

PER with vinylidene end group has been prepared by copolymerization of propylene with ethylene using Cp_2ZrCl_2/MAO (Al/Zr=1000) catalyst system at 50 ºC for 5 h.

Hydroxylation of PER

PER (50 g, 0.071 mol as vinylidene end group) and toluene (250 mL) were placed in 500-mL glass reactor and stirred. Then DIBAL-H (50 mL, 0.28 mol) was added, and the system was then heated at 110 ºC for 6 h. Dried air at 110 ºC was then continuously fed (100 L/h) into the system. After 3 h, the reaction mixture was washed with *aq.*HCl and distilled water. After evaporation of solvent, hydroxylated PER was obtained as a yellow viscous liquid.

Synthesis of Methacryloyl-terminated PER (PERM)

After hydroxylated PER (20 g, 12.7 mmol as hydroxyl group) and toluene (30 mL) was placed in a 100-mL Schlenk tube, triethylamine (2.7 mL) and methacryloyl chloride (2.5 mL) were added to the tube, and then the mixture was stirred at room temperature for 3.5 h. The reaction mixture was washed with *aq.*HCl and distilled water. After the solvent was evaporated, the product was purified by liquid chromatography.

Homopolymerization of PERM

After PERM (3.0 g, 2.98 mmol as methacryloyl group) was placed in a 100-mL Schlenk tube, toluene (20 mL) and AIBN (75 mg) were added to the tube, and the mixture was heated at 70 ºC for 30 h. The reaction mixture was washed with *aq.*HCl

and distilled water. After the solvent was evaporated, a viscous liquid was obtained.

Polymer Fractionation

First, the polymer obtained by homopolymerization of PERM was dissolved in *n*-hexane and poured into a glass column packed with silica gel. Then, the first fraction was eluted by *n*-hexane and the second fraction by *n*-hexane/CH_2Cl_2 (2:1) mixed solvent. After evaporation of the solvent, each fraction was analyzed by GPC, ^{1}H NMR, and ^{13}C NMR.

Analytical Procedures

^{1}H NMR and ^{13}C NMR spectra were recorded by JEOL GSX-270 or GSX-400 spectrometers using chloroform-*d* or 1,2-dichlorobenzene-d_4 as a solvent at 25 ^{o}C or 120 ^{o}C. The gel permeation chromatograms (GPC) calibrated with PS standard were recorded by using a Waters Alliance GPC2000 equipped with four TSKgel columns (two sets of TSKgelGMH$_6$-HT and two sets of TSKgelGMH$_6$-HTL) and a refractive index detector at 140 ºC and 1,2-dichlorobenzene.

Results and Discussion

Synthesis of PERM

The synthetic route of PERM developed in this study is shown in Scheme 1. Vinylidene-terminated PERs were obtained by propylene copolymerization with ethylene by using typical metallocene catalysts. Unsaturated chain ends of the polymer were converted into hydroxyl end groups by hydroalumination or hydroboration and subsequent oxidation, as previously reported [8,9]. Hydroalumination of vinylidene end groups by DIBAL-H was then carried out at 110 ºC in toluene, as recommended in the literature [8]. Then, dried air was fed into the resulting mixture at 110 ºC to convert the alkylaluminum end groups to hydroxyl end groups. The obtained hydroxyl end groups easily reacted with methacryloyl chloride in the presence of a Lewis base at room temperature to produce methacryloyl end groups. The PER with a methacryloyl end group was useful as PERM owing to the polymerizable methacryloyl end group. By selecting the polymerization conditions and catalyst, we prepared two types of functionalized PERs with different molecular weights (PER1 and PER2).

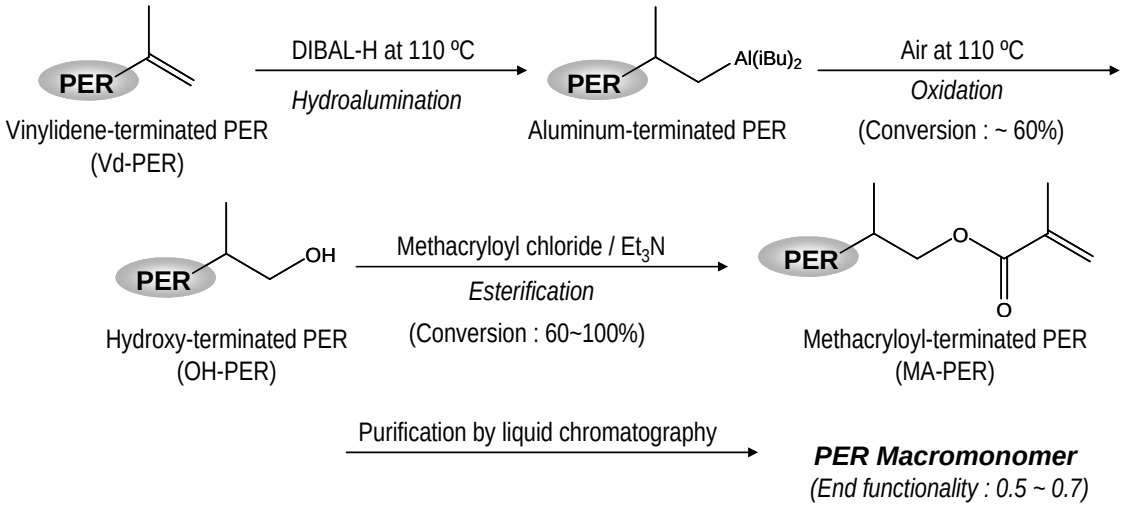

Scheme 1. Synthetic route of PER macromonomer.

Figures 1(i), (ii), and (iii) show the ^{1}H NMR spectra of PER1 with a vinylidene end group (Vd-PER1), with a hydroxyl end group (OH-PER1), and with a methacryloyl end group (MA-PER1), respectively. In Figure 1(i), the signals assigned to the vinylidene group protons (*c*; 4.6-4.8 ppm), were detected in addition to the signals of PER main chain protons at 0.7 to 1.8 ppm. These additional signals are generated from the chain transfer reaction induced by monomers when the propagating chain end was a propylene unit [10]. The content of vinylidene, ethylene, and propylene units was 4.0, 38, and 58 mol%, respectively, calculated from the relative intensities of the protons of each unit in the ^{1}H NMR spectrum. In Figure 1(ii), the new signals assigned to the hydroxymethylene group protons (*e*; 3.3-3.6 ppm) were detected in addition to the signals of unreacted vinylidene protons. The calculated content of the hydroxymethylene and vinylidene groups in OH-PER1 was 2.4 mol% and 0.09 mol%, respectively, indicating that about 60% of the vinylidene end groups in Vd-PER1 were hydroxylated and that the other vinylidene end groups were converted to the saturated end groups. This hydroxylation efficiency of 60% would be reasonable, because we previously reported that the hydroxylation efficiency of alkylaluminum-terminated PP was 52% [11]. In Figure 1(iii), the new signals assigned to the methacryloyl end group protons (*a*, *b*, *d* and *f*; 6.1, 5.5, 3.8-4.2 and 1.95 ppm, respectively) were detected. From the relative intensities of the protons of each group, the calculated content of the methacryloyl, hydroxymethylene, and vinylidene groups was 2.4, 0.37, and 0.08 mol%, respectively, indicating that almost all hydroxyl end groups in OH-PER1 were converted to methacryloyl end groups.

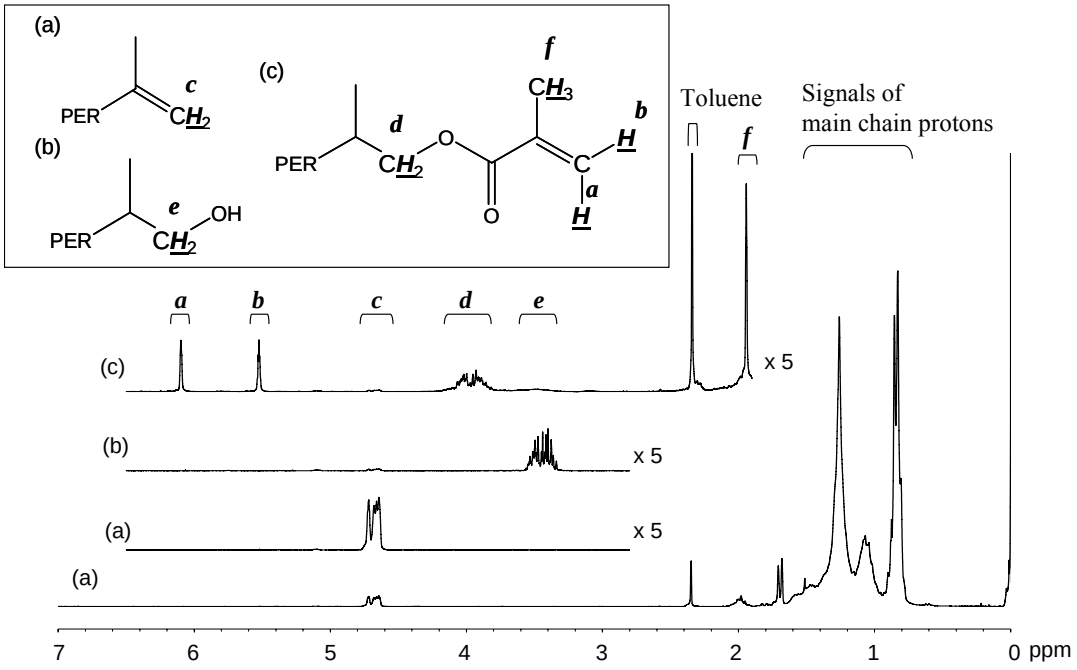

Figure 1. ^{1}H NMR spectra of (a)Vd-PER1, (b)OH-PER1 and (c) MA-PER1 (270 MHz, in $CDCl_3$ at 25 ^{o}C)

To remove the undesirable PER that has a saturated vinylidene or hydroxyl end group, the obtained MA-PER1 was purified by liquid chromatography. The content of the methacryloyl, ethylene, and propylene units of the purified MA-PER1 was 3.9, 35, and 61 mol%, respectively, calculated from ^{1}H NMR analysis, and the number average molecular weight (M_n) was 670 estimated from the GPC measurement. Therefore, the estimated end functionality (f_{MA}) of the obtained MA-PER1 was 0.68. The absence of vinylidene and hydroxymethylene end groups in the ^{1}H NMR spectrum indicates that residual chain ends were saturated end groups. Using the same purification method as for MA- PER1, MA-PER2 with higher M_n than MA-PER1 was obtained. Table 1 summarizes these functionalization results. For the synthesis of MA-PER2, both the conversion of the vinylidene end groups to hydroxyl end groups and that of the hydroxyl end groups to methacryloyl end groups were about 60 %. Such low conversion of the hydroxyl end groups to methacryloyl end groups in PER2 is probably due to the higher viscosity of PER2 than that of PER1. After purification, the estimated f_{MA} of the obtained MA-PER2 was 0.53 from ^{1}H NMR analysis and GPC measurement. The obtained MA-PER1 (f_{MA} = 0.68) and MA-PER2 (f_{MA} = 0.53) were then used as PERMs for free-radical polymerization without further purification.

Table 1. Functionalization Results for PER Chain Ends

		Vd-PER [a]	OH-PER	MA-PER	
				before purification	after purification
PER1	M_n [b]	520	520	690	670
	Content of vinylidene end group (mol%)[c]	4.0	0.09	0.08	n.d. [d]
	hydroxy end group (mol%)[c]	-	2.4	0.37	n.d. [d]
	methacryloyl end group (mol%)[c]	-	-	2.4	3.9
	(End functionality; f_{MA})				(0.68)
PER2	M_n [b]	1,550	1,650	1,960	1,330
	Content of vinylidene end group (mol%)[c]	1.4	0.04	n.d. [d]	n.d. [d]
	hydroxy end group (mol%)[c]	-	0.85	0.01	0.10
	methacryloyl end group (mol%)[c]	-	-	0.52	1.6
	(End functionality; f_{MA})				(0.53)

[a] Polymerization conditions: (PER1) 0.01 mmol of Cp_2ZrCl_2, 10 mmol of MAO, ethylene/propylene flowrate of 10/90 (l/h), in 800 ml of toluene, 50 ºC, 5 h, (PER2) 0.02 mmol of $(1,3\text{-}Me_2Cp)_2ZrCl_2$, 20 mmol of MAO, ethylene/propylene flowrate of 20/80 (l/h), in 800 ml of toluene, 50 ºC, 2 h.
[b] Determined by GPC.
[c] Calculated from ^{1}H NMR.
[d] Not detected.

Homopolymerization of PERM

Homopolymerization of the PER1 macromonomer (PERM1) and PER2 macromonomer (PERM2) was carried out at 70 ºC and 60 ºC, respectively, in toluene in the presence of AIBN as a radical initiator. Each resulting product was pale yellow viscous oil. Figure 2 shows the GPC traces for PERMs and the corresponding homopolymerized products. Each GPC trace of the homopolymerized product showed a new peak at a higher M_n region (over 10^4 mol/g) in addition to a peak of PERM at a lower M_n region (under 10^4 mol/g). These peaks indicate the formation of polymacromonomer. The estimated M_n of poly(PERM1) and poly(PERM2) was 18,760 and 45,920, respectively, from the higher M_n part of GPC traces. From a calculation based on M_n values for the two PERMs (670 for PERM1 and 1,330 for PERM2), the estimated D_p of these poly(PERM1) and poly(PERM2) was about 28 and 35, respectively. Although these two D_p values cannot be directly compared due to differences in polymerization conditions, these two macromonomers indicate nearly equal efficiency of polymerization, despite the different M_n.

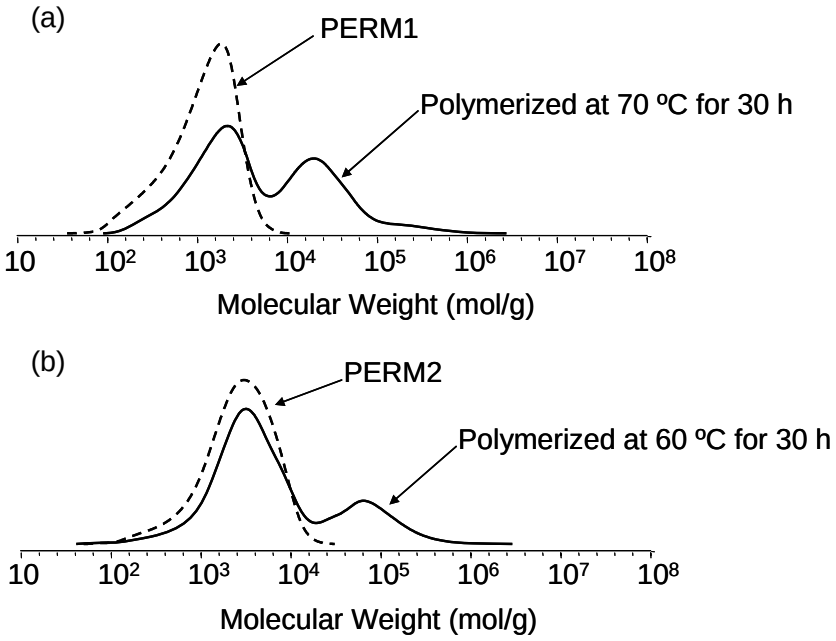

Figure 2. GPC traces for homopolymerization of (a)PERM1 and (b)PERM2.

Fractionation and Characterization of Poly(PERM1)

To isolate the higher M_n region, the mixture was fractionated by liquid chromatography using a silica gel column into two fractions, *n*-hexane and *n*-hexane / dichloromethane (2:1) eluates. The GPC traces of these two fractions were shown in Figure 3. From a calculation based on M_n value (670) for the PERM1, the first fraction was estimated to be the poly(PERM1) (D_p = 30) and the second fraction the unpolymerized PERM1 containing the oligomer of PERM1 (D_p = 2~3). Based on the ^{1}H NMR spectrum, the second fraction contained unreacted methacryloyl end groups.

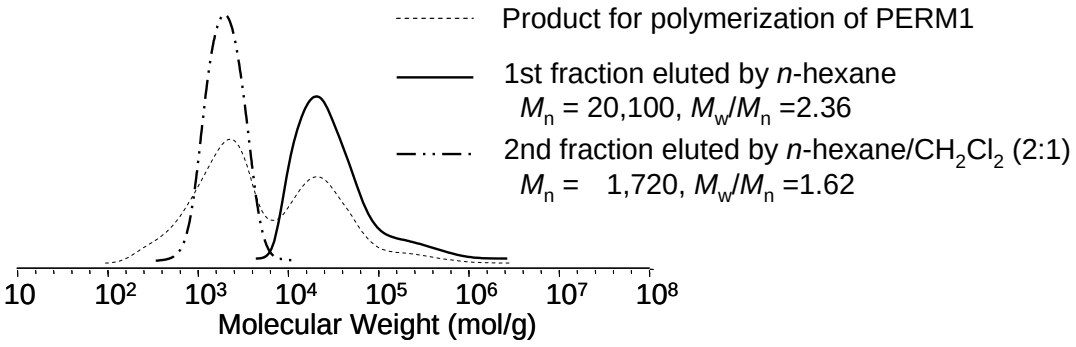

Figure 3. GPC traces of the product for polymerization of PERM1 and fractions obtained by liquid chromatography.

Figures 4 and 5 show the ^{1}H and ^{13}C NMR spectra of the isolated poly(PERM1), respectively. In the ^{1}H NMR spectrum, the signals of methacryloyl group protons of PERM1 (1.95, 5.5, and 6.1 ppm) disappeared and the signals of methylene protons adjoining ester group shifted from 3.8-4.2 ppm to 3.4-4.1 ppm (*a*) in comparison with the ^{1}H NMR spectrum of PERM1 in Figure 1(iii) (MA-PER1). In addition, the signals of methylene protons in polymethacrylate backbone appeared at 1.7-2.0 ppm (*b*). In the ^{13}C NMR spectrum, in addition to the signals of PER chain carbons, signals appeared at 15-20, 45, 52-55, 70, and 176-178 ppm. Based on the ^{13}C NMR measured in DEPT mode, these signals are respectively assigned to methyl carbon (*e*), quaternary carbon (*d*) and methylene carbon (*c*) in the polymethacrylate main chain, methylene carbon (*b*) adjoining ester group, and carbonyl carbon (*a*), respectively. Thus, NMR analyses revealed the formation of poly(PERM1).

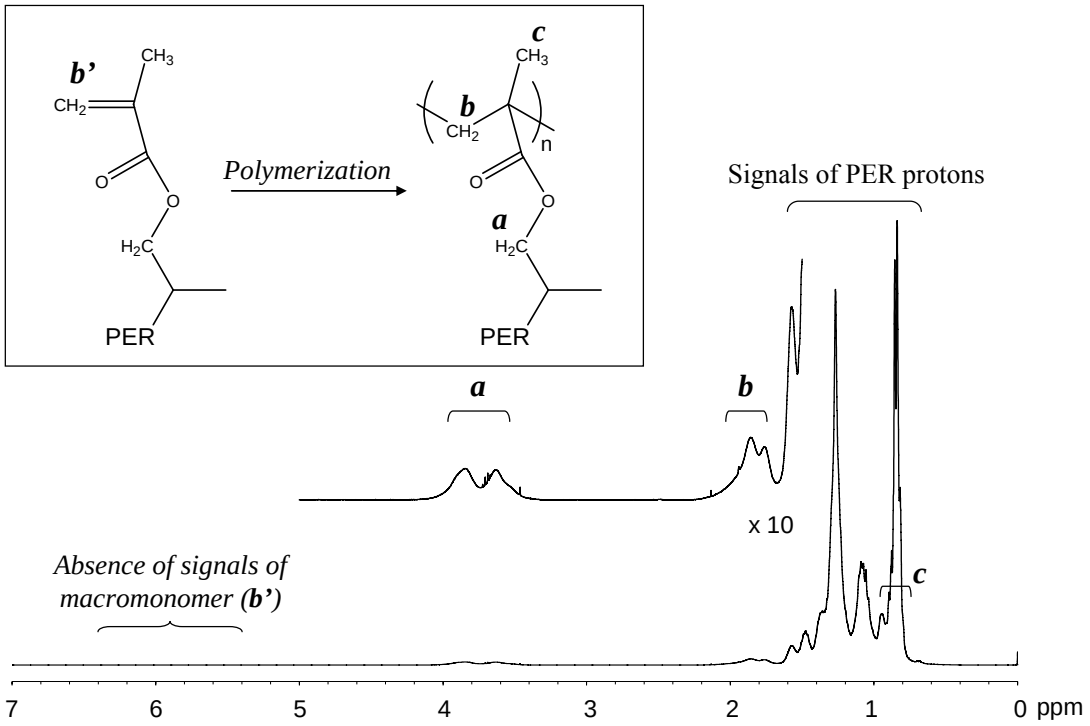

Figure 4. ^{1}H NMR spectrum of poly(PERM1) (400 MHz, in 1,2-dichlorobenzene-d_4 at 120 ºC).

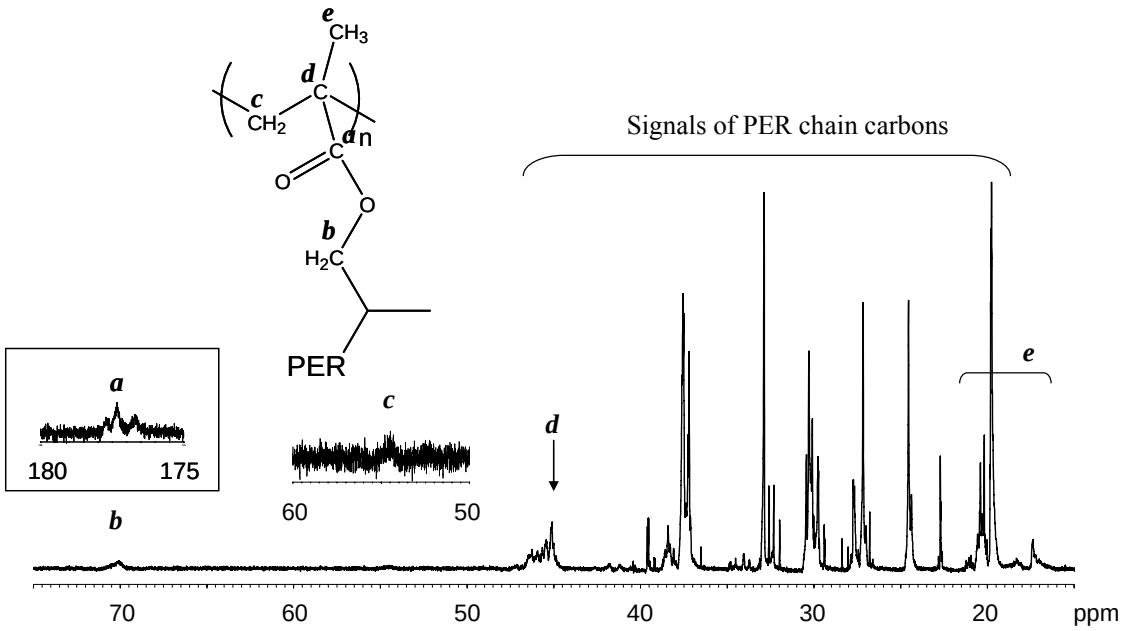

Figure 5. ^{13}C NMR spectrum of poly(PERM1) (100 MHz, in 1,2-dichlorobenzene-d_4 at 120 ºC).

Based on the D_p obtained by GPC measurement, this poly(PERM1) consists of a polymethacrylate backbone (M_n = 2,550) and 30 PER branch chains (M_n = 585). This is the first report of such unique polymer architecture, which is expected to be the hybrid materials consisting of polyolefins and polar polymers. Despite having the polymethacrylate backbone, this poly(PERM1) is a viscous liquid polymer and soluble even in non-polar hydrocarbon solvents such as *n*-hexane, due to the high branch density and the high content of PER segment (87 wt%).

In addition, the result of liquid chromatography indicates that the polarity of this poly(PERM1) was lower than that of unpolymerized macromonomers in *n*-hexane, despite having the same composition (the molar ratio of methacryloyl segment to PER segment was considered to be equal). One interpretation of this lower polarity for poly(PERM1) than that for PERM1 is as follows. This poly(PERM1) consists of two different segments, polar polymethacrylate and non-polar PER. Therefore, in non-polar solvent such as *n*-hexane, this poly(PERM1) would form a core-shell type structure, in which the polar core of the polymethacrylate backbone is inside the non-polar shell formed by PER side branches. Consequently, the apparent polarity of the poly(PERM1) in *n*-hexane is decreased.

The relationship between M_w and the intrinsic viscosity ([η]; measured in decalin at 135 ºC) of PERs obtained by using metallocene catalysts is shown in Figure 6. In the

case of linear PER, a linear relationship was observed independent of monomer composition. On the other hand, the obtained poly(PERM1) located obviously below this line. This result shows that poly(PERM1) has a lower viscosity than the linear PER with the same molecular weight owing to its unique polymer topology and composition.

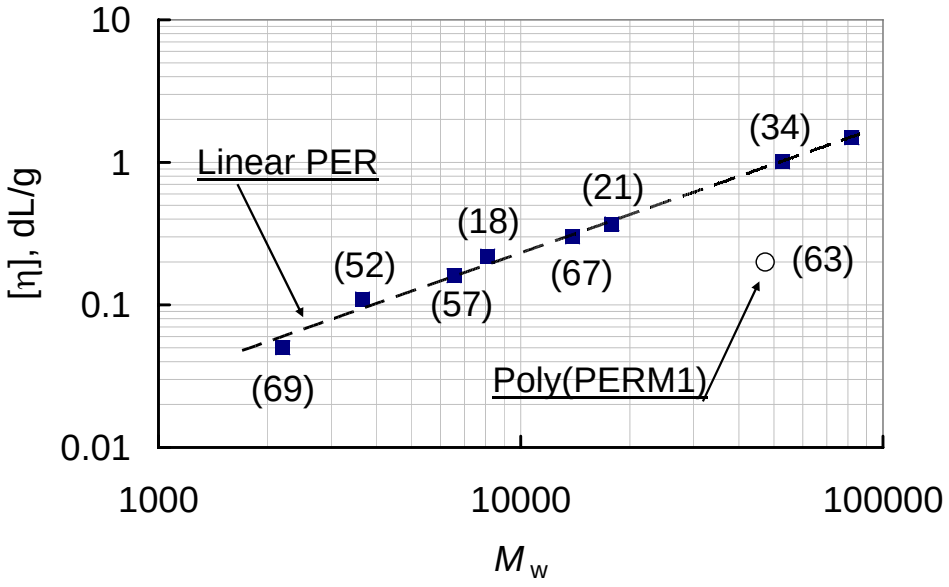

Figure 6. Double-logarithmic plots of [η] vs M_w for linear PERs and poly(PERM1). (Values in parentheses are the propylene content (mol%) in PER.)

Conclusions

Polymacromonomers with polyolefin branches were successfully synthesized by homopolymerization of methacryloyl-terminated PER macromonomer, which were synthesized by the conversion of the vinylidene-terminated PER obtained by metallocene-catalyzed polymerization. The obtained polymacromonomer could be isolated by liquid chromatography with a silica gel column. Based on ^{1}H and ^{13}C NMR analyses and GPC measurement, the obtained polymer consisted of a polymethacrylate backbone and 30 PER branch chains. This novel polymacromonomer exhibited the nature of PER rather than the nature of polymethacrylate because of its unique polymer architecture such as the high concentration of polyolefin branches. It is expected that various unique polymers having both polar polymer segment and polyolefin segment could be synthesized by applying this synthetic route.

References

[1] Tsukahara, Y.; Mizuno, K.; Segawa, A.; Yamashita, Y. Macromolecules 1989, 22, 1546-1552.

[2] Terao, K.; Hokajo, T.; Nakamura, Y.; Norisuye, T. Macromolecules 1999, 32, 3690-3694.

[3] Wintermantel, M.; Gerie, M.; Fisher, K.; Schmidt, M.; Wataoka, I.; Urakawa, H.; Kajiwara, K.; Tsukahara, Y. Macromolecules 1996, 29, 978-983.

[4] Gerle, M.; Fisher, K.; Roos, S.; Müller, A. H. E.; Schmidt, M.; Sheiko, S. S.; Prokhorova, S.; Möller, M. Macromolecules 1999, 32, 2629-2637.

[5] Sheiko, S. S.; Gerle, M.; Fisher, K.; Schmidt, M.; Möller, M. Langmuir 1997, 13, 5368-5372.

[6] Duschek, T.; Mülhaupt, R. Polym Prepr 1992, 33, 170-171.

[7] Hong, S. C.; Jia, S.; Teodorescu, M.; Kowalewski, T.; Matyjaszewski, K.; Gottfried, A. C.; Brookhart, M. J Polym Sci Part A: Polym Chem 2002, 40, 2736-2749.

[8] Kang, K. K.; Shiono, T.; Ikeda, T. Macromolecules 1997, 30, 1231-1233.

[9] Chung, T. C.; Lu, H. L.; Janvikul, W. Polymer 1997, 38, 1495-1502.

[10] Tsutsui, T.; Mizuno, A.; Kashiwa, N. Polymer 1989, 30, 428-431.

[11] Kojoh, S.; Tsutsui, T.; Kioka, M.; Kashiwa, N. Polym J 1999, 31, 332-335.

Chapter 6

Syntheses of Graft and Star Copolymers Possessing Polyolefin Branches by Using Polyolefin Macromonomer

Abstract

Graft and star copolymers having poly(methacrylate) backbone and ethylene–propylene random copolymer (EPR) branches were successfully synthesized by radical copolymerization of an EPR macromonomer with methyl methacrylate (MMA). EPR macromonomers were prepared by sequential functionalization of vinylidene chain-end group in EPR via hydroalumination, oxidation, and esterification reactions. Their copolymerizations with MMA were carried out with monofunctional and tetrafunctional initiators by atom transfer radical polymerization (ATRP). Gel permeation chromatography and NMR analyses confirmed that poly(methyl methacrylate) (PMMA)-*g*-EPR graft copolymers and four-arm (PMMA-*g*-EPR) star copolymers could be synthesized by controlling EPR contents in a range of 8.6–38.1 wt% and EPR branch numbers in a range of 1–14 branches. Transmission electron microscopy of these copolymers demonstrated well-dispersed morphologies between PMMA and EPR, which could be controlled by the dispersion of both segments in the range between 10 nm and less than 1 nm. Moreover, the differentiated thermal properties of these copolymers were demonstrated by differential scanning calorimetry analysis.

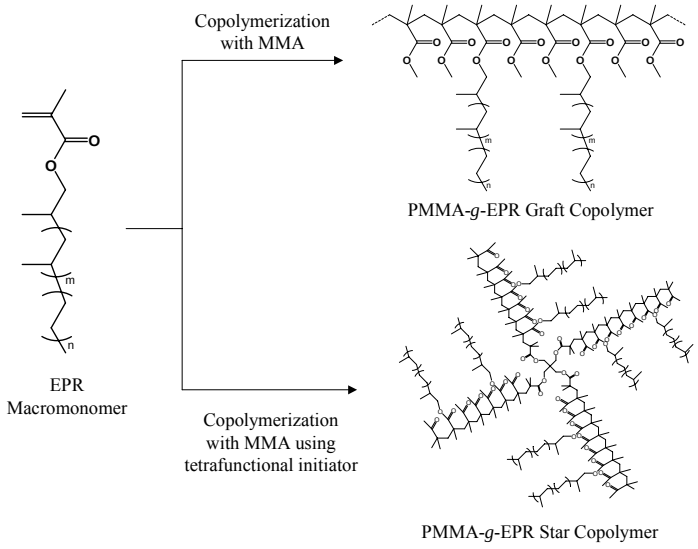

Introduction

Polyolefins represented by polyethylene (PE) and polypropylene (PP) are indispensable materials with certain social impact in countless beneficial ways. Their excellent properties, such as high mechanical strength, flexibility, chemical stability, and processability, led to their current widespread use. To broaden their applications to highly profitable fields, it has been desired to create new olefinic polymers with various topologies, such as block-, graft-, and star-shaped polymers, based on polyolefin. In particular, combination of polyolefin with the other polyolefin or non-polyolefin segments by chemical linkage has been attracting much attention as hybrid polymers between immiscible segments, such as crystalline and amorphous or polar and non-polar segments, leading to creation of novel and unique polymer materials. As mentioned in *General Introduction*, these new hybrid polymers could be synthesized by using functionalized polyolefin as three kinds of effective tools, which are polyolefin macroinitiator, polyolefin macromonomer and reactive polyolefin. In this chapter, the polyolefin macromonomer is focused and discussed to create novel polyolefin hybrids.

Polyolefin macromonomers possessing a polymerizable chain end were also reported to be useful to produce graft copolymers with polyolefin branches. Duschek *et al.* synthesized a polypropylene macromonomer with a methacryloyl end group, which was used to prepare poly(methyl methacrylate)-*g*-polypropylene graft copolymers by conventional free radical copolymerization [1]. Hong *et al.* reported the preparation of poly(*n*-butyl acrylate)-*g*-polyethylene graft copolymers by using Pd-mediated olefin polymerization and atom transfer radical polymerization [2]. However, it is inevitable that unreacted polyolefin macromonomers remain in the resulting polymers in any methods using polyolefin macromonomers. To overcome this disadvantage, we used polyolefin macromonomers on the basis of ethylene–propylene random copolymer (EPR) backbone, namely EPR macromonomer. EPR macromonomer is so easy to dissolve into organic solvents at a wide range of its molecular weights, and thus, it has an advantage in removing the unreacted polyolefin macromonomers. In *Chapter 5*, the authors reported the homopolymerization of propylene-ethylene random copolymer (PER) macromonomer to obtain pure poly(PER macromonomer) by removing the unreacted PER macromonomer [3,4].

In this chapter, EPR macromonomer is further studied to control the structures of poly(methyl methacrylate)(PMMA)-*g*-EPR graft and star copolymers variously, with keeping the well-defined manner, as summarized in Figure 1. Besides, the authors also discuss their nanostructures and thermal properties, focusing on the contents of EPR

segment and the topologies, and the practical function of the PMMA-*g*-EPR graft copolymer as a compatibilizer for the immiscible combination of EPR and PMMA.

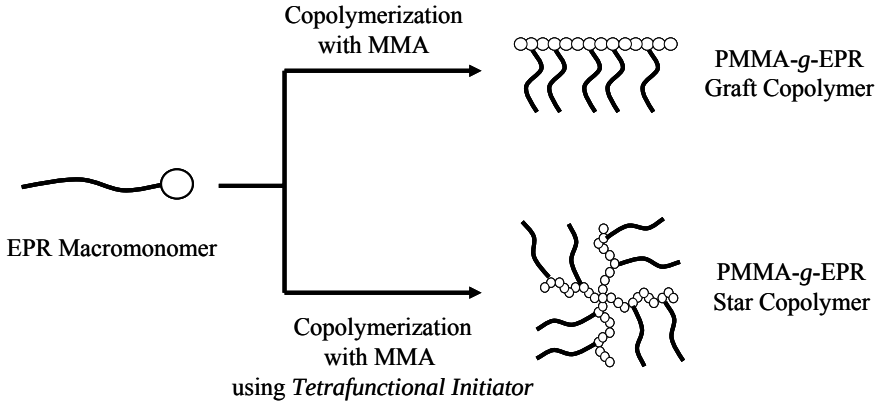

Figure 1. Target graft and star copolymers.

Experimental

General Procedures and Materials

All manipulations of air- and water-sensitive materials were performed under dry nitrogen atmosphere in a conventional nitrogen-filled glove box. Dicyclopentadienylzirconium dichloride (Cp_2ZrCl_2) and bis(1,3-dimethylcyclopenta-dienyl)zirconium dichloride [$(1,3\text{-}Me_2Cp)_2ZrCl_2$] were commercially obtained and used without further purification. Pentaerythritol, methacryloyl chloride, triethylamine, 2,2'-azobis(isobutyronitrile) (AIBN), copper bromide (CuBr), *N*,*N*,*N'*,*N"*,*N"*-pentamethyldiethylenetriamine (PMDETA), (1-bromoethyl)benzene (BEB), and 2-bromoisobutyryl bromide (BiBB) were purchased from Wako Pure Chemical Industries and used without further purification. MMA (Wako Pure Chemical Industries) was dried over CaH_2 and distilled *in vacuo*. Ethylene was purchased from Sumitomo Seika, and propylene was obtained from Mitsui Chemicals. Methylalminoxane (MAO) was purchased from Albemarle as 1.2 M toluene solution, and trimethylaluminum, which is considered an impurity, was evaporated in vacuo before use. Toluene and *o*-xylene (Wako Pure Chemical Industries) used as a polymerization solvent were dried over Al_2O_3 and degassed by bubbling with nitrogen gas. Diisobutylaluminum hydride (DIBAL-H) was purchased from Tosoh-Finechem. The EPR [number- average molecular weight (M_n) = 40,000; polydispersity index (M_w/M_n) = 2.01] for the polymer blend was prepared with Cp_2ZrCl_2/MAO catalyst system. The homo-PMMA (M_n = 22,800; M_w/M_n = 1.76) for the polymer blend was prepared by the polymerization of MMA with AIBN as an initiator. All other chemicals

were obtained commercially and used as received.

Synthesis of EPR Macromonomer

A typical process is as follows: toluene (800 mL) was placed in a 1-L glass reactor equipped with a mechanical stir bar, and then ethylene (20 L/h) and propylene gas (80 L/h) were fed into the reactor. MAO (10 mmol) and Cp_2ZrCl_2 (0.01 mmol) were added at 50 ^oC. After the copolymerization at atmospheric pressure at 50 ^oC for 2 h, DIBAL-H (50 mL, 0.28 mol as an aluminum atom) was added, and the mixture was heated at 110 ^oC for 5.5 h under stirring. Dried air at 110 ^oC was then continuously fed (100 L/h) into the system. After 6 h, the system was purged with nitrogen gas and then cooled to room temperature. The reaction mixture was washed three times with aqueous hydrochloric acid solution (0.5 N) and three times with distilled water. The resulting polymer was separated as a yellow viscous liquid by the evaporation of toluene and then dried *in vacuo* at 80 ^oC for 10 h to give hydroxyl-terminated EPR (125.4 g, 0.802 mmol of OH/g of polymer according to ^1H NMR analysis). After hydroxyl-terminated EPR (120 g, 96.2 mmol as a hydroxyl end group) and toluene (250 mL) were placed in a 500-mL glass reactor equipped with a mechanical stir bar, the system was degassed by bubbling with nitrogen gas. Triethylamine (13.4 mL, 96.2 mmol) and methacryloyl chloride (18.8 mL, 192.5 mmol) were added to the reactor, and then the mixture was stirred at room temperature for 6 h. The reaction mixture was filtered to remove the white precipitated powder, and EPR with a methacryloyl end group was separated as a yellow viscous liquid by the evaporation of toluene. Then, 130 g of this EPR with a methacryloyl end group was dissolved in 50 mL of *n*-hexane and poured into a glass column packed with silica gel. The first fraction was eluted by using *n*-hexane and the second fraction by *n*-hexane/chloroform (4:1) mixed solvent. The second fraction was evaporated and dried *in vacuo* at 30 ^oC for 10 h to give 50.6 g of methacryloyl-terminated EPR. By selecting the reaction conditions and catalysts, two kinds of methacryloyl-terminated EPRs with different molecular weights were obtained and then used as EPR macromonomer, EPRM (0.9 K) and EPRM (3 K). The details of the reaction conditions and characteristics for each EPR macromonomer are shown later in Table 1.

Synthesis of PMMA-g-EPR Graft Copolymers by ATRP

A typical copolymerization process is as follows: after EPRM (0.9 K) (0.24 g, 0.20 mmol as a methacryloyl group) was placed in a 30-mL Schlenk tube equipped with a stirring bar, *o*-xylene (6.3 mL), a solution of CuBr/PMDETA in *o*-xylene (1.36 mL, 0.10 mmol as a copper atom), MMA (2.14 mL, 20.0 mmol) and a solution of BEB in

o-xylene (0.20 mL, 0.10 mmol) were added to the tube and the mixture was heated at 90 °C for 6 h. The polymerization was stopped by cooling the mixture in an ice bath and then quenched by the addition of methanol (*ca.* 5 mL). The reaction mixture was poured into 400 mL of methanol and the obtained white solid was collected by filtration, washed by using *n*-hexane and methanol and dried at 120 °C *in vacuo*. As shown later in Table 2, seven kinds of PMMA-*g*-EPR graft copolymers were obtained. The details of the polymerization conditions and the characteristics of the obtained polymers are also shown later in Table 2.

Synthesis of PMMA-g-EPR Graft Copolymers by Using AIBN as an Initiator

A typical copolymerization process is as follows: after EPRM (0.9 K) (0.98 g, 0.80 mmol as a methacryloyl group) was placed in a 30-mL Schlenk tube equipped with a stirring bar, toluene (10 mL), MMA (2.14 mL, 20 mmol), and a solution of AIBN in toluene (3.26 mL, 0.10 mmol) were added to the tube and the mixture was heated at 60 °C for 4 h. The reaction mixture was poured into 2000 mL of methanol and the obtained white solid was collected by filtration, washed by using *n*-hexane and methanol and dried at 120 °C *in vacuo*. As shown later in Table 7, two kinds of PMMA-*g*-EPR graft copolymers were obtained by selecting the polymerization conditions.

Preparation of Tetrafunctional Initiator

In a dried 50-mL Schlenk tube, pentaerythritol (1 g, 7.34 mmol), triethylamine (8.20 mL, 58.8 mmol), and tetrahydrofuran (10 mL) were placed and the mixture was stirred at 0 °C. Then, BiBB (7.26 mL, 58.8 mmol) was added and the mixture was stirred at ambient temperature for 24 h. The reaction mixture was washed with aqueous hydrochloric acid and water. After the solvent evaporated, the obtained black solid was purified by liquid chromatography to give a white crystalline pentaerythritol tetrakis(2-bromoisobutyrate) (3.7 g).

Synthesis of PMMA-g-EPR Star Copolymers by Using a Tetrafunctional Initiator

A typical copolymerization process is as follows: after EPRM (0.9 K) (2.44 g, 2.0 mmol as a methacryloyl group) was placed in a 100-mL Schlenk tube equipped with a stirring bar, *o*-xylene (34.7 mL), a solution of CuBr/PMDETA in *o*-xylene (1.19 mL, 0.336 mmol as a copper atom), MMA (2.14 mL, 20.0 mmol), and a solution of pentaerythritol tetrakis(2-bromoisobutyrate) in *o*-xylene (2.0 mL, 0.10 mmol) were added to the tube and the mixture was heated at 90 °C for 6 h. The polymerization was stopped by cooling the mixture in an ice bath and then quenched by the addition of

methanol (*ca.* 5 mL). The reaction mixture was poured into 400 mL of methanol and the obtained white solid was collected by filtration, washed by using *n*-hexane and methanol and dried at 120 ^{o}C *in vacuo*. As shown later in Table 4, two kinds of PMMA-*g*-EPR star copolymers were obtained by using different polymerization conditions.

Preparation of the Blended Polymers

The blended polymers, used for transmission electron microscopy (TEM) images shown later in Figure 10, were prepared in solution to obtain molecular-level mixing. The polymers (*ca.* 0.6 g) and *o*-xylene (20 mL) were added to a 100-mL Schlenk tube equipped with a stirring bar and were stirred at 130 ^{o}C, until the polymer mixture was homogeneous (*ca.* 1 h). The blended polymer was precipitated in 1000 mL of methanol and then filtered and dried at 80 ^{o}C *in vacuo*.

Analytical Procedures

^{1}H NMR spectra were recorded on JEOL GSX-270 (270 MHz) or GSX-400 (400 MHz) spectrometers using chloroform-*d* or 1,2-dichlorobenzene-d_4 as a solvent at 25 ^{o}C or 120 ^{o}C. The gel permeation chromatograms (GPC) of the EPR macromonomer at 140 ^{o}C in 1,2-dichlorobenzene were recorded by using Waters Alliance GPC2000 equipped with four TSKgel columns (two sets of TSKgelGMH6-HT and two sets of TSKgelGMH6-HTL) calibrated with EPR. The GPC of the graft and star copolymers at 40 ^{o}C in chloroform were recorded by using GL Sciences RI-504R differential refractometer with three Waters STYRAGEL columns (two sets of STYRAGEL HT 6E and STYRAGEL HR 5E) calibrated with PS. The glass transition temperatures of the polymers were measured by using Seiko Instruments RDC220 differential scanning calorimeter (DSC). The DSC curves were recorded during the second heating cycle from -100 to 200 ^{o}C, with a heating rate of 10 ^{o}C/min.

TEM Analysis

Ultrathin (*ca.* 100 nm) sections of the polymer, which had been pressed into a sheet, were cut on a Reica Ultracut microtome equipped with a diamond knife at a low temperature and were then stained with RuO_4. TEM observations were made with a Hitachi H-7000 TEM at an acceleration voltage of 75 kV and at a magnification of 20,000× and 100,000×.

Results and Discussion

Synthesis of EPR Macromonomers

The synthetic route of EPR macromonomer studied here is shown in Scheme 1. EPR with a vinylidene end group was obtained by ethylene copolymerization with propylene by using a typical metallocene catalyst. Unsaturated chain ends of the polymer were converted into hydroxyl end groups by hydroalumination or hydroboration and subsequent oxidation, as previously reported [5]. Hydroalumination of the obtained vinylidene end groups by DIBAL-H was then carried out at 110 ^{o}C in toluene. Then, dry air was fed into the resulting mixture at 110 ^{o}C to convert the alkylaluminum end groups to hydroxyl end groups. The obtained hydroxyl end groups were reacted with methacryloyl chloride in the presence of a Lewis base at room temperature to be converted into methacryloyl end groups. To remove the undesirable EPR that has saturated, vinylidene and hydroxyl end groups, the obtained EPR was purified by liquid chromatography. This EPR with a methacryloyl end group was then used as an EPR macromonomer. By selecting the polymerization conditions and catalyst, two kinds of EPR macromonomers with different molecular weights, EPRM (0.9 K) and EPRM (3 K), were obtained.

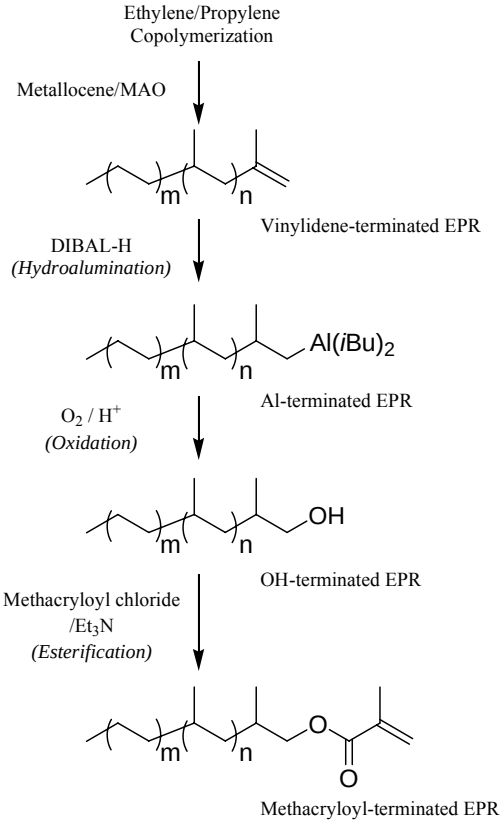

Scheme 1. Synthetic route of EPR macromonomer.

Figure 2 shows the ^{1}H NMR spectrum of EPRM (0.9 K). The spectrum indicates all the key signals arising from EPR backbone unit (*e–j*) and methacryloyl end group (*a–d*). From the relative intensities of these signals, the contents of ethylene, propylene, and methacryloyl unit were calculated to be 42.2, 54.7, and 3.10 mol %, respectively. In addition, the number-average molecular weight (M_n) calibrated with EPR was estimated to be 940 by GPC measurement. The number-average end functionality (F_n) was derived from the unit composition and M_n was found to be 0.78. The absence of vinylidene and hydroxyl end groups in the ^{1}H NMR spectrum indicates that the residual chain ends were saturated end groups. Table 1 summarizes the synthesis and characterization of EPR macromonomers.

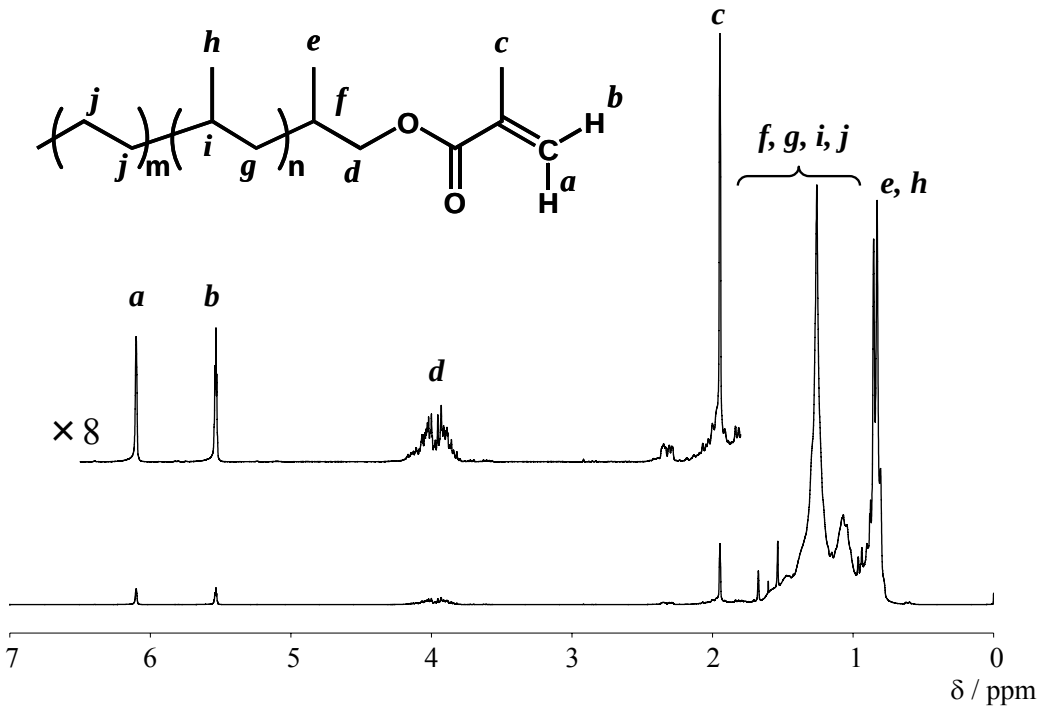

Figure 2. ^{1}H NMR Spectrum of EPRM(0.9K) (270 MHz in $CDCl_3$ at 25 ^{o}C).

Table 1. Characterization of EPR Macromonomer

Macromonomer	Composition[c] (mol%)			M_n[d] (g mol^{-1})	M_n[e] (g mol^{-1})	M_w/M_n[e]	F_n[f] (unit/chain)
	Ethylene	Propylene	Methacryloyl				
EPRM(0.9K)[a]	42.2	54.7	3.10	1,700	940	2.34	0.78
EPRM(3K)[b]	45.5	53.5	0.97	5,800	3,020	1.63	0.81

[a] Polymerization conditions: [MAO]/[Cp_2ZrCl_2] = 0.025/2.5×10^{-5} M, C_2H_4/C_3H_6 = 20/80 L/h, in toluene 800 mL at 50 °C for 2 h; Hydroalumination conditions: DIBAL-H 50 mL at 110 °C for 5.5 h; Oxdation Conditions: Dried air 100 L/h at 100 °C for 6 h; Esterification conditions: EPR-OH/Methacryloyl chloride/Et_3N = 1/2/1 *eq.* in toluene 250 mL at 25 °C for 6 h.

[b] Polymerization conditions: [MAO]/[(1,3-$Me_2Cp)_2ZrCl_2$] = 0.025/2.5×10^{-5} M, C_2H_4/C_3H_6 = 40/60 L/h, in toluene 800 mL at 60 °C for 2 h; Hydroalumination conditions: DIBAL-H 44 mL at 100 °C for 4 h; Oxdation Conditions: Dried air 100 L/h at 100 °C for 7 h; Esterification conditions: EPR-OH/Methacryloyl chloride/Et_3N = 1/10/5 *eq.* in toluene 50 mL at 25 °C for 21 h.

[c] Determined by ^{1}H NMR.

[d] Molecular weight was determined by GPC at 40 °C in $CHCl_3$ and calibrated with PS.

[e] Molecular weight was determined by GPC at 140 °C in 1,2-dichlorobenzene and calibrated with EPR.

[f] Number-average end functionality (F_n) was calculated from unit compositions and M_n.

Synthesis of PMMA-g-EPR Graft Copolymers

PMMA-*g*-EPR graft copolymers were synthesized by copolymerization of EPR macromonomers with MMA by using ATRP method, as shown in Scheme 2. The copolymerization of EPR macromonomer with MMA was carried out by using BEB as an initiator in combination with CuBr and PMDETA in *o*-xylene at 90 °C. After the copolymerization, the reaction mixture was poured into methanol and the obtained white precipitate was filtered and washed by using *n*-hexane to remove the unreacted EPR macromonomer.

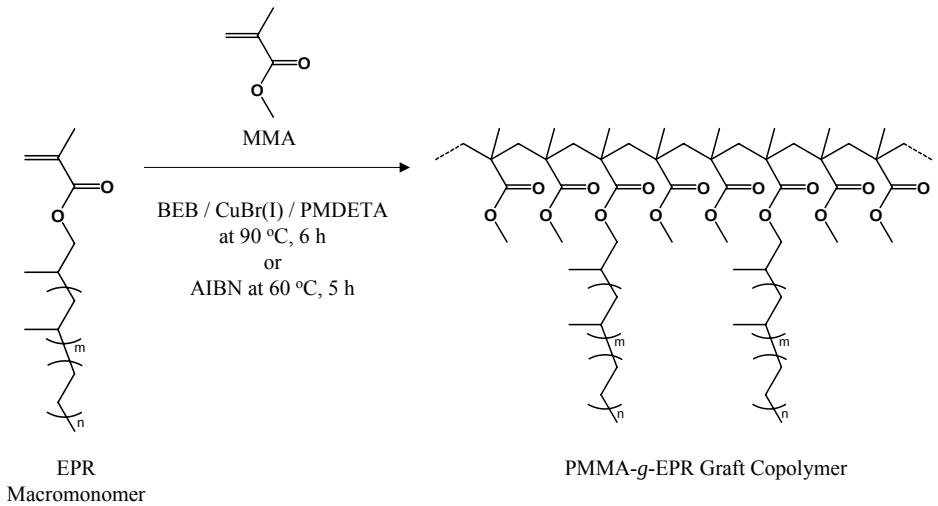

Scheme 2. Synthesis of PMMA-*g*-EPR graft copolymer.

By changing the feed ratio of EPR macromonomer/MMA and using two kinds of EPR macromonomers having different molecular weight, EPRM (0.9 K) and EPRM (3 K), seven kinds of the polymers were synthesized. The obtained polymers were characterized by GPC measurement and ^{1}H NMR analysis, as shown in Table 2. Figure 3 shows the GPC traces of the EPRM (0.9 K) and the obtained graft copolymer (**G1**). These GPC traces show that the obtained polymer could be completely purified and had relatively narrow molecular weight distribution (M_w/M_n = 1.45).

Table 2. Preparation of PMMA-*g*-EPR Graft Copolymers[a]

	EPR Macromonomer		MMA	$[MMA]_0$ /	Yield	M_n[b]		EPR content[c]	
		(g)	(mL)	$[EPRM]_0$	(g)	(g mol^{-1})	M_w/M_n[b]	(mol%)	(wt%)
G1	EPRM(0.9K)	4.88	4.28	10	2.77	28,200	1.40	6.2	38.1
G2	EPRM(0.9K)	1.95	4.28	25	2.52	27,500	1.41	2.6	19.9
G3	EPRM(0.9K)	0.49	2.14	50	1.06	29,300	1.39	2.0	15.9
G4	EPRM(0.9K)	0.24	2.14	100	1.01	32,300	1.45	1.0	8.6
G5	EPRM(3K)	1.49	2.14	50	1.49	27,700	1.48	1.1	24.9
G6	EPRM(3K)	0.93	2.14	80	1.19	34,600	1.56	0.72	18.0
G7	EPRM(3K)	0.37	2.14	200	1.00	29,000	1.62	0.37	10.0

[a] Polymerization conditions: [BEB]/[CuBr]/[PMDETA]/[MMA] = 0.01/0.01/0.02/2.0 M in *o*-xylene at 90 °C for 6 h.
[b] Molecular weight was determined by GPC at 40 °C in $CHCl_3$ and calibrated with PS.
[c] Determined by ^{1}H NMR.

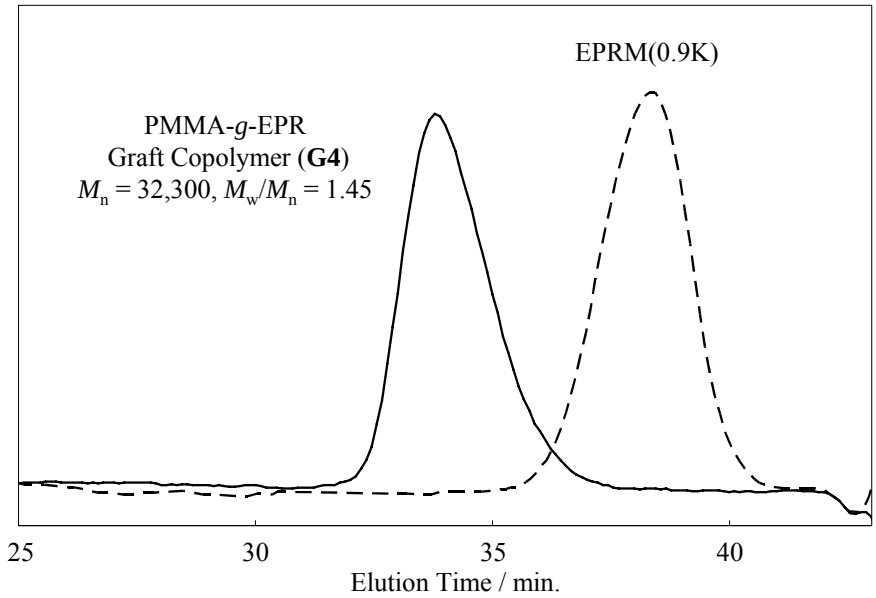

Figure 3. GPC traces of the EPRM(0.9K) and PMMA-*g*-EPR graft copolymer (**G4**).

^{1}H NMR spectrum of this graft copolymer (**G1**) is shown in Figure 4. The signals at δ 7.0–7.2 ppm can be assigned to the phenyl ring protons, based on the initiator (*a*, *b*), and the signals at δ 3.6 and 3.8–4.0 ppm can be assigned to the ester group protons of MMA and EPRM (0.9 K) (*c*, *d*), respectively. In addition, the signals of the poly(methacrylate) backbone and the EPR branch protons were observed at δ 0.7–2.0 ppm. This result of ^{1}H NMR analysis shows the formation of PMMA-*g*-EPR graft copolymers obviously. From the relative intensities of each signal, the unit composition of the initiator, EPRM (0.9 K), and MMA was estimated to be 0.45, 6.2, and 93.4 mol %, respectively.

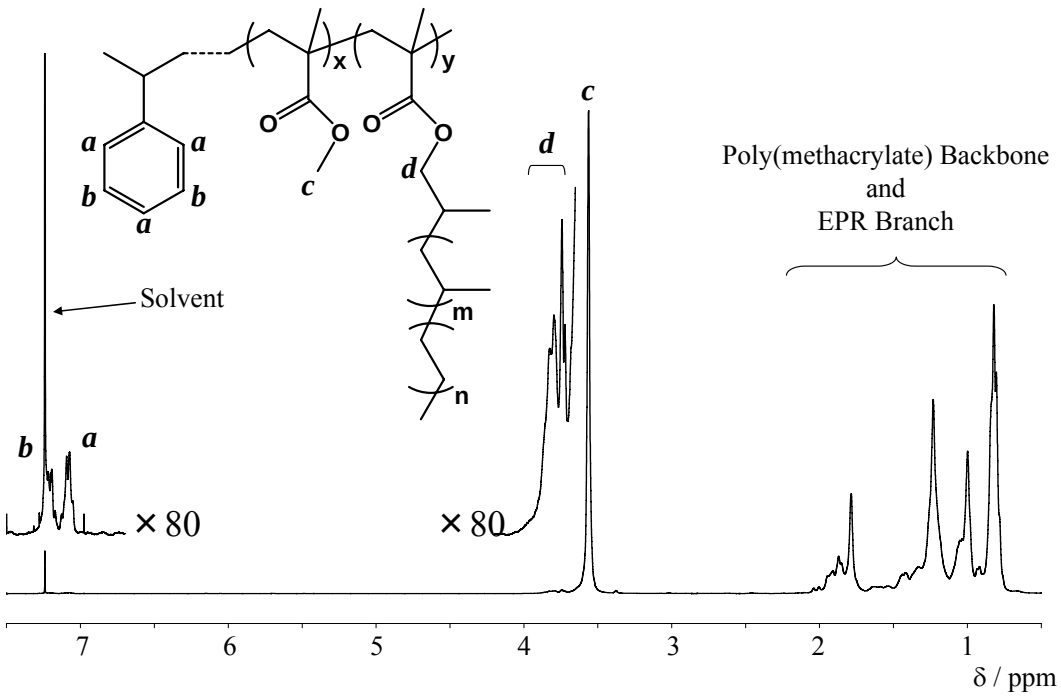

Figure 4. ^{1}H NMR Spectrum of PMMA-*g*-EPR graft copolymer (**G4**) (400 MHz in $CDCl_3$ at 50 ^{o}C).

As shown in Table 2, all graft copolymers had the considerably narrow molecular weight distribution (M_w/M_n = 1.39–1.62). As the feed ratio of EPR macromonomer to MMA increased, the content of EPR in the obtained graft copolymer increased. In the case of EPRM (0.9 K), the weight fraction of EPR in the obtained graft copolymer was controlled from 8.6 to 38.1 wt % and in the case of EPRM (3 K), the weight fraction of EPR was controlled in the range of 10.0–24.9 wt %. When the initial feed ratio of $[MMA]_0/[EPRM\ (0.9\ K)]_0$ decreased less than 10, the obtained graft copolymer dissolved in *n*-hexane and the isolation of the graft copolymer was very difficult. Because *n*-hexane is a poor solvent to PMMA and a good solvent to EPR, the solubility

of the obtained graft copolymer in *n*-hexane depends on the weight fraction of EPR segment in the graft copolymer. These results indicate that the borderline of the solubility to *n*-hexane is around 40 wt % of EPR weight fraction in this type of graft copolymer.

Assuming that the chain end of the obtained graft copolymers consists of the initiator, the unit composition of EPR macromonomer, and MMA per polymer chain, average EPR branch number and number-average molecular weight can be calculated from ^{1}H NMR analysis, as shown in Table 3. In the case of EPRM (0.9 K), average EPR branch number was controlled from 2 (**G4**) to 14 (**G1**). On the other hand, in the case of EPRM (3 K), average EPR branch number was 1 or 2 due to less reactivity of the higher molecular weight of EPR macromonomer. It is considered that the smaller branch numbers in the case of EPRM (3 K) with higher molecular weight were caused by increase of viscosity in the polymerization system.

Table 3. Characterization of PMMA-*g*-EPR Graft Copolymers

	Unit Composition			EPR Branch Number (Average)/chain	$M_{n,NMR}$ (g mol^{-1})
	Initiator	EPRM	MMA		
G1	1	13.6	207	14	33,700
G2	1	5.3	200	5	25,100
G3	1	4.3	212	4	25,300
G4	1	2.1	207	2	22,800
G5	1	2.1	187	2	25,100
G6	1	1.4	192	1	23,600
G7	1	0.8	216	1	24,200

Synthesis of (PMMA-g-EPR) Star Copolymers

It is well known that a selection of the multifunctional initiator in the ATRP of polar monomers realizes generation of the star polymers with various arm numbers, lengths, and compositions. Matyjaszewski *et al.* reported the synthesis of styrenic and (meth)acrylic star polymers by the ATRP method, using multifunctional initiators [6,7]. In this study, it was combined with the copolymerization of the EPR macromonomer with MMA as discussed earlier. The tetrafunctional initiator was prepared by a reaction between pentaerythritol and BiBB, as shown in Scheme 3. By copolymerization of EPRM (0.9 K) with MMA using the tetrafunctional initiator, the star polymers having PMMA-*g*-EPR graft copolymer arms could be synthesized in combination with CuBr/PMDETA in *o*-xylene at 90 ^{o}C, as shown in Scheme 4.

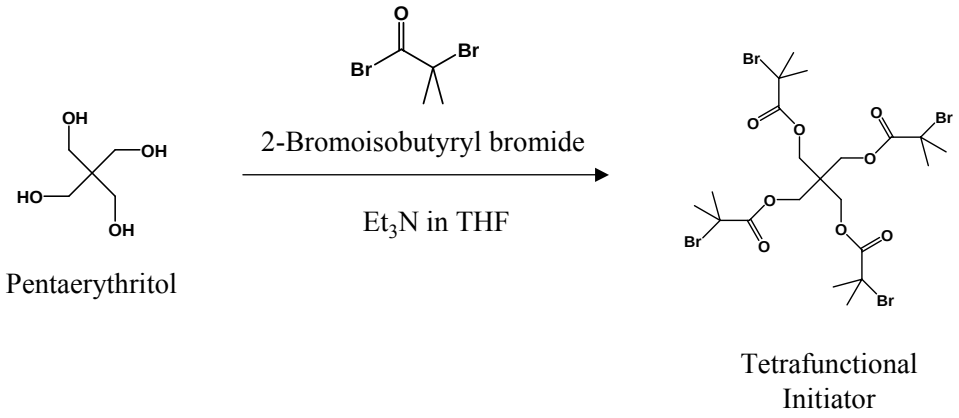

Scheme 3. Preparation of a tetrafunctional initiator.

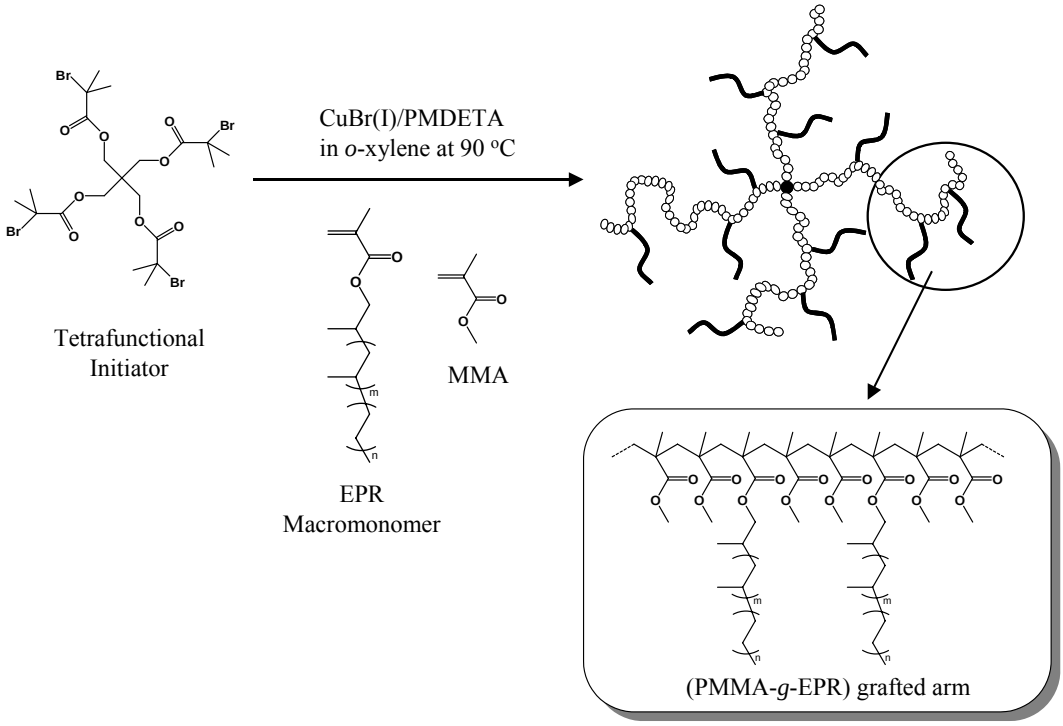

Scheme 4. Synthesis of the four-arms (PMMA-*g*-EPR) star copolymer.

After the copolymerization, the obtained polymer was purified by the same method as have been done earlier for the graft copolymers. The obtained polymers were characterized by GPC measurement and ^{1}H NMR analysis. Table 4 summarized the characterization results of the obtained polymers. From the GPC traces, the obtained star copolymer (**S1**) did not contain unreacted EPR macromonomer and had narrow molecular weight distribution (M_w/M_n = 1.32), as shown in Figure 5.

Table 4. Preparation of PMMA-*g*-EPR Star Copolymers[a]

	EPRM(0.9K) (g)	MMA (mL)	$[MMA]_0$ / $[EPRM(0.9K)]_0$	Yield (g)	M_n[b] (g mol^{-1})	M_w/M_n[b]	EPR content[c] (mol%)	EPR content[c] (wt%)
S1	2.44	2.14	10	0.82	27,100	1.32	5.3	36.3
S2	0.98	2.14	25	0.92	28,200	1.41	2.3	21.0

[a] Polymerization conditions: [Tetrafunctional initiator]/[CuBr]/[PMDETA]/[MMA] = 0.01/0.01/0.02/2.0 M in *o*-xylene at 90 °C for 6h.
[b] Molecular weight was determined by GPC at 40 °C in $CHCl_3$ and calibrated with PS.
[c] Determined by ^{1}H NMR.

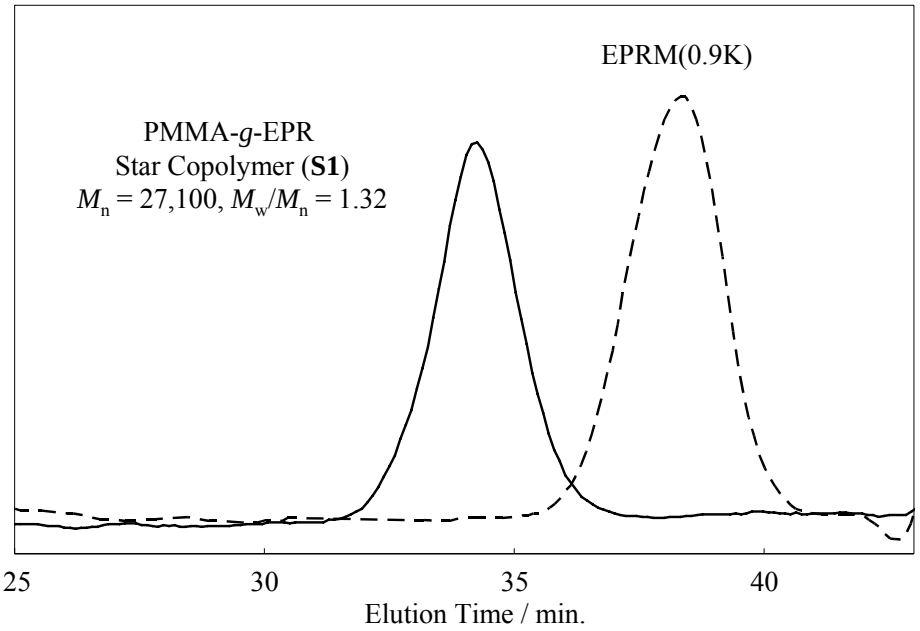

Figure 5. GPC traces of the EPRM(0.9K) and PMMA-*g*-EPR star copolymer (**S1**).

Figure 6 shows a ^{1}H NMR spectrum of this star copolymer (**S1**). In this spectrum, some specific signals were observed at δ 3.9–4.2 ppm (*a*: the ester group protons of EPR macromonomer), δ 3.8 ppm (*b*: the ester group protons of MMA), and δ 4.5 ppm (*c*: the methylene protons of the initiator). In addition, the signals were observed at a low magnetic field (δ 5.5–6.5 ppm), which would be assigned to the carbon–carbon double bond protons generated by the elimination of HBr from the bromine-end structure of each arm. On the other hand, from ^{1}H NMR analysis, the used tetrafunctional initiator has not only bromine-end structure as an initiation site but also small amount of vinylidene-, isopropyl-, and hydroxyl-end structures as a noninitiation site as shown in Figure 7. Therefore, it is considered that the average number of arms can be estimated from the relative intensities between these end structures as a

noninitiation site and the methylene unit bonded to the center carbon in the tetrafunctional initiator. Figure 8 shows a magnification of the low magnetic field in Figure 6. In this magnified spectrum, the signal observed at δ 6.2 ppm would assign the vinylidene-end proton as a noninitiation site. The other that signals as a noninitiation site, such as isopropyl- and hydroxyl-end structures, were too weak to be detected in this ^{1}H NMR spectrum. This would be a reasonable result considering the existence ratio of each structure in the tetrafunctional initiator. From the relative intensities between the vinylidene-end and the methylene unit protons, the average number of arms in the obtained polymer was estimated to be 3.8. Therefore, the obtained polymer was confirmed to be the star structure having about four (PMMA-*g*-EPR) graft copolymer arms. Furthermore, the average EPR branch number per arm was calculated to be 1.6 from the unit composition of MMA and EPR macromonomer. Table 5 summarizes the average number of arms and the average branch number per arm in these star copolymers.

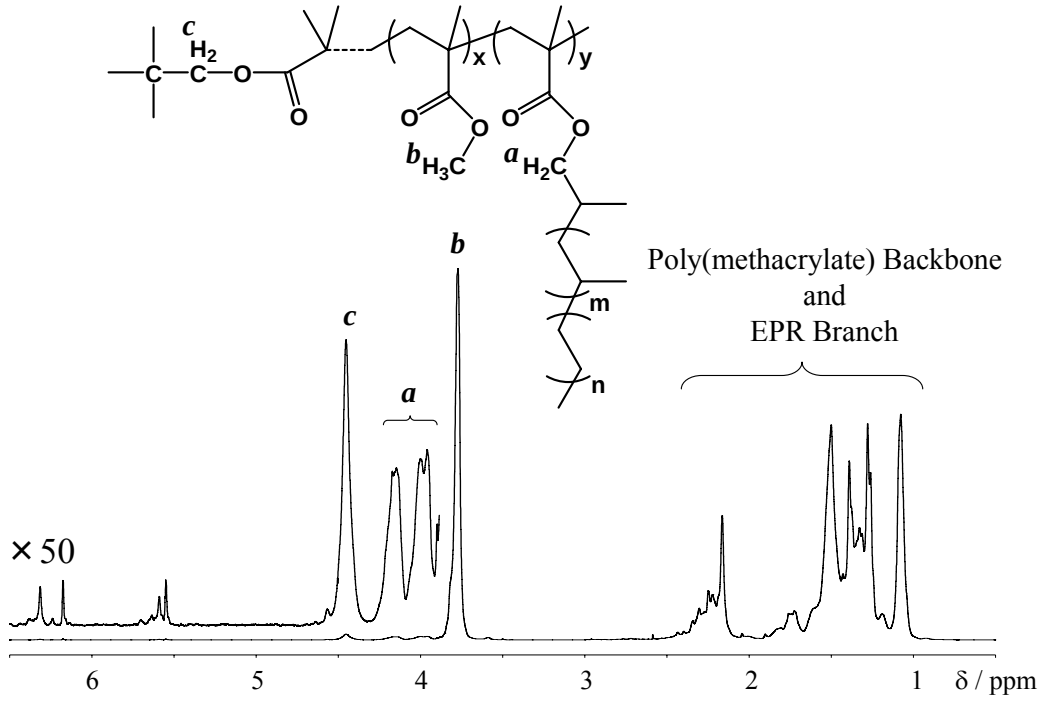

Figure 6. ^{1}H NMR Spectrum of PMMA-*g*-EPR star copolymer (**S1**) (400 MHz in 1,2-Dichlorobenzene-d_4 at 120 ^{o}C).

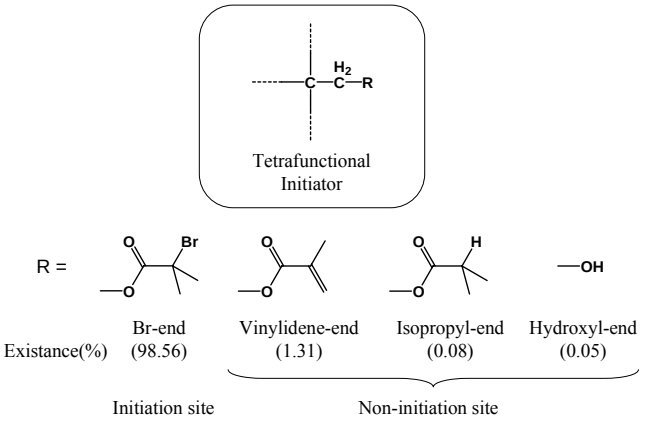

Figure 7. End structures on the tetrafunctional initiator observed by ^{1}H NMR.

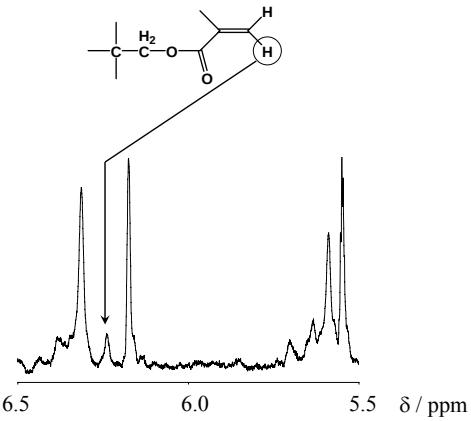

Figure 8. Magnified ^{1}H NMR spectrum of PMMA-*g*-EPR star copolymer (**S1**) (400 MHz in 1,2-Dichlorobenzene-d_4 at 120 ^{o}C).

Table 5. Average Arm Number and Branch Number in the Star Copolymers

	Average arm number	Average EPR branch number (unit/arm)
S1	3.81	1.60
S2	3.87	0.73

Morphologies of PMMA-g-EPR Graft and Star Copolymers

The morphologies of these PMMA-*g*-EPR graft and star copolymers were observed by TEM, as shown in Figure 9. Although all of them demonstrated microphase-separated morphologies, they were definitely different. Figure 9a shows morphology of PMMA-*g*-EPR graft copolymer with low EPR content (8.6 wt %, **G4**) obtained by ATRP method. In this picture, the black domain of EPR was observed in the white PMMA matrix, and the average size of the EPR domain was estimated to be about 10 nm. On the other hand, in the case of PMMA-*g*-EPR graft copolymer with high EPR content (38.1 wt %, **G1**) obtained by ATRP method, each segment dispersed more finely in comparison with that with low EPR content, as shown in Figure 9b. Those nano-order phase-separated morphologies consisting of PMMA and EPR domains have never been reported because of their immiscible combination. However, intermolecular aggregation of EPR branches should be still considered in Figure 9a. By increasing EPR branches, the average size of the dispersed phase became finer drastically and distinguishing which segment was matrix was impossible in the case of **G1**, as shown in Figure 9b. It is considered that many EPR branches prevent each segment from aggregating themselves. Figure 9c shows morphology of four-arm (PMMA-*g*-EPR) star copolymer

with higher EPR content (36.3 wt %, **S1**). Although the EPR content of this star copolymer is similar to that of the graft copolymer, **G1**, the segmental dispersion in this star copolymer seems much finer than that in the graft copolymer, **G1**, and the average size of each segment in this star copolymer was estimated to be less than 1 nm. Part of this is because a PMMA backbone in the star copolymer has a unique conformation that four PMMA arms spread through from a center molecule radially and the movement of the PMMA backbone in the star polymer would be restricted. In addition, the entanglement of the backbone in the star copolymer is considered to be less than that in the graft copolymer. Therefore, the intermolecular aggregation of each segment in the star copolymer would become more difficult, resulting to give extremely well-dispersed structure between each segment. These results demonstrate that the morphology of the graft and star copolymer can be controlled by the composition of each segment, the number of branches, and the topology of the backbone.

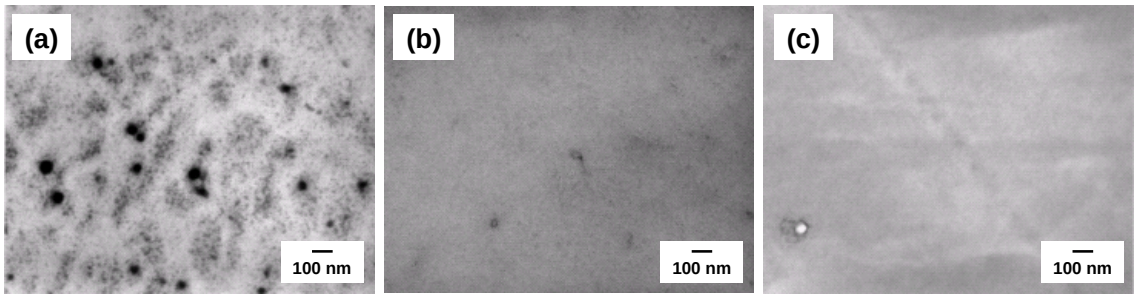

Figure 9. TEM Images of (a) PMMA-*g*-EPR graft copolymer (EPR content = 8.6 wt%; **G4**), (b) PMMA-*g*-EPR graft copolymer (38.1 wt%; **G1**) and (c) four-arms (PMMA-*g*-EPR) star copolymer (36.3 wt%; **S1**).

Compatibility of PMMA-g-EPR Graft Copolymer for EPR and PMMA Blend

Because the copolymers obtained in this study consist of two segments with a different nature, such as EPR and PMMA, these copolymers can be expected to be a compatibilizer for immiscible combination such as polyolefin/non-polyolefin blend. Figure 10a shows morphology of EPR/PMMA (50/50 wt %) blend observed by TEM. In this picture, the white PMMA domain was observed in the black EPR matrix and the size of the PMMA domain was estimated to be more than 10 lm in diameter. After adding 10 wt % of the graft copolymer with high EPR content, **G1**, to this polymer blend, morphology remarkably changed as shown in Figure 10b. The PMMA domain finely dispersed up to about 10 nm. This result demonstrates that PMMA-*g*-EPR graft copolymer effectively worked as a compatibilizer for EPR/PMMA polymer blend.

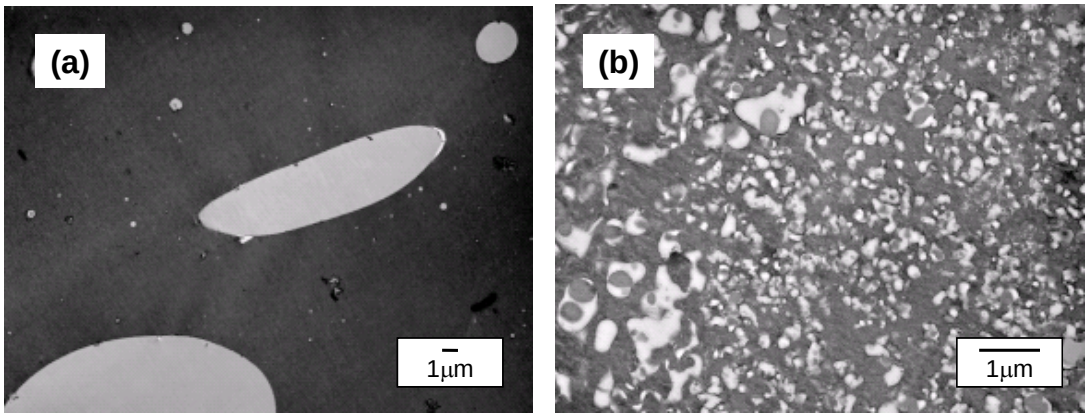

Figure 10. TEM Images of EPR / PMMA blend (a) before adding PMMA-*g*-EPR graft copolymer (EPR / PMMA = 50 / 50 wt%) and (b) after adding PMMA-*g*-EPR graft copolymer (EPR / PMMA-*g*-EPR / PMMA = 45 / 10 / 45 wt%).

DSC Analysis of the PMMA-g-EPR Graft and Star Copolymers

The glass transition temperatures (T_gs) of the obtained graft and star copolymers were measured by DSC analysis. The results for a series of the obtained graft and star copolymers were summarized in Table 6. In all cases, one or two clearly distinguished T_g peaks were observed, as shown in Figure 11.

Table 6. DSC Results for the PMMA-*g*-EPR Graft and Star Copolymers

Sample	EPR content (mol%)	EPR content (wt%)	$T_{g,\ PMMA}$ (°C)	$T_{g,\ EPR}$ (°C)
homo-PMMA (linear)[a]	-	-	101.7	-
homo-PMMA (star)[b]	-	-	110.0	-
PMMA-*g*-EPR (**G7**)	0.37	10.0	108.0	n.d.[c]
PMMA-*g*-EPR (**G6**)	0.72	18.0	101.4	-65.8
PMMA-*g*-EPR (**G5**)	1.1	24.9	101.9	-68.3
PMMA-*g*-EPR (**G4**)	1.0	8.6	104.2	n.d.[c]
PMMA-*g*-EPR (**G2**)	2.6	19.9	90.2	n.d.[c]
PMMA-*g*-EPR (**G1**)	6.2	38.1	74.9	-64.7
(PMMA-*g*-EPR) star (**S2**)	2.3	21.0	89.3	n.d.[c]
(PMMA-*g*-EPR) star (**S1**)	5.3	36.3	57.9	-64.9

[a] Homo-PMMA (M_n = 22,800, M_w/M_n = 1.76) was prepared by the polymerization of MMA with AIBN.
[b] Four-arms PMMA star polymer (M_n = 6,600 per arm) was prepared by the polymerization of MMA by ATRP using a tetrafunctional initiator.
[c] Not detected.

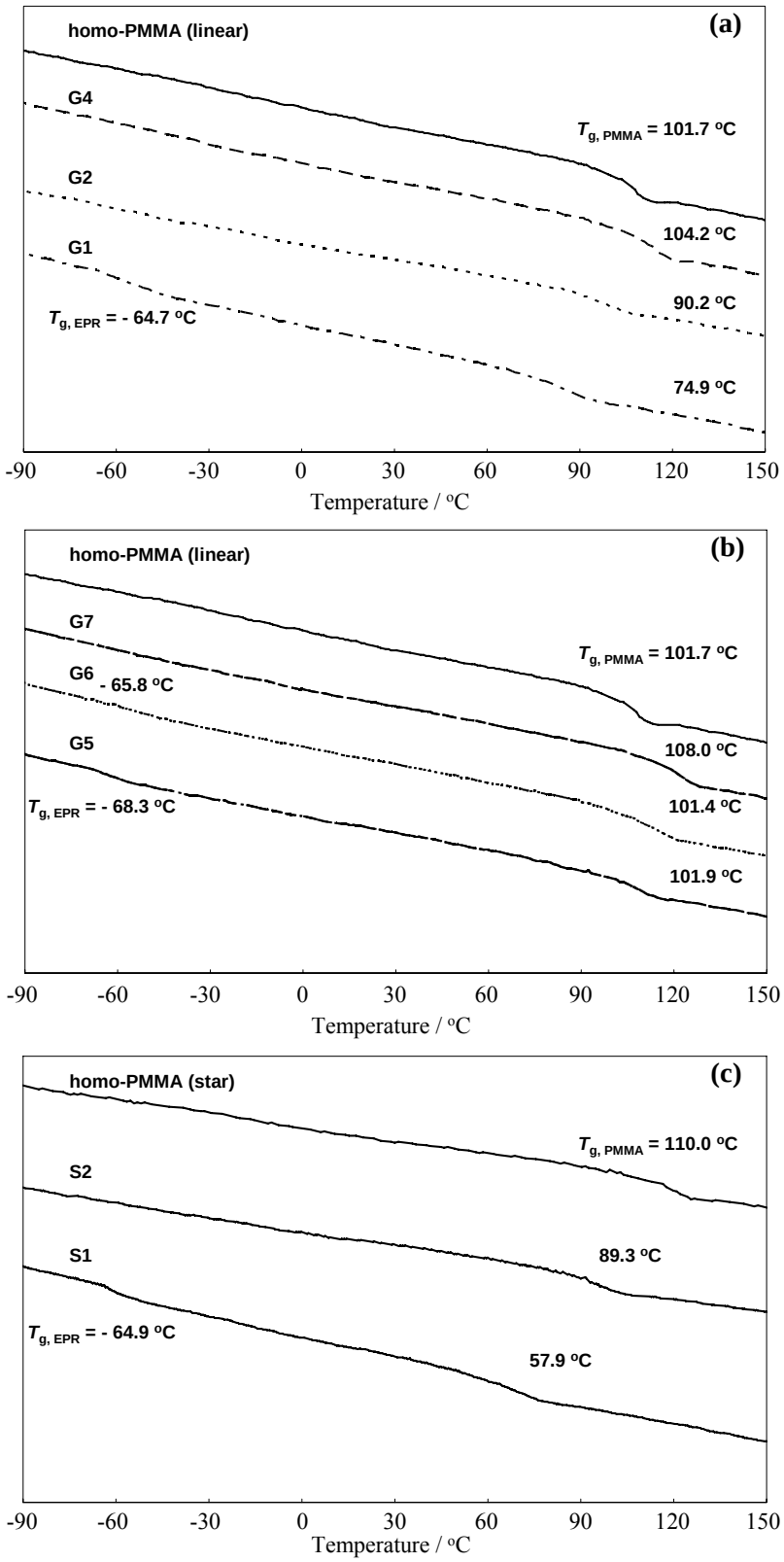

Figure 11. DSC thermograms of (a) PMMA-*g*-EPR graft copolymers (**G1**, **G2** and **G4**), (b) PMMA-*g*-EPR graft copolymers (**G5**-**G7**) and (c) PMMA-*g*-EPR star copolymers (**S1** and **S2**).

Figure 11a shows the DSC thermograms of PMMA-*g*-EPR graft copolymers obtained by the copolymerization of EPRM (0.9K) with MMA (**G1**, **G2**, and **G4**) and homo-PMMA as a reference. The T_g value of homo-PMMA was observed at 101.7 ^oC, and the T_g values of the graft copolymers gradually decreased with increasing EPR content. In the case of **G1**, a second T_g value appeared at -64.7 ^oC in addition to a T_g value based on the PMMA backbone at 74.9 ^oC. This second T_g value can be assigned to the EPR branch segment. It is well known that the incorporation of comonomers, such as ethyl, *n*-butyl, isobutyl and *t*-butyl methacrylate, decreases the T_g value of PMMA backbone. However, in the case of these comonomers more than 50 mol % of the comonomer content is needed to decrease T_g up to 75 ^oC [8]. Therefore, EPR macromonomer is more effective than these comonomers to control the T_g value of the PMMA backbone because of the high molecular weight of the EPR macromonomer.

On the other hand, in the case of PMMA-*g*-EPR graft copolymers obtained by using EPRM (3 K), T_g value hardly changed even at 24.9 wt % of the EPR content as shown in Figure 11b. These results demonstrate that the decreases of T_g values in the graft copolymers from that in the homo-PMMA can be attributed not to weight fraction but to mole fraction that is the number of EPR branches. In Figure 11c, the star copolymers obviously showed lower T_g values than those in the graft copolymers having similar compositions to them. It shows that the T_g value can be controlled by not only mole fraction of EPR branch but also topology of PMMA backbone.

Comparison with the PMMA-g-EPR Graft Copolymers Obtained by Conventional Free Radical Polymerization

The copolymerization of EPRM (0.9 K) with MMA were carried out using AIBN as an initiator in toluene at 60 ^oC. By changing the feed ratio between EPRM (0.9 K) and MMA, two graft copolymers with different compositions were synthesized, as shown in Table 7. Similar to the copolymerization, by using ATRP method, ^1H NMR and GPC analyses confirmed the formation of PMMA-*g*-EPR graft copolymers. In conventional free radical polymerization (CFRP) method, the number-average molecular weights were higher than those in ATRP method and the molecular weight distributions were broader than those in ATRP method. In this case of higher molecular weight, the detection of chain ends based on the initiator in the ^1H NMR spectrum was so difficult that the number-average molecular weight (M_n) and EPR branch number per chain cannot be estimated from ^1H NMR analysis. Then, the EPR branch numbers of these graft copolymers were roughly estimated to be about 10–30 from the M_n by GPC measurement and the EPR contents by ^1H NMR analysis.

Table 7. Preparation of PMMA-*g*-EPR Graft Copolymers by Using AIBN

	$[MMA]_0$ / $[EPRM(0.9K)]_0$	Yield (g)	M_n[c] (g mol^{-1})	M_w/M_n[c]	EPR content[d] (mol%)	EPR content[d] (wt%)	$T_{g,\ PMMA}$[e] (^oC)	$T_{g,\ EPR}$[e] (^oC)
G8[a]	10	0.99	94,700	1.70	4.8	32.0	89.9	-60.0
G9[b]	25	0.74	60,000	1.90	2.1	16.5	98.6	n.d.[f]

[a] Polymerization conditions: EPRM(0.9K) 2.44 g, MMA 2.14 mL, AIBN 0.1 mmol in toluene 10 mL at 60 ^oC for 5h.
[b] Polymerization conditions: EPRM(0.9K) 0.98 g, MMA 2.14 mL, AIBN 0.1 mmol in toluene 10 mL at 60 ^oC for 5h.
[c] Molecular weight was determined by GPC at 40 ^oC in $CHCl_3$ and calibrated with PS.
[d] Detaermined by ^1H NMR.
[e] From DSC analysis.
[f] Not detected.

Figure 12 shows morphology of the PMMA-*g*-EPR graft copolymer obtained by using CFRP method (**G8**). Although this graft copolymer has the same EPR content as that obtained by using ATRP method (**G1**), morphologies between them differed remarkably. In the case of this graft copolymer, it seems to be two immiscible phases with the different brightness. In addition, T_g values of these graft copolymers tend to be higher than those of the graft copolymers obtained by ATRP method. The reason of these phenomena is not clear at present, but it might be due to the differences of molecular weight and molecular weight distribution of the graft copolymers.

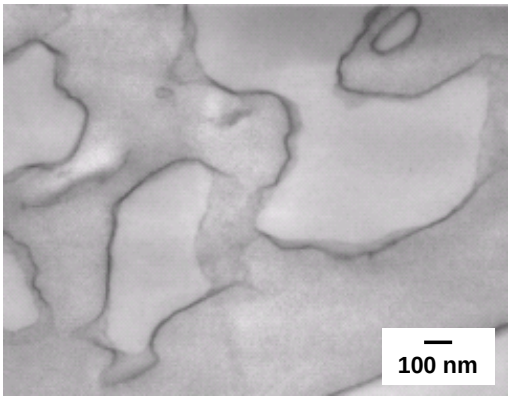

Figure 12. TEM Image of PMMA-*g*-EPR graft copolymer obtained by using CFRP method (EPR content = 32.0 wt%; **G8**).

Conclusions

Graft and star copolymers possessing poly(methacrylate) backbone and EPR branches were successfully synthesized by copolymerization of EPR macromonomers with MMA. EPR macromonomers were prepared by the sequential end functionalization of EPRs with vinylidene end group via hydroalumination, oxidation,

and esterification. ATRP method could be used for the copolymerization reaction to give PMMA-*g*-EPR graft copolymers with various EPR contents (8.6–38.1 wt %) and EPR branch numbers (1–14 branches). Furthermore, by using ATRP method with a tetrafunctional initiator, the star copolymers consisting of four PMMA-*g*-EPR graft copolymer arms were also synthesized. These unique topologies of the obtained copolymers could be confirmed by GPC measurement and NMR analysis. From TEM observation, the morphologies of these graft and star copolymers were remarkably altered by changing EPR branch number and the structure of PMMA backbone, which can control the segmental dispersion of PMMA and EPR segments in the range between more than 10 nm and less than 1 nm. Moreover, it was clearly demonstrated that the PMMA-*g*-EPR graft copolymer with 38.1 wt % of EPR content efficiently worked as a compatibilizer for EPR/PMMA polymer blend. DSC analysis revealed the effect of EPR branch on T_g value of PMMA backbone and a few incorporation of EPR branch remarkably caused a large deviation of T_g value from homo-PMMA. On the other hand, the PMMA-*g*-EPR graft copolymers obtained using CFRP method showed different morphology and thermal property from those using ATRP method. The obtained EPR/PMMA hybrid polymers having the unique characteristics could be expected to be novel polyolefin-based materials for the future.

References

[1] Duschek, T.; Mülhaupt, R. Polym Prepr 1992, 33, 170-171.

[2] Hong, S. C.; Jia, S.; Teodorescu, M.; Kowalewski, T.; Matyjaszewski, K.; Gottfried, A. C.; Brookhart, M. J Polym Sci Part A: Polym Chem 2002, 40, 2736-2749.

[3] Kaneko, H.; Matsugi, T.; Kojoh, S.; Kawahara, N.; Matsuo, S.; Kashiwa, N. PMSE Preprints 2003, 89, 664-665.

[4] Kaneko, H.; Kojoh, S.; Kawahara, N.; Matsuo, S.; Matsugi, T.; Kashiwa, N. Macromol Symp 2004, 213, 335-345.

[5] Shiono, T.; Kurosawa, H.; Ishida, O.; Soga, K. Kobunshi Ronbunshu 1992, 49, 847-854.

[6] Matyjaszewski, K.; Miller, P. J.; Pyun, J.; Kickelbick, G.; Diamanti, S. Macromolecules 1999, 32, 6526-6535.

[7] Matyjaszewski, K.; Qin, S.; Boyce, J. R.; Shirvanyants, D.; Sheiko, S. S. Macromolecules 2003, 36, 1843-1849.

[8] Penzel, E.; Rieger, J.; Schneider, H. A. Polymer 1997, 38, 325-337.

PART III

REACTIVE POLYOLEFIN APPROACH

Chapter 7

Terminal Hydroxylation of Isotactic Polypropylene and Its Utilization for Creating Polymer Hybrids

Abstract

The well-defined functionalized polyolefins are expected not only for improving such properties as adhesion or printability but also for creating hybrid polymers. As the examples, terminally hydroxylated isotactic polypropylenes (PPs) were synthesized via oxidization of Al-functionalized PPs obtained by predominant chain transfer with Et_3Al and hydroalumination of pyrolysis PP. They could be coupled with ethylene-propylene random copolymer (EPR) possessing maleic anhydride groups to give polymer hybrids consisting of PP and EPR segments. Impressively, the polymer hybrid demonstrated unique nano-order phase separation morphology of PP and EPR and indicated to work as a compatibilizer between PP and EPR.

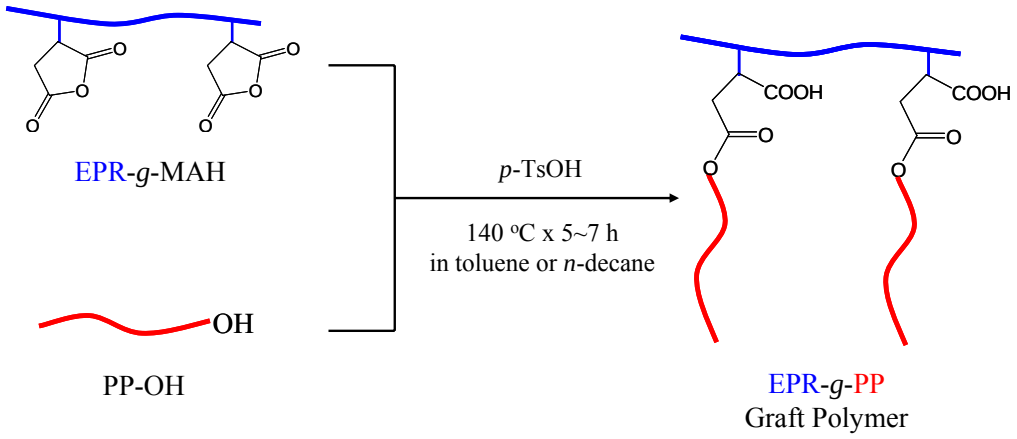

Introduction

Continuous innovations for controlling primary structures of polyolefin have contributed to broaden their application fields. For example, the latest $MgCl_2$-supported $TiCl_4$ catalyst can control the structure of isotactic polypropylene (PP) almost completely [1]. Therefore, worldwide production volume of polyolefins has grown to more than 80,000,000 tons per year and is predicted to rise continuously at a high rate. However, there is still large room to create new polymers on the basis of these well-established polyolefins. The typical example is to create functionalized polyolefins under precise structure control.

The well-defined functionalized polyolefins are expected not only for improving such properties as adhesion or printability but also for creating polymer hybrids. Utilizing them as macroinitiators, macromonomers and reactive polymers allowed us to synthesize novel polymer hybrids such as polyethylene-*b*-(polar polymer) or polyethylene-*g*-(polar polymer) [2, 3]. Needless to say, PP segment is also so important to create the polymer hybrids that studies on chain transfer reactions in propylene polymerization and their application to synthesizing terminally functionalized PP should be involved in the league. Through the long-term investigation about the chain transfer reactions [4], it has been reported the influences of electron donors [5] and alkylaluminums [6] on the reactions and an example of terminal functionalization of PP [7]. On the basis of these previous reports, the authors would like to introduce our current studies concerning to novel polymer hybrids.

Experimental

Catalyst Preparation

An $MgCl_2$-supported $TiCl_4$ catalyst was prepared as follows. $MgCl_2$ (7 g), *n*-decane (38 mL) and 2-ethylhexyl alcohol (35 mL) were reacted at 130 ºC for 2 h. Into the obtained uniform solution, phthalic anhydride (1.7 g) was added and stirred at 130 ºC for 1 h. The uniform solution thus obtained was cooled to room temperature and added dropwise into 200 mL of $TiCl_4$ at -20 ºC for 1 h. Then, the solution was heated to 110 ºC and diisobutyl phthalate (DIBP; 5 mL) was added at this temperature. It was further stirred at that temperature for 2 h and the resulting solid portion was collected by filtration. The solid portion was suspended with 275 mL of $TiCl_4$ and stirred at 110 ºC for 2 h. The resulting solid portion was collected by filtration and washed with *n*-decane and *n*-hexane to obtain DIBP included $MgCl_2$-supported $TiCl_4$ catalyst.

Polymers

Pyrolysis PP (py-PP) used here was commercially available from Mitsui Chemicals, Inc. who thermally decompose PP prepared with DIBP included $MgCl_2$-supported $TiCl_4$ catalyst to obtain it. Its weight average molecular weight (M_w) was 8,000 and its molecular weight distribution (M_w/M_n) was 2.4. It was iPP copolymerized with 2 mol% of ethylene. Two kinds of maleic anhydride grafted ethylene/propylene random copolymers (EPR-*g*-MAH-1 and EPR-*g*-MAH-2) that were obtained in the conventional way [8]. M_w of both was 130,000 and composition of both was 80 mol% of ethylene and 20 mol% of propylene. The contents of MAH were 0.5 wt% and 1.0 wt%, respectively.

Synthesis of PP-OH-1

In a 500-mL glass autoclave equipped with a stirrer, *n*-decane (250 mL) was added and the system was charged with propylene. Then, triethylaluminum (5 mmol), cyclohexylmethyldimethoxysilane (0.5 mmol) and the solid catalyst (0.1 mmol as Ti atom) were added at 100 ºC in this order. Polymerization was carried out under atmospheric pressure at that temperature for 1 h. During the polymerization, 50 L/h of propylene was supplied continuously. After the polymerization, the feed of the propylene monomer was stopped and replaced by a stream of nitrogen. The resulting slurry was contacted with molecular oxygen as follows. Into the slurry, 200 L/h of dry air was continuously supplied at 100 ºC for 5h. Then the whole product was poured into 2 L of methanol at room temperature. The resulting slurry was stirred for 5 min and settled overnight. Subsequently, 2 mL of hydrochloric acid was added into the slurry and the obtained mixture was stirred for 5 min, settled for 30 min and filtered. The resulting polymer was washed with plenty of methanol and vacuum-dried at 80 ºC for 10 h (yield 2.5 g).

Synthesis of PP-OH-2

Into a nitrogen-purged 1-L glass reactor equipped with a mechanical stirrer, py-PP (26.6 g) was added with $(i\text{-Bu})_2AlH$ (34.6 mmol) and *n*-decane (800 mL). It was heated to 100 ºC and that temperature was maintained for 7 h with stirring. Then, dried air was fed into it at a rate of 200 L/h at that temperature for 6 h. The resulting solution was poured into a mixture of 2 L of methanol, 2 L of acetone and small amount of HCl, followed by stirring for 2 h. Thus-obtained polymer (PP-OH-2) was recovered by filtration, washed with 1 L of methanol, and dried at 80 ºC for 5 h.

Coupling Reaction

Into a nitrogen-purged glass reactor equipped with a mechanical stirrer, PP-OH-1 or PP-OH-2 (1.0 g) was added with toluene (250 mL) or *n*-decane (150 mL), catalyst amount of *p*-toluenesulfonic acid and EPR-*g*-MAH-1 (0.1 g) or EPR-*g*-MAH-2 (2.8 g), respectively. It was heated to 80 or 140 ºC and the temperature was maintained for 5 or 7 h with stirring, respectively. Then, it was poured into a mixture of 1.5 L of methanol and 1.5 L of acetone, followed by stirring with a magnetic stirrer chip for 5 min. The recovered polymer by filtration was stirred in 2 L of acetone with a magnetic stirrer chip for 2 h. Thus-obtained polymer was recovered by filtration, washed with 0.5 L of acetone, and vacuum-dried at 80 ºC for 10 h.

Polymer Blend

Same procedures as described in coupling reaction except for using py-PP instead of PP-OH-2 were carried out to prepare polymer blend for the comparison with the polymer obtained by coupling reaction between PP-OH-2 and EPR-*g*-MAH-2. Then, for evaluating the polymer obtained by the coupling reaction between PP-OH-2 and EPR-*g*-MAH-2, it was added to the above polymer blend at a weight ratio of 1 to 9 and stirred in decane at 140 ºC for 3 h.

GPC Measurement

Molecular weights were measured by a Millipore Waters 150C gel permeation chromatograph (GPC) equipped with a refractive index detector using a TSK mixed polystyrene gel column (G3000-G7000) in 1,2-dichlorobenzene as a solvent at 140 ^{o}C.

TEM Observation

Morphologies were observed with a transmission electron microscopy (TEM) as following. Ultra-thin (*ca.* 100 nm) section of the polymer that had been pressed to give a sheet and dyed with RuO_4 was prepared with a Reica Ultracut microtome equipped with a diamond knife. The specimen was examined with a HITACHI H-810 transmission electron microscopy operated at 100 KV at 10,000 and 150,000 magnifications.

Measurement of C_{10} Sol.

Solubility to *n*-decane at 23 ºC (C_{10} Sol) was measured as following. Into a 1-L flask, the polymer sample (1 g) was added with 2,6-di-*t*-butyl-4-methylphenol (10 mg) and *n*-decane (500 mL). The mixture was heated to 150 ºC in order to dissolve the polymer

sample. The obtained solution was cooled to 23 ºC during 8 h and kept at that temperature for 8 h. The resulting slurry was filtered and the liquid phase portion was vacuum-dried until it reached constant weight. The percentage of thus-obtained constant weight in the weight of the initial polymer sample was C_{10} Sol.

Results and Discussion

Terminal hydroxylation of PP

Two kinds of terminally hydroxylated PP were synthesized. One of them was obtained by the same manner described in a previous paper [7] except for using the DIBP-included $MgCl_2$-supported $TiCl_4$ catalyst instead of using the dioctyl phthalate included one and the resulting M_w was 170,000 and hydroxylated chain end was 52 mol% (PP-OH-1). The other was produced by hydroxylation of py-PP, which M_w was 8,000 (PP-OH-2). The chain-end structures of py-PP were investigated with ^{13}C NMR and the major group was vinylidene group as shown in Table 1, which is accordance with the literature on pyrolysis of PP [9]. The chain-end structures of PP-OH-2 were also analyzed with ^{13}C NMR and summarized in Table 1. The formation of 45 mol% of hydroxyl chain-end group from the vinylidene group accounting for 81 mol% in py-PP means comparable conversion with that observed in the hydroxylation for producing PP-OH-1 having the higher molecular weight. Consequently, the obtained polymer possessed hydroxyl chain end in the content of 45 mol% of both ends of the polymer chain, namely, 0.9 units of hydroxyl group per chain on the average, although it would be a mixture of di-hydroxylated, mono-hydroxylated and non-hydroxylated polymers.

Table 1. Proportions of Chain-End Groups of Pyrolysis and Hydroxylated PP.

	Chain-End Group[a] (mol%)				
Sample	Vd	*n*Pr	*i*Pr	*i*Pr-OH	others
py-PP	81	17	2	n.d.[b]	n.d.[b]
PP-OH-2	6	15	34	45	n.d.[b]

[a] Vd: vinylidene, *n*Pr: *n*-propyl, *i*Pr: *i*-propyl, *i*Pr-OH: hydroxyl *i*-propyl.

[b] Not detected.

Coupling Reaction of PP-OH with EPR-g-MAH

Thus-obtained PP-OH-1 and PP-OH-2 were used for coupling reaction with EPR-*g*-MAH-1 and EPR-*g*-MAH-2, respectively, because the polymer hybrid consisting of the crystalline polyolefin and the amorphous polyolefin is of importance to create new class of plastic materials.

The coupling reaction between PP-OH-1 and EPR-*g*-MAH-1 was carried out at 80 ºC for 5 h at the weight ratio of 1 to 10 of EPR-*g*-MAH-1 to PP-OH-1 to synthesize the polymer hybrid (EPR-*g*-PP-1). The C_{10} Sol of the resulting polymer was 8.1 wt%. From C_{10} Sol of EPR-*g*-MAH-1 and PP-OH-1 (97 and 6.0 wt%, respectively) and the weight ratio of EPR-*g*-MAH-1 and PP-OH-1, the C_{10} Sol should be 14 wt%, if the coupling reaction did not occur. Therefore, it indicated the occurrence of the coupling reaction.

PP-OH-2 was reacted with EPR-*g*-MAH-2 at 140 ºC for 7 h in *n*-decane with a molar ratio of 6 to 1 to synthesize the polymer hybrid (EPR-*g*-PP-2). For its comparison, py-PP was blended with EPR-*g*-MAH-2 under the same conditions as the coupling reaction expect for the replacement of PP-OH-2 by py-PP. In the coupling reaction, its non-viscous initial solution changed to jelly-like product through highly viscous solution, although that in blending the polymers kept the state of non-viscous solution. It strongly suggests the proceeding of the aimed coupling reaction. Each product was poured into a mixture of methanol and acetone, then the polymer recovered by filtration was washed with acetone followed by vacuum dry to be compared in C_{10} Sol. The C_{10} Sol of the polymer blend was 75.3 wt% corresponding nearly to the weight proportion of EPR in it, while that of the polymer hybrid (EPR-*g*-PP-2) was 8.8 wt% suggesting that PP segment bonded to EPR prevented the EPR segment from dissolving in *n*-decane.

Morphological Study on Polymer Hybrid and Polymer Blend

Figure 1 shows morphologies observed with TEM for press sheets from the respective polymers. Microphase separation morphology was observed in the polymer blend, where the matrix was EPR segment and the dispersed phase was PP segment (Figure 1(b)). It was common morphology for polyolefins and the dispersed phase was found to be considerably large and non-uniform. On the contrary, EPR-*g*-PP demonstrated unique lamella microstructure as shown in Figure 1(a). Furthermore, its phase boundary was not distinct at high magnification as seen in Figure 1(c), although the phase boundary was clear in the polymer blend even at high magnification (Figure 1(d)). Namely, the lamellar domains looked black or white at low magnification were turned out to include the other component on a nano-order scale by the observation at

high magnification. Eventually, it was found that iPP could form nano-order phase separation structures with EPR to give the novel lamellar morphology by this coupling reaction.

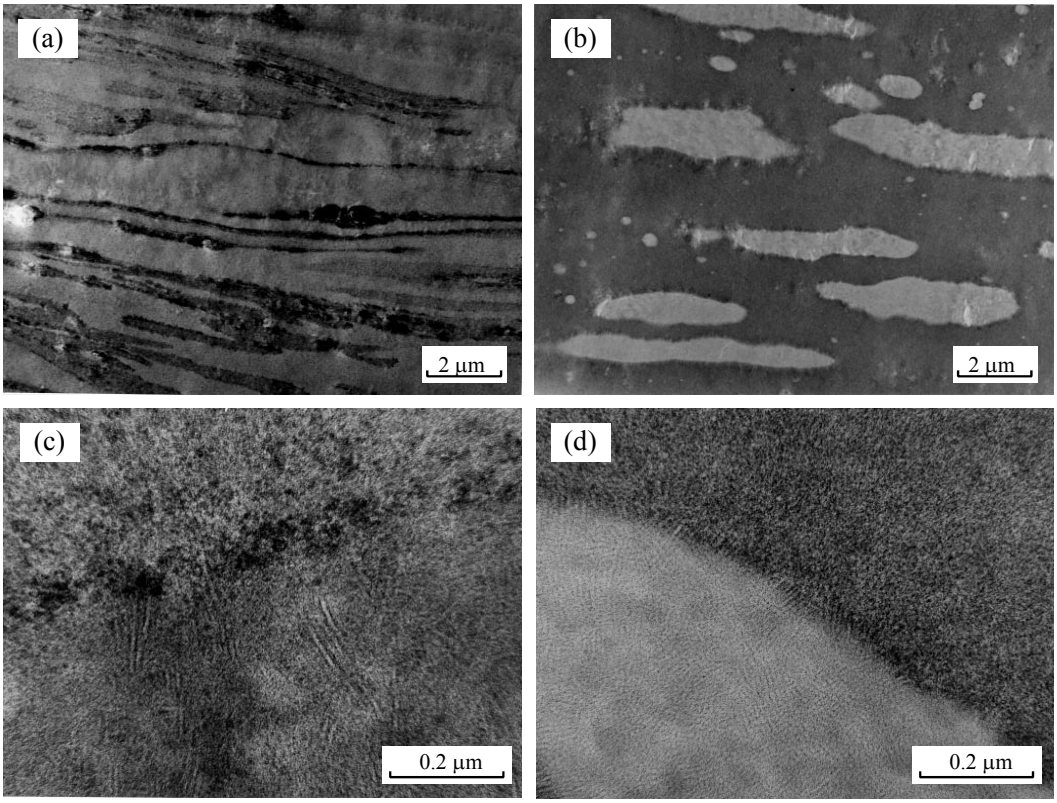

Figure 1. TEM micrographs at 10,000 magnification from (a) EPR-*g*-PP-2 produced by coupling reaction between PP-OH-2 and EPR-*g*-MAH-2 and (b) polymer blend consisting of py-PP and EPR-*g*-MAH-2 and at 150,000 magnification of (c) the EPR-*g*-PP-2 and (d) the polymer blend. The molar ratio of iPP segment to EPR segment is 6 to 1 in any of the both samples.

Evaluation of EPR-g-PP

EPR and PP are so immiscible that the microphase separation morphology obtained by blending them is usually coarse and irregular as shown in Figure 1(b), meaning that its polymer properties are not good. The nano-order phase separation morphology of EPR-*g*-PP was expected that it played an important role for improving it as a compatibilizer. In fact, its addition to the polymer blend observed in Figure 1(b) at a weight ratio of 1 to 9 led to much smaller sizes of the dispersed PP domains as shown in Figure 2, demonstrating its high ability as a compatibilizer. This result would coincidently support the above-mentioned suggestion that the coupling reaction linked EPR with PP.

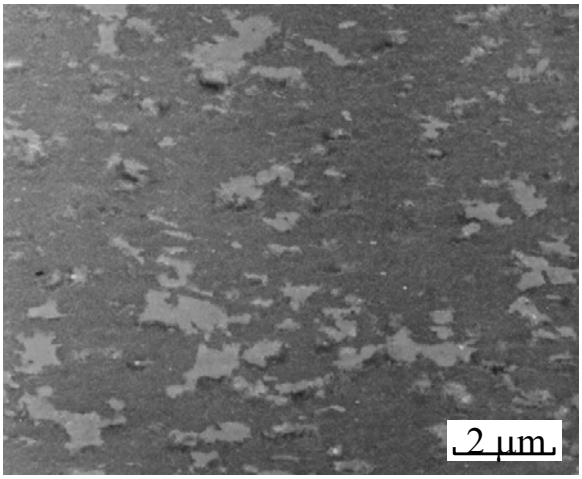

Figure 2. TEM micrographs at 10,000 magnification from the EPR-*g*-PP-2 added polymer blend consisting of py-PP and EPR-*g*-MAH-2 at a weight ratio of 1(EPR-*g*-PP-2): 2.4(py-PP):6.6(EPR-*g*-MAH-2).

Conclusion

Both predominant chain transfer by Et_3Al and hydroalumination of py-PP gave terminally hydroxylated PP via oxidation and methanolysis. They could be coupled with ethylene/propylene random copolymer (EPR) possessing MAH to form polymer hybrids consisting of PP and EPR segments. Impressively, the obtained polymer hybrid demonstrated unique nano-order phase separation morphology of PP and EPR and indicated to work as a compatibilizer between PP and EPR.

References

[1] Kashiwa, N.; Kojoh, S.; Imuta, J.; Tsutsui, T. In Metalorganic Catalysts for Synthesis and Polymerization: Recent Results by Ziegler-Natta and Metallocene Investigations; Kaminsky, W., Ed.; Springer-Verlag: Berlin Heidelberg, 1999; p 30.

[2] Kojoh, S.; Matsugi, T.; Ono, S. S.; Kizu, K.; Mori, R.; Nobori, T.; Imuta, J.; Fujita, T.; Yamamoto, S.; Kashiwa, N. In Proceedings of the FLEXPO2002, Houston, 2002; p 221.

[3] Kojoh, S.; Matsugi, T.; Kaneko, H.; Matsuo, S.; Kawahara, N.; Kashiwa, N. In

Proceedings of the EUPOC 2003, Milan, 2003; p 249.

[4] Kojoh, S.; Kioka, M.; Kashiwa, N.; Itoh, M.; Mizuno, A. Polymer 1995, 36, 5015-5018.

[5] Kojoh, S.; Tsutsui, T.; Kashiwa, N.; Itoh, M.; Mizuno, A. Polymer 1998, 39, 6309-6313.

[6] Kojoh, S.; Kioka, M.; Kashiwa, N. Eur Polym J 1999, 35, 751-755.

[7] Kojoh, S.; Tsutsui, T.; Kioka, M.; Kashiwa, N. Polym J 1999, 31, 332-335

[8] Yamanaka, T.; Miura, E. JP Patent, Kokai 4-57808, 1992.

[9] Sawaguchi, T.; Ikemura, T.; Seno, M. Macromolecules 1995, 28, 7973-7978.

GENERAL CONCLUSIONS

This thesis has dealt with the study on polyolefin-based polymer hybrids with multiple polymer segments, named “Polyolefin Hybrids”. In this thesis, the author has developed new synthetic methodologies for polyolefin hybrids with designed topologies and compositions by a combination of the functionalized polyolefins, including polyolefin macroinitiator, polyolefin macromonomer and reactive polyolefin, and post-polymerization processes. Furthermore, he also discussed the structures and characteristics of the obtained polyolefin hybrids using several analytical methods. Those studies are aimed at a creation of new value-added polyolefins with the improved and unique properties. The brief conclusions of each part and chapter are as follows.

PART I concerned the synthesis and utilization of PP macroinitiators to give a variety of PP-based block and graft copolymers. In ***Chapter 1***, PP macroinitiators were prepared by a series of end-functionalization of pyrolysis PP via hydroalumination, oxidation and esterification. The controlled radical polymerizations of MMA or NIPAAm with these PP macroinitiators were carried out to give PP-*b*-PMMA and PP-*b*-PNIPAAm block copolymers. TEM observation demonstrated the microphase-separation morphology at the nanometer level between PP and PNIPAAm segments and its morphology was remarkably altered by the length of the attached PNIPAAm segment.

Chapter 2 includes the first example of PP macroinitiator prepared by a direct allylic bromination of terminally-unsaturated PP. The brominated PP was successfully employed as a macroinitiator for controlled radical polymerization of typical polar monomers, such as St, MMA and nBA, to give the corresponding block copolymers. From GPC measurements, successful chain extensions from the brominated PP were achieved and block copolymers having polar segments of controlled molecular weight were conveniently synthesized. Furthermore, thus obtained PP-based block copolymers demonstrated the unique thermal properties and morphologies due to the microphase separation between both segments. This new synthetic method is simpler and more facile than the other existing methods for the synthesis of polyolefin hybrids.

In ***Chapter 3***, PP macroinitiator was prepared by the reaction between maleic anhydride-modified PP and ethanolamine and the subsequent reaction with 2-bromoisobutyryl bromide. The obtained PP macroinitiator was successfully employed for the controlled radical polymerization of MMA to give the PP-*g*-PMMA graft copolymers. From TEM observations, both segments finely dispersed at the nanometer level and the PP-*g*-PMMA worked as a good compatibilizer for the PP/PMMA polymer

blend. On the other hand, HEMA polymerization on the PP macroinitiator particles gave a hydrophilic core-shell polymer consisting of a PP-rich core and a PHEMA-rich shell. The introduction of PMMA and PHEMA segments into PP improved its low interfacial interaction with polar polymers or water and thus obtained PP hybrids are expected to be used as not only compatibilizer and modifier but also the other new applications such as antistatic agent, antifog additive, aqueous coating and aqueous emulsion.

In ***Chapter 4***, PP macroinitiator was prepared by a metallocene-catalyzed copolymerization of propylene/10-undecen-1-ol and subsequent reaction with 2-bromoisobutyryl bromide. The controlled radical polymerizations of MMA, St and nBA with the obtained PP macroinitiator were carried out to give the corresponding PP-based graft copolymers. The flexural and Izod impact tests revealed that the incorporation of PMMA and PS into the PP backbone effectively enhanced stiffness and concerning PnBA remarkably improved toughness.

PART II concerned the synthesis and utilization of EPR or PER-based macromonomers to give the graft or star copolymers possessing polyolefin branches. In ***Chapter 5***, poly(PER macromonomers) were successfully synthesized by homopolymerization of methacryloyl-terminated PER macromonomer, which were synthesized by the conversion of the vinylidene-terminated PER. From ^{1}H and ^{13}C NMR analyses and GPC measurement, the obtained polymer consisted of a polymethacrylate backbone and 30 PER branches. This novel polymacromonomer exhibited the nature of PER rather than the nature of polymethacrylate because of its unique polymer architecture such as the high concentration of polyolefin branches.

In ***Chapter 6***, the controlled radical copolymerization of EPR macromonomer with MMA was carried out to give the PMMA-*g*-EPR graft copolymers with various EPR contents (8.6-38.1 wt%) and EPR branch numbers (1-14 branches), and the star copolymers consisting of four PMMA-g-EPR arms. Their unique topologies were confirmed by GPC measurement and NMR analysis. From TEM observation, the morphologies of these graft and star copolymers were remarkably altered by changing EPR branch number and the structure of PMMA backbone. Moreover, the PMMA-*g*-EPR graft copolymer efficiently worked as a compatibilizer for EPR/PMMA polymer blend. On the other hand, the PMMA-*g*-EPR graft copolymers obtained by conventional free radical polymerization showed different morphology and thermal property from those by controlled radical polymerization.

PART III concerned the synthesis and utilization of reactive polyolefins to give the graft copolymers consisting of different polyolefin segments. In ***Chapter 7***, the terminally-hydroxylated PPs were prepared by a sequential functionalization of

Al-functionalized PP via oxidation and methanolysis. They could be coupled with ethylene-propylene random copolymer (EPR) possessing MAH to form polymer hybrids consisting of PP and EPR segments. Impressively, the obtained polymer hybrid demonstrated unique nano-order phase separation morphology of PP and EPR and indicated to work as a compatibilizer between PP and EPR.

Thus, these new synthetic methodologies by combination of the functionalized polyolefins and post-polymerization processes have enabled a creation of various polyolefin hybrids with designed topologies and compositions. Because of a chemical linkage among the multiple polymer segments, such polyolefin hybrids demonstrate microphase separation morphology and unique and improved properties reflecting the kind and content of the introduced segments. In the future, polyolefin hybrids are expected to be used in various fields as a new value-added polyolefin material.

LIST OF PUBLICATIONS

Papers (included in this thesis)

1. Polypropylene-*block*-Poly(methyl methacrylate) and -*block*-Poly(*N*-isopropylacrylamide) Block Copolymers Prepared by Controlled Radical Polymerization with Polypropylene Macroinitiator (***Chapter 1***)

   Hideyuki Kaneko, Tomoaki Matsugi, Nobuo Kawahara, Shingo Matsuo, Shin-ichi Kojoh and Norio Kashiwa, *Kinetics and Catalysis,* **2006**, *47*, 227-233.

2. Synthesis and Characterization of Polypropylene-Based Block Copolymers Possessing Polar Segments via Controlled Radical Polymerization (***Chapter 2***)

   Hideyuki Kaneko, Junji Saito, Nobuo Kawahara, Shingo Matsuo, Tomoaki Matsugi and Norio Kashiwa, *Journal of Polymer Science: Part A: Polymer Chemistry*, **2009**, *47*, 812-823.

3. Synthesis and Characterization of Polypropylene-Based Polymer Hybrids Linking Poly(methyl methacrylate) and Poly(2-hydroxyethyl methacrylate) (***Chapter 3***)

   Hideyuki Kaneko, Junji Saito, Nobuo Kawahara, Shingo Matsuo, Tomoaki Matsugi and Norio Kashiwa, *Polymer*, **2008**, *49*, 4576-4584.

4. Synthesis and Mechanical Properties of Polypropylene-Based Polymer Hybrids via Controlled Radical Polymerization (***Chapter 4***)

   Hideyuki Kaneko, Shingo Matsuo, Nobuo Kawahara, Junji Saito, Tomoaki Matsugi and Norio Kashiwa, *Macromolecular Symposia*, **2007**, *260*, 9-14.

5. Polymacromonomers with Polyolefin Branches Synthesized by Free-radical Homopolymerization of Polyolefin Macromonomer with a Methacryloyl End Group (***Chapter 5***)

   Hideyuki Kaneko, Shin-ichi Kojoh, Nobuo Kawahara, Shingo Matsuo, Tomoaki Matsugi and Norio Kashiwa, *Macromolecular Symposia*, **2004**, *213*, 335-345.

6. Syntheses of Graft and Star Copolymers Possessing Polyolefin Branches by using Polyolefin Macromonomer (***Chapter 6***)

   Hideyuki Kaneko, Shin-ichi Kojoh, Nobuo Kawahara, Shingo Matsuo, Tomoaki Matsugi and Norio Kashiwa, *Journal of Polymer Science: Part A: Polymer Chemistry*, **2005**, *43*, 5103-5118.

7. Terminal Hydroxylation of Isotactic Polypropylene and Its Utilization for Creating Polymer Hybrids (***Chapter 7***)

   Shin-ichi Kojoh, **Hideyuki Kaneko**, Nobuo Kawahara, Shingo Matsuo, Tomoaki Matsugi and Norio Kashiwa, *In Current Achievements on Heterogeneous Olefin Polymerization Catalysts; Terano, M., Ed.; Sankeisha: Nagoya,* **2004**; pp 234-239.

Papers (not included in this thesis)

1. Hydrocarbon Anions with High Stability. Part 2. Structure and Stability of Cyclopentadienide Ions with Condensed Aromatic Rings

   Tomomi Kinoshita, Masaya Fujita, **Hideyuki Kaneko**, Ken'ichi Takeuchi, Kazunari Yoshizawa and Tokio Yamabe, *Bulletin of the Chemical Society of Japan*, **1998**, *71*, 1145-1149.

2. Synthesis and Characterization of Highly Processable LLDPE obtained by $Et(Ind)_2ZrCl_2$/MAO Catalyst System

   Norio Kashiwa, **Hideyuki Kaneko**, Shin-ichi Kojoh, Shingo Matsuo, Toshiyuki Tsutsui and Terunori Fujita, *In Proceedings of the symposium of PACIFICHEM2000*, pp. 115-129.

3. Synthesis and characterization of metallocene-catalyzed propylene-ethylene copolymer with end-capped functionality

   Akinori Toyota, Akira Mizuno, Toshiyuki Tsutsui, **Hideyuki Kaneko** and Norio Kashiwa, *Polymer*, **2002**, *43*, 6351-6355.

4. Functionalization of Polyethylene Based on Metallocene Catalysis and Its Application to Syntheses of New Graft Copolymers Possessing Polar Polymer Segments

   Norio Kashiwa, Tomoaki Matsugi, Shin-ichi Kojoh, **Hideyuki Kaneko**, Nobuo

Kawahara, Shingo Matsuo, Tadahito Nobori and Jun-ichi Imuta, *Journal of Polymer Science: Part A: Polymer Chemistry*, **2003**, *41*, 3657-3666.

5. Synthesis and Morphology of Polyethylene-block-poly(methyl methacrylate) through the Combination of Metallocene Catalysis with Living Radical Polymerization

   Tomoaki Matsugi, Shin-ichi Kojoh, Nobuo Kawahara, Shingo Matsuo, **Hideyuki Kaneko** and Norio Kashiwa, *Journal of Polymer Science: Part A: Polymer Chemistry*, **2003**, *41*, 3965-3973.

6. Direct Introduction of Primary Amine into Nonpolar Polyolefins Mediated by a New Metallocene IFZ Catalyst. A New Synthetic Approach for One-pot Synthesis of Allyl Amine-capped Polyolefins

   Jun-ichi Imuta, Yoshihisa Toda, Tomoaki Matsugi, **Hideyuki Kaneko**, Shingo Matsuo, Shin-ichi Kojoh and Norio Kashiwa, *Chemistry Letter*, **2003**, *32*, 656-657.

7. New Methodology for Synthesizing Polyolefinic Graft Block Copolymers and Their Morphological Features

   Norio Kashiwa, Shin-ichi Kojoh, Nobuo Kawahara, Shingo Matsuo, **Hideyuki Kaneko** and Tomoaki Matsugi, *Macromolecular Symposia*, **2003**, *201*, 319-326.

8. New Olefin Polymerization Catalyst Systems Comprised of Bis(phenoxy-imine) Titanium Complexes and $MgCl_2$-Based Activators

   Yasushi Nakayama, Hideki Bando, Yoshiho Sonobe, **Hideyuki Kaneko**, Norio Kashiwa and Terunori Fujita, *Journal of Catalysis*, **2003**, *215*, 171-175.

9. Study on Chain End Structures of Polypropylenes Prepared with Different Symmetrical Metallocene Catalysts

   Nobuo Kawahara, Shin-ichi Kojoh, Shingo Matsuo, **Hideyuki Kaneko**, Tomoaki Matsugi, Yoshihisa Toda, Akira Mizuno and Norio Kashiwa, *Polymer*, **2004**, *45*, 2883-2888.

10. Effect of Various Alkyl Groups of External Silane Donors on $MgCl_2$-Supported $TiCl_4$ Catalyst Performance in Propylene, 1-Butene and 4-Methyl-1-pentene Polymerizations

Hideyuki Kaneko, Shin-ichi Kojoh, Nobuo Kawahara, Shingo Matsuo, Tomoaki Matsugi and Norio Kashiwa, *In Current Achievements on Heterogeneous Olefin Polymerization Catalysts; Terano. M., Ed.; Sankeisha: Nagoya*, **2004**; pp 18-22.

11. Investigation of Insertion Reaction of 10-Undecen-1-ol Protected with Alkylaluminum in En(Ind)$_2$ZrCl$_2$/MAO Catalyst System
    Nobuo Kawahara, Shin-ichi Kojoh, Shingo Matsuo, **Hideyuki Kaneko**, Tomoaki Matsugi and Norio Kashiwa, *Journal of Molecular Catalysis A: Chemical*, **2005**, *241*, 156-161.

12. Creation of New Polyolefin Hybrids on The Surface of Molded Polypropylene Sheet
    Shingo Matsuo, Tomoaki Matsugi, Junji Saito, Nobuo Kawahara, **Hideyuki Kaneko** and Norio Kashiwa, *Studies in Surface Science and Catalysis*, **2006**, *161*, 1-6.

13. Synthetic Method of Polyethylene-poly(methyl lmethacrylate) (PE-PMMA) Polymer Hybrid via Reversible Addition-Fragmentation Chain Transfer (RAFT) Polymerization with Functionalized Polyethylene
    Nobuo Kawahara, Shin-ichi Kojoh, Shingo Matsuo, **Hideyuki Kaneko**, Tomoaki Matsugi, Junji Saito and Norio Kashiwa, *Polymer Bulletin*, **2006**, *57*, 805-812.

14. Study on Unsaturated Structures of Polyhexene, Poly(4-methylpentene) and Poly(3-methylpentene) Prepared with Metallocene Catalysts
    Nobuo Kawahara, Junji Saito, Shingo Matsuo, **Hideyuki Kaneko**, Tomoaki Matsugi, Yoshihisa Toda and Norio Kashiwa, *Polymer*, **2007**, *48*, 425-428.

15. New Methodology for Synthesizing Polypropylene-*graft*-Polystyrene (PP-*g*-PS) by Coupling Reaction with Brominated Polypropylene
    Norio Kawahara, Junji Saito, Shingo Matsuo, **Hideyuki Kaneko**, Tomoaki Matsugi, Shin-ichi Kojoh and Norio Kashiwa, *Polymer Bulletin*, **2007**, *59*, 177-183.

16. Syntheses, Structures and Functions of Polyolefin/non-Polyolefin Hybrids
    Junji Saito, Nobuo Kawahara, Shingo Matsuo, **Hideyuki Kaneko**, Tomoaki Matsugi and Norio Kashiwa, *Kobunshi Ronbunshu*, **2007**, *64*, 897-906.

17. Polymer Hybrids Based on Polyolefins - Syntheses, Structures, and Properties
    Nobuo Kawahara, Junji Saito, Shingo Matsuo, **Hideyuki Kaneko**, Tomoaki Matsugi and Kashiwa, *Advances in Polymer Science*, **2008**, *217*, 79-119.

18. Novel Polyolefin Hybrids via Controlled/Living Radical Polymerization
    Junji Saito, Nobuo Kawahara, Shingo Matsuo, **Hideyuki Kaneko**, Tomoaki Matsugi and Norio Kashiwa, *In Progress in Controlled/Living Radical Polymerization; Matyjaszewski, K., Ed.; ACS Symposium Series; American Chemical Society: Washington, DC*, **2009**; *submitted*.

19. Polypropylene-*graft*-poly(methyl methacrylate) Graft Copolymers: Synthesis and Compatibilization of Polypropylene/Polylactide
    Hideyuki Kaneko, Junji Saito, Nobuo Kawahara, Shingo Matsuo, Tomoaki Matsugi and Kashiwa, *In Progress in Controlled/Living Radical Polymerization; Matyjaszewski, K., Ed.; ACS Symposium Series; American Chemical Society: Washington, DC*, **2009**; *submitted*.

ACKNOWLEDGEMENTS

This thesis is a part of the studies that the author carried out at the Organo-Metal Complexes Catalyzation Laboratory, the Research Center, Mitsui Chemicals, Inc. during the period of 2002 to 2008.

The author would like to express his sincere gratitude to Professor Mitsuo Sawamoto, Kyoto University, for his kind guidance, invaluable suggestions and important discussion. He is equally grateful to Professor Yoshiki Chujo and Professor Kazuo Akagi, Kyoto University, for their insightful comments. He is also grateful to Assistant Professor Takaya Terashima, Kyoto University, for his helpful suggestions and support.

He wishes to express his deep gratitude to Dr. Norio Kashiwa, the Senior Research Fellow of Mitsui Chemicals, Inc. for his support, invaluable discussion and warm encouragement.

He wishes to thank Dr. Akinori Toyota, Dr. Noriaki Kihara, Dr. Terunori Fujita, Dr. Toshiyuki Tsutsui and Dr. Kenji Fujiwara for their helpful supports and understanding.

He is grateful to Dr. Jun-ichi Imuta, Dr. Shin-ichi Kojoh, Dr. Junji Saito, Dr. Nobuo Kawahara, Mr. Shingo Matsuo and Dr. Tomoaki Matsugi for their kind help, suggestions and collaborations.

He also wishes to thank Dr. Akira Todo, Dr. Ryuichi Sugimoto and Mr. Takayuki Onogi for their kind help, informative discussion and advice.

He deeply appreciates his parents, Mr. Hideo Kaneko and Mrs. Toshimi Kaneko for their education and support.

Finally, he would like to express his many thanks to his wife, Kumie, and his sons, Takumi and Hiroto, for their continuous encouragement and kind support.

Sodegaura, January 2009

Hideyuki Kaneko